ECO LOGY

Combined effects of ocean acidification and tidal emergence on the performance and gene expression in the intertidal brown seaweed *Fucus serratus*

AWI

Master thesis proposed by

Anique Stecher

Bremen, August 2011

University of Bremen, Faculty 02: Biology/Chemistry

Conducted at the Alfred Wegener Institute for Polar and Marine Research, Bremerhaven in the working group:

"Seaweed Biology"

1. Examiner: Prof. Dr. Christian Wiencke

                      Alfred Wegener Institute Bremerhaven, Germany

2. Examiner: Prof. Dr. Martin Diekmann

                      University of Bremen, Germany

Declaration

Herewith, I declare that this master thesis "Combined effects of ocean acidification and tidal emergence on the performance and gene expression in the intertidal brown seaweed *Fucus serratus*" was written only by myself and without the assistance from third parties. Additionally, I conform that no other sources than those indicated as such, were used. This thesis, in same or similar form, has not been proposed to any other faculty or institution.

Bremerhaven, 31 August 2011   _____

                                                                    Anique Stecher

Abstract

Marine macroalgae are important components of coastal ecosystems, providing food and habitat for numerous species. Since the atmospheric CO_2 concentration increases, the CO_2 concentration of the upper surface layers of the global oceans increases as well, causing an alteration of the seawater chemistry. This shift can affect marine macroalgae which depend on carbon to efficiently run photosynthesis. Thus, the performance of marine macroalgae might be influenced by ocean acidification with as yet unpredictable consequences for the entire ecosystem. Intertidal macroalgae are not only affected by enhanced atmospheric CO_2 concentrations but also by severe alterations in their abiotic environment due to the diurnal tidal cycle (e.g. tidal emergence). This study aimed to provide the first data on the combined effects of enhanced CO_2 and tidal emergence on the physiological performance and the expression of specific enzymes involved in carbon fixation in the common intertidal brown macroalga *Fucus serratus*. Furthermore, the applicability of molecular tools for this macroalgal species should be tested. *F. serratus* was cultured for two weeks at two different CO_2 concentrations (280 and 1200 ppm) and two different tidal regimes (regular emergence and permanent submersion). Physiological traits were unaffected by enhanced CO_2 concentrations and tidal emergence. Photosynthesis, growth and chlorophyll *a* content remained constant in each of the tested treatments. The insensitivity of physiological traits might be the result of an actively running carbon concentrating mechanism (CCM). By this CCM, photosynthesis of *F. serratus* is already carbon saturated at present CO_2 concentrations. Gene expression analysis was performed by a quantitative real-time polymerase chain reaction (qRT-PCR), investigating the expression of genes encoding for carbonic anhydrase (CA), ribulose-1,5-bisphosphate carboxylase oxygenase (RubisCO) and phosphoenolpyruvate carboxykinase (PEPCK). Enhanced CO_2 and tidal emergence did not affect the expression of the tested genes. The combination of both parameters led, however, to an up-regulation of all tested genes. Gene expression was unaffected by either CO_2 or desiccation what might be due to the activity of the CCM. The up-regulation of the genes under the combined influence of the two factors cannot be explained by the present study. However, this study proved that (1) molecular tools are applicable to *F. serratus* and (2) that the two tested abiotic parameters interact, leading to a change in the transcriptional abundance of the tested enzymes. Although gene expression was affected by the interaction of the abiotic parameters, physiological traits remained unchanged, indicating that *F. serratus* is well adapted to its abiotic environments by a dynamical reaction without a change in fitness. The present study did not investigate enzyme activity and content. Future investigations should consider proteomic analysis to explain the effects of changing environments and different abiotic stresses in a more comprehensive way.

Zusammenfassung

Marine Makrolagen sind wichtige Bestandteile von Küstenökosystemen, indem sie Nahrung und Habitat für zahlreiche verschiedene Arten zur Verfügung stellen. Der Anstieg der atmosphärischen CO_2 Konzentration führt zu einem gleichzeitigen Anstieg der CO_2 Konzentration im Oberflächenwasser der Ozeane. Dadurch kommt es zu einer Veränderung der Karbonatchemie der Meere, welche die Photosynthese und das Wachstum mariner Makrolagen und dadurch auch komplette Ökosysteme beeinflussen könnte. Algen des Gezeitenbereichs sind jedoch nicht nur den erhöhten CO_2 Konzentration ausgesetzt, sondern auch der Veränderung ihres abiotischen Lebensraumes durch den täglichen Gezeitenwechsel. Faktoren wie Trockenfallen und Austrocknung können Gezeitenalgen stark beeinflussen. Die vorliegende Arbeit stellt die erste Untersuchung dar, in der die kombinierten Effekte erhöhter CO_2 Konzentrationen und Gezeitensimulation auf die physiologische Leistung und gleichzeitig auf die Expression verschiedener Gene der Kohlenstofffixierung in der braunen Gezeitenalge *Fucus serratus* untersucht werden. Gleichzeitig soll mit dieser Studie untersucht werden, ob molekulargenetische Methoden für diese spezielle Braunalge anwendbar sind. *F. serratus* wurde über zwei Wochen unter verschiedenen CO_2 Konzentrationen (280 und 1200 ppm) und verschiedenen Gezeitenregimen (regelmäßiges Trockenfallen und kein Trockenfallen) kultiviert. Physiologische Parameter wurden weder von erhöhten CO_2 Konzentrationen noch von Gezeiten beeinflusst. Die Photosyntheserate, das Wachstum und der Chlorophyll *a*-Gehalt der Alge blieben unverändert. Diese Unempfindlichkeit physiologischer Parameter kann auf einen aktiven Kohlenstoffkonzentrierungsmechanismus (CCM) zurückgeführt werden. Durch den CCM ist die Photosynthese unter derzeitigen CO_2 Konzentrationen bereits gesättigt, was weder einen Anstieg noch eine Abnahme physiologischer Parameter zur Folge hatte. Die Expressionsanalysen wurden mittels einer quantitativen Echtzeit Polymerasen Kettenreaktion (qRT-PCR) durchgeführt, mit welcher die Expression der Gene untersucht wurde, die für die Carboanhydrase (CA), Ribulose-1,5-bisphosphat Carboxylase Oxygenase und Phosphoenolpyruvate Carboxykinase (PEPCK) kodieren. Weder die CO_2 Konzentration noch der Gezeiteneffekt hat die Genexpression der getesteten Gene beeinflusst. Der kombinierte Effekt der beiden abiotischen Faktoren führte jedoch zu einer Hochregulation aller getesteten Gene. Die Genexpression unter dem Einfluss der einzelnen Faktoren könnte aufgrund des aktiven CCM unbeeinflusst gewesen sein. Die Hochregulierung der Gene durch die Interaktion der abiotischen Faktoren konnte allerdings mittels der vorliegenden Arbeit nicht erklärt werden. Dennoch bestätigt diese Arbeit, dass (1) molekulargenetische Methoden auf *F. serratus* anwendbar sind und (2) dass die beiden getesteten Faktoren interagieren, was zu einer Veränderung der Transkriptabundanz führt. Obwohl die

Genexpression der getesteten Enzyme durch die Interaktion der Faktoren beeinflusst wurde, wurden die physiologischen Parameter dadurch nicht beeinflusst. Diese Beobachtung deutet darauf hin, dass *F. serratus* gut an die abiotischen Faktoren seines Lebensraums angepasst ist und die Fitness nicht beeinflusst wird, obwohl auf molekulargenetischer Ebene Änderungen stattfinden. In der vorliegenden Arbeit wurde weder die Enzymaktivität noch die Enzymmenge bestimmt. Zukünftige Studien sollten Proteinanalysen integrieren, um die Effekte eines sich ändernden Lebensraums und abiotische Stressoren ganzheitlich untersuchen zu können.

List of abbreviations

µmol:	Micro mole
A:	Absorption
A:	Adenosine
ADP:	Adenosine diphosphate
ANOVA:	Analysis of variance
ATP:	Adenosine triphosphate
BLAST:	Basic Local Alignment Search Tool
bp:	Base pairs
CA:	Carbonic anhydrase
cDNA.	Complementary desoxyribonucleic acid
Chl *a*:	Chlorophyll *a*
CO_2:	Carbon dioxide
cO_2:	Oxygen concentration
CO_3^{2-}:	Carbonate ions
C_t:	Cycle threshold
ddNTP:	Dideoxynucleotide triphosphates
DNA:	Desoxyribonucleic acid
dNTP:	Deoxynucleotide triphosphates
E. coli:	*Escherichia coli*
e.m.f:	Electromotive force
EST:	Expressed sequence tags
EtOH:	Ethanol
GOGAT:	Glutamine oxoglutarate aminotransferase
GOI:	Gene of interest
h:	Hours
H^+:	Hydrogen ions
HCO_3^-:	Bicarbonate
LB:	Luria-Bertani medium
MA:	Major allergen
mRNA:	Messenger ribonucleic acid

NSP:	Nitrile specifier protein
OAA:	Oxaloacetic acid
PAR:	Photosynthetically active radiation
PCR:	Polymerase chain reaction
PEP:	Phosphoenolpyruvate
PEPC:	Phosphoenolpyruvate carboxylase
PEPCK:	Phosphoenolpyruvate carboxykinase
ppm:	Parts per million
qRT-PCR:	Quantitative real-time polymerase chain reaction
rcf:	Relative centrifugal force
RNA:	Ribonucleic acid
rpm:	Rounds per minute
rRNA:	Ribosomal ribonucleic acid
RubisCO:	Ribulose-1,5-bisphosphate carboxylase oxygenase
S.O.C.:	Super Optimal Broth
SGR:	Specific growth rate
T:	Thymine
UTR:	Untranslated region
UV:	Ultra violet
WW:	Wet weight

List of figures

(ddNTPs, black quadrates) will be size determined within a (b) gel electrophoresis. Due to the fluorescent characteristics of the ddNTPs, a fluorescence detector can detect these nucleotides and a (c) chromatogram can be produced. A specific software will back translate the sequence of the chromatogram into the (d) target sequence.

Fig. 10:   Schematic graphic showing the position of the two different primer types used for quantitative real-time polymerase chain reaction (qRT-PCR) approach. Outer primers will be used within a PCR reaction to produce larger sequences used for a standard curve for the qRT-PCR (indicated as yellow boxes). Smaller and inner primers will be used to quantify the gene expression of specific enzymes integrated into carbon fixation of *Fucus serratus* within the qRT-PCR (different coloured boxes). A) One outer primer pair (yellow) and two distinct inner primer pairs (blue) used for sequences reassembled from expressed sequence tags (ESTs). B) If sequences were too long, they were split (dashed line) into two distinct sequences with each one outer primer pair (yellow) and one inner primer pair (orange). Arrows indicate the length of the PCR and qRT-PCR products.

Fig. 11:   Growth of apical tips of *Fucus serratus* cultured at a combination of two CO_2 concentrations (280 and 1200 ppm) and two tidal regimes (tidal emersion and permanent submersion) over a period of 14 days. Symbols give mean biomass [g_{WW}] of the three to four algal tips per 2L beaker for all replicates ± standard deviation (n = 5).

Fig. 12:   Specific growth rate (SGR) [% d^{-1}] of apical tips of *Fucus serratus* cultured at two different CO_2 concentrations (280 and 1200 ppm) and two tidal regimes (tidal emergence and permanent submersion). The SGR was calculated over an experimental period of 14 days. Bars give mean values ± standard deviation (n = 5).

Fig. 13:   Dark respiration as oxygen consumption [$\mu mol\ O_2\ h^{-1}\ g_{WW}^{-1}$] of apical tips of *Fucus serratus* cultured at two different CO_2 concentrations (280 and 1200 ppm) and two different tidal regimes (with and without the simulation of tides). Bars give means ± standard deviation (n = 4 - 5).

Fig. 14:   Gross photosynthetic activity as oxygen production [$\mu mol\ O_2\ h^{-1}\ g_{WW}^{-1}$] of apical tips of *Fucus serratus* cultured at two different CO_2 concentrations (280 and 1200 ppm) and two different tidal regimes (with and without the simulation of tides). Bars give means ± standard deviation (n = 5).

Fig. 15:   Net photosynthetic activity as oxygen production [$\mu mol\ O_2\ h^{-1}\ g_{WW}^{-1}$] of apical tips of *Fucus serratus* cultured at two different CO_2 concentrations (280 and 1200 ppm) and two different tidal regimes (with and without the simulation of tides). Bars give means ± standard deviation (n = 5).

further analysis. DNA ladder: peqGOLD ladder-mix (0.5 mg DNA/ µl; PeqLab, Erlangen, Germany).

Fig. 24:   PCR products amplified by specific designed primers to obtain large sequence used within the standard curve of the quantitative real-time PCR (a = CA1, b = CA2, c = RubisCO). DNA ladder: peqGOLD ladder-mix (0.5 mg DNA/ µl; PeqLab, Erlangen, Germany).

List of tables

1. Introduction

1.1 Increasing atmospheric CO_2 concentrations and ocean acidification

Since the beginning of the 18th century and the accompanied industrialization, man-made carbon-dioxide (CO_2) emissions are increasing drastically. Burning of fossil fuels and deforestation cause large quantities of CO_2 to enter the atmosphere (Sabine et al. 2004). From 1970 to 2004 the annual CO_2 emission grew from 21 to 38 gigatonnes (Gt) and the annual growth increment during the last decade was even greater than during the previous decade (IPCC 2007). The continuous emissions caused the atmospheric CO_2 concentration to increase from pre-industrial 280 ppm (parts per million) to recently ~ 380 ppm CO_2. The Intergovernmental Panel on Climate Change (IPCC 2007) predicted that the atmospheric CO_2 concentration will increase to ~ 750 ppm by the end of this century (IPCC scenario IS92a). Based on different assumptions and model calculations the atmospheric CO_2 concentration could even rise to more than 1000 ppm by the end of this century. The rate of the current and the predicted increase is about 100 times higher than any increase that occurred over the past 650.000 years (The Royal Society 2005). These changes in the atmospheric CO_2 concentration will also alter the oceanic CO_2 concentrations. The oceans cover 70% of the earth's surface and, therefore, possess a large potential to absorb large amounts of the atmospheric CO_2. Over the past 200 years, the oceans and the terrestrial biosphere took up together nearly half of the total anthropogenic CO_2 emissions (The Royal Society 2005). Due to the rapid air-sea gas exchange the CO_2 concentration of the upper-surface water layers of the global oceans rises along with the atmospheric CO_2 concentration (Wolf-Gladrow et al. 1999). When CO_2 dissolves in seawater it reacts with water to form carbonic acid (H_2CO_3), which dissociates to bicarbonate (HCO_3^-) and hydrogen ions (H^+), which in turn can form additional HCO_3^- when reacting with carbonate (CO_3^{2-}):

$$CO_2 + H_2O \rightarrow H_2CO_3$$
$$H_2CO_3 \rightarrow H^+ + HCO_3^-$$
$$H^+ + CO_3^{2-} \rightarrow HCO_3^-$$
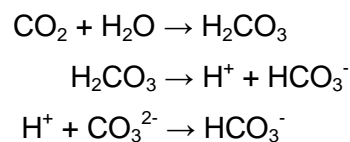
These chemical reactions allow the global oceans to take up large amounts of atmospheric CO_2 and store it in other carbon sources (Pörtner 2008; Rost et al. 2008; The Royal Society 2005; Wolf-Gladrow et al. 1999). Most of the dissolved inorganic carbon (DIC) in the water column is present as HCO_3^- (~ 90%) and CO_3^{2-} (~ 9%). Less than 1 % of the total DIC is made up of CO_2 (and very small amounts of H_2CO_3) (Wolf-Gladrow et al. 1999). If more CO_2 is taken up by the surface layers of the oceans, more DIC will be available and the chemical

balance will shift towards higher CO_2 and HCO_3^- concentrations, whereas the amount of CO_3^{2-} and H^+ will decrease, causing a shift in the seawater chemistry (Fig. 1).
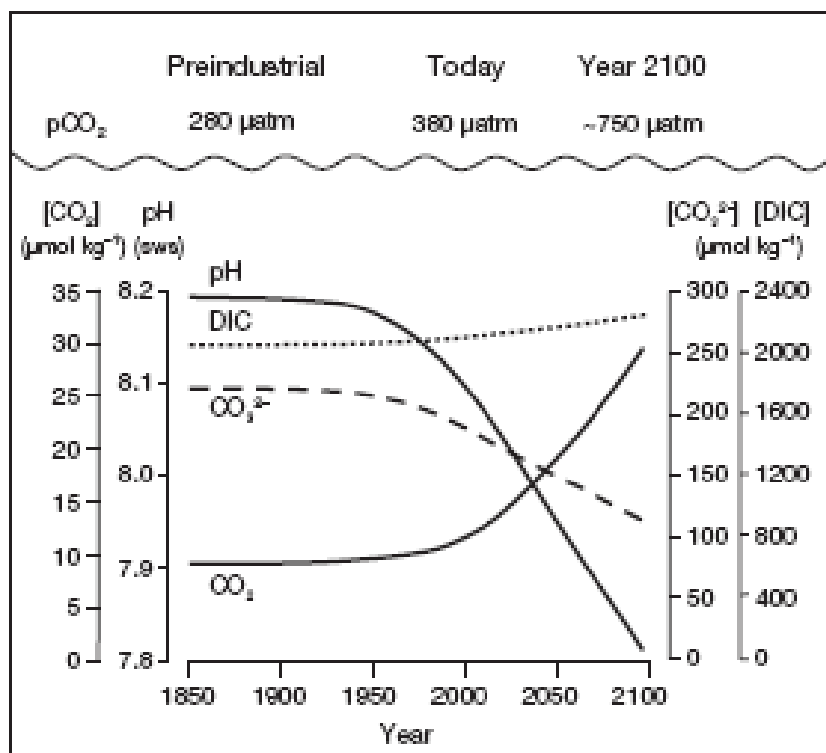
Fig. 1: Predicted changes of the carbonate chemistry of the upper surface layers of the global oceans caused by rising atmospheric CO_2 concentrations assumed by the IS92a Scenario of the Intergovernmental Panel on Climate Change (modified after Wolf-Gladrow et al. 1999 in Rost et al. 2008).

The higher amount of H^+ in the upper surface layers of global oceans will lower the seawater pH. The global ocean pH has already decreased by about 0.1 pH units since 1800 (Wolf-Gladrow et al. 1999). Different emission scenarios predict the global pH to decrease by about 0.3 – 0.5 pH units by the end of this century (Caldeira and Wickett 2005). This drop in the pH of the slightly alkaline surface waters (pH of 8.2) is termed ocean acidification. The intense shift in the seawater chemistry of the ocean surface waters is probably unique for the period of the last 20 million years (Feely et al. 2004). An alteration of the oceans carbon balance might have substantial effects on marine organisms.

Especially, marine calcifying organisms such as reef building corals (Kleypas et al. 2006; The Royal Society 2005), coccolithophorids (Delille et al. 2005; Sciandra et al. 2003), mollusks (Gazeau et al. 2007; Kurihara et al. 2007) and coralline algae (Kleypas et al. 2006) are sensitive to changes in the carbonate chemistry and will be particularly affected by ocean acidification. Enhanced CO_2 concentration in the surface waters will decrease the availability of CO_3^{2-} and lowers the saturation state for major shell-forming minerals like aragonite and

calcite (Kleypas et al. 2006). Furthermore, this alteration of the saturation state might cause the dissolution of biogenic carbonate and thus of shells and calcareous material (Kleypas et al. 2006; The Royal Society 2005).

1.2 The effect of ocean acidification on marine macroalgae – state of the art

Marine macroalgae depend on inorganic carbon as a substrate for photosynthesis. For submerged algae, inorganic carbon for photosynthesis is available for marine macroalgae from two sources: HCO_3^- and CO_2. The only inorganic carbon species that can be used by the primary carbon fixation enzyme ribulose-1,5-bisphosphate carboxylase oxygenase (RubisCO) in photosynthetic carbon fixation (Calvin cycle) is CO_2 (Cooper et al. 1969). Since the concentration of CO_2 in the water column is low (12 µmol kg^{-1}), photosynthesis of marine macroalgae would be limited if it exclusively depended on exogenous CO_2 (Larsson and Axelsson 1999), because the half saturation concentration for CO_2 of RubisCO is 20 – 70 µmol l^{-1} (Badger et al. 1998).Together with the slow, uncatalyzed conversion from HCO_3^- to CO_2 (Wolf-Gladrow and Riebesell 1997) and the slow diffusion of CO_2 in water (Israel and Hophy 2002), these circumstances might have favored the evolution of a carbon concentrating mechanism (CCM) in several algal species to overcome these limiting conditions. Many macroalgae have evolved a CCM that allows for an efficient photosynthesis (Wu et al. 2008) by the additional use of HCO_3^- as a carbon source (Giordano et al. 2005). HCO_3^- is 160 times more abundant in seawater than CO_2 (Larsson and Axelsson 1999). The enzyme external carbonic anhydrase (CA) dehydrates extracellular HCO_3^- to CO_2 which in turn can diffuse into the algal thallus (Badger et al. 1998; Zou 2005). The absorbed CO_2 will then be accumulated or concentrated at the active site of RubisCO (Thoms et al. 2001). Thus, the carboxylation efficiency of RubisCO is enhanced by an active CCM. Another effect of this CO_2 concentration is the depression of photorespiration by enhanced CO_2 concentrations which in turn causes an enhancement of the carboxylation activity of RubisCO by a depressed oxygenase activity (Giordano et al. 2005). Therefore, marine seaweeds are able to efficiently run photosynthesis and grow although the seawater CO_2 concentration is low (Thoms et al. 2001). Due to this concentration process, photosynthesis of many marine macroalgae is already carbon saturated at present CO_2 concentrations (Mercado et al. 1998). Nevertheless, ocean acidification can have diverse and heterogeneous effects on marine macroalgae. *Gracilaria* sp. (Andría et al. 2001), *Cladophora vagabunda* (Rivers and Peckol 1995) and *Porphyra yezoensis* (Gao et al. 1991) increased their photosynthetic activity and growth rate when cultured at enhanced CO_2 concentrations. Photosynthesis of these macroalgae appears to be unsaturated at present CO_2

concentrations leading to a stimulation of photosynthesis and growth by enhanced CO_2 concentrations. Contrarily, growth and photosynthesis of *Gracilaria tenuistipitata* (García-Sánchez et al. 1994) and *Porphyra leucosticta* (Mercado et al. 1999) decreased as CO_2 concentration increased. García-Sánchez et al. (1994) found a higher concentration of carbohydrates and a decreased CA activity and amount of RubisCO. Several authors state that carbohydrates can inhibit the expression of genes involved in photosynthesis, thus leading to a depression of photosynthesis (Mercado et al. 1999; Van Oosten and Besford 1996; Webber et al. 1994). Another common phenomenon in macroalgae which have been grown under elevated CO_2 concentrations is a non-photosynthetic growth enhancement. Growth of several macroalgae such as *Hizikia fusiforme* (Zou 2005), *Ulva rigida* (Gordillo et al. 2001), *Porphyra leucosticta* (Mercado et al. 1999) and *Gracilaria lemaneiformis* (Xu et al. 2010) was enhanced by elevated CO_2 concentrations although photosynthesis was already saturated at ambient CO_2 concentrations. High CO_2 may enhance the uptake of nitrogen and the activity of the nitrate reductase. Thus, nitrogen accumulation is stimulated which can enhance growth. Thus, the effects of ocean acidification on marine macroalgae can be very species-specific.

Most studies on the effects of ocean acidification on marine seaweeds were conducted on algae that were permanently submerged. However, marine macroalgae often inhabit the rocky intertidal zone (Lüning 1985) where they experience continuous fluctuations of the abiotic environment due to the diurnal tidal cycle and might thus be affected by severe changes in abiotic factors such as temperature, radiation (Bischof et al. 2006; Wiencke et al. 2007) and desiccation (Davison and Pearson 1996). Photosynthesis of intertidal seaweeds appears to be highly affected by emersion (Davison and Pearson 1996; Zou et al. 2007). During emersion, the only available carbon source for photosynthesis is CO_2. CO_2 diffuses 10.000 times faster in air than in seawater (Zou and Gao 2004). The substantially reduced diffusion layer on top of the algal thallus increases the uptake of CO_2 (Ji and Tanaka 2002) and allows intertidal algae to efficiently drive photosynthesis during emersion. At the beginning of a desiccation event, photosynthesis might be enhanced (Dring and Brown 1982; Zou and Gao 2002). However, as the desiccation event proceeds, photosynthesis decreases. Thus, several authors stated that photosynthesis during emersion is more limited than during submersion (Zou and Gao 2002; Zou et al. 2007). However, if the atmospheric CO_2 concentration increases, this constraint might be overcome. Therefore, marine intertidal seaweeds are expected to benefit particularly from rising atmospheric CO_2 concentrations.

The intertidal zone is a highly productive environment (Tait and Schiel 2010) which is inhabited by a high number of different species (see Lüning 1985). Algae are an important part of intertidal ecosystems, providing food and nursery habitat for various animal species

(Carlsen et al. 2007; Tait and Schiel 2010). Important members of intertidal ecosystems are fucoid brown algae which belong to the order *Fucales* in the division Phaeophyceae. Fucoid brown algae occur in high abundances in rocky intertidal areas (Chapman 1995). Their geographic distribution extends from arctic to tropical regions where the species are always restricted to the intertidal zone (Lüning 1985). Typical and important fucoid species in the German Bight (North Sea) are *Fucus spiralis*, *F. vesiculosus* and *F. serratus* which occupy different areas in the intertidal zone (Lüning 1985). Fucoids are important food sources for many marine herbivores (Chapman 1995). Thus, negative effects of ocean acidification on *Fucus* sp. might thus propagate through the food chain. For this reason, it is crucial to understand how such important species will be affected by changing conditions due to climate change and the accompanied ocean acidification.

So far, relatively high effort has been made to investigate the effects of ocean acidification on marine macroalgae, including several brown algal species (Gao et al. 1999; Israel and Beer 2000; Israel and Hophy 2002; Swanson and Fox 2007; Wu et al. 2008; Zou and Gao 2005), at the ecological or physiological level. However, the effect of ocean acidification on fucoid species is less studies (Johnston and Raven 1990). Some studies investigated the effect of desiccation on *Fucus* sp. (Brinkhuis et al. 1976; Dring and Brown 1982; Kawamitsu and Boyer 1999; Kawamitsu et al. 2000; Quadir et al. 1979) but little attention has been paid on the effects of ocean acidification and other abiotic factors (see Pearson et al. 2001, 2010) on the genetic level of marine macroalgae. Molecular tools will provide information about the transcripts of genes that are present in certain cells, tissues or the complete organism at a certain time (referred to as "transcriptome") (López 2007). By combining genomic tools with physiological measurements, it will be possible to investigate more completely the responses of species to specific stressors. Thus, molecular ecology improves the understanding of complex interactions. Especially transcription profiling gives the opportunity to investigate how a species will respond dynamically to environmental cues, leading to a higher understanding of stress responses (Dupont et al. 2007). Therefore, molecular tools will complement ecological and physiological observations, leading to a more complete understanding of specific mechanisms. Besides studies that aim to reveal the complete genomes of species by sequencing (Cock et al. 2010), studies concerning the effects of ocean acidification in combination with other abiotic factors on macroalgae are missing. As to my knowledge, the only studies which investigated the effect of abiotic parameters (desiccation) on gene expression level in fucoid algae were conducted by Pearson et al. (2001, 2010), indicating the need for incorporating molecular methods into future studies.

1.3 Characterization of *Fucus serratus*

The present study used *Fucus serratus* as a model organism. *F. serratus* is a common brown seaweed of the intertidal zone of N Atlantic rocky shores. Its distribution limits are the arctic White Sea in the North and Northern Portugal in the South, but it will also occur in the Gulf of St. Lawrence and Nova Scotia (Lüning 1985). Within these habitats, it provides food and habitat for several invertebrates and plays a crucial role in intertidal food webs (Chapman 1995). *F. serratus* is characterized by a specific serrated apical morphology (Fig. 2). The apical parts of the thallus represent the meristematic zone and the site where reproductive tissues develop (Kornmann and Sahling 1977). Due to the high abundance of this brown algal species and its crucial role in intertidal ecosystems, it is important to understand how this species might be affected by a changing environment due to ocean acidification.

Fig. 2: *Fucus serratus* during low tide at the rocky intertidal zone of Helgoland.

1.4 Aim of the study

The present study aims to investigate the effects of enhanced CO_2 concentrations and/or tidal emergence on *Fucus serratus* by answering the following questions:

- How will the performance of the intertidal brown seaweed *F. serratus* be affected by enhanced CO_2 concentrations during submersion?
- Will *F. serratus* benefit from increased CO_2 concentrations during emersion?
- Do these abiotic factors affect the expression of specific genes involved in carbon fixation in *F. serratus*?
- If the selected genes will be affected by enhanced CO_2 concentrations and desiccation, how will they be regulated under the described conditions?
- Are molecular tools applicable for the brown macroalga *F. serratus*?

By answering these questions, this study provides the first investigation testing whether physiological parameters and gene expression will be affected by these abiotic factors in *F. serratus.*

2. Materials and methods

2.1 Physiological part

2.1.1 Algal material

Fucus serratus was collected in March 2011 during low tide in the northern rocky intertidal zone of Helgoland (54° 18' 8'' N, 7° 87' 12' E, Fig. 3). Apical parts (4 – 5 cm) of mature *F. serratus* sporophytes were cut off from mature individuals. Only non-fertile and non-furcated apical tips were taken. 6 – 7 apical tips were selected from each randomly chosen individual to have sufficient genetically identical tissue for each analytical procedure (see next section). After collection, the algae were stored at 5°C in darkness until transportation to the laboratory of the Alfred Wegener Institute in Bremerhaven for culturing procedures.

Fig. 3: Sampling area of *Fucus serratus* individuals in the northern rocky intertidal zone of Helgoland during low tide.

2.1.2 Culturing conditions and experimental design

Each algal tip was cut to a total length of 2 cm by a razor blade. The initial wet weight (WW) was determined after gently blotting the algal tips with tissue paper to remove surface water. The initial biomass of the apical algal tips ranged from 0.15 to 0.18 g and did not differ statistically between the treatments (df = 3, F = 0.99, p = 0.42, one-way ANOVA). Four tips of *Fucus serratus* were cultured simultaneously in each of five replicate 2 L glass beakers (Schott Duran, Germany) per treatment filled with sterile filtered (pore size: 0.2 µm) and

pasteurized North Sea water (see Fig. 4 and 5). To avoid excessive growth of epibionts, no nutrients were added to the seawater medium. Instead, the culture medium was exchanged every two days during the experimental duration to avoid depletion of nutrients and accumulation of algal metabolic waste products. After the first week the seawater medium became brownish. From this day onwards, the medium was exchanged every day.

The seawater carbonate chemistry was adjusted to the respective CO_2 concentration by incubating the medium for at least 24 h before each usage. A treatment consisted of a combination of two CO_2 concentrations (280 and 1200 ppm) and one out of two tidal regimes (tidal emergence and permanent submersion) (see Fig. 5). The CO_2 concentration of the seawater medium was adjusted by continuously incubating the seawater medium with CO_2-enriched artificial air (80% nitrogen and 20% oxygen; gas-mixer: HTK Hamburg GmbH, Germany) through air stones. The flow-through rate of the artificial air was regulated by flow-meters (RMA-14-SSV, Dwyer, cc/min Air X 100, Michigan, USA) to ensure an even gas supply of all replicates.
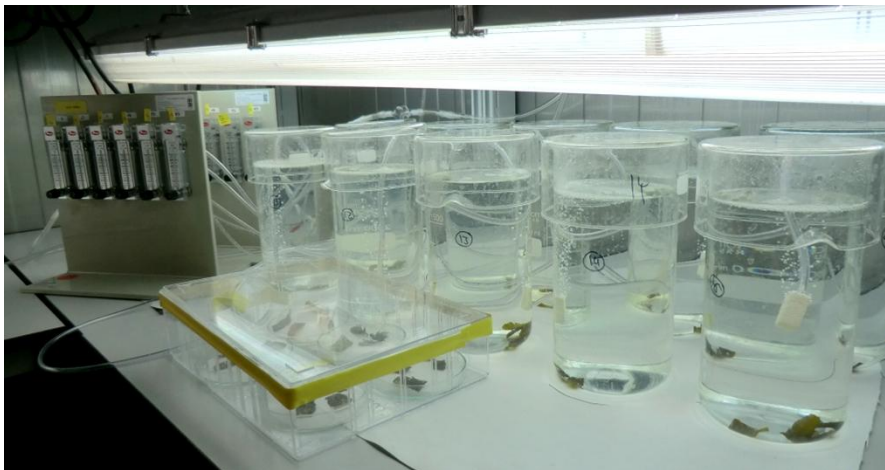
Fig. 4: Experimental set-up for 280 ppm CO_2 within the temperature controlled culture room. In the back, 2 L beakers containing four apical tips of *Fucus serratus* are shown. In front of the beakers, the humid chamber containing the apical tips during tidal emergence is placed. An identical experimental set-up was used for 1200 ppm CO_2.
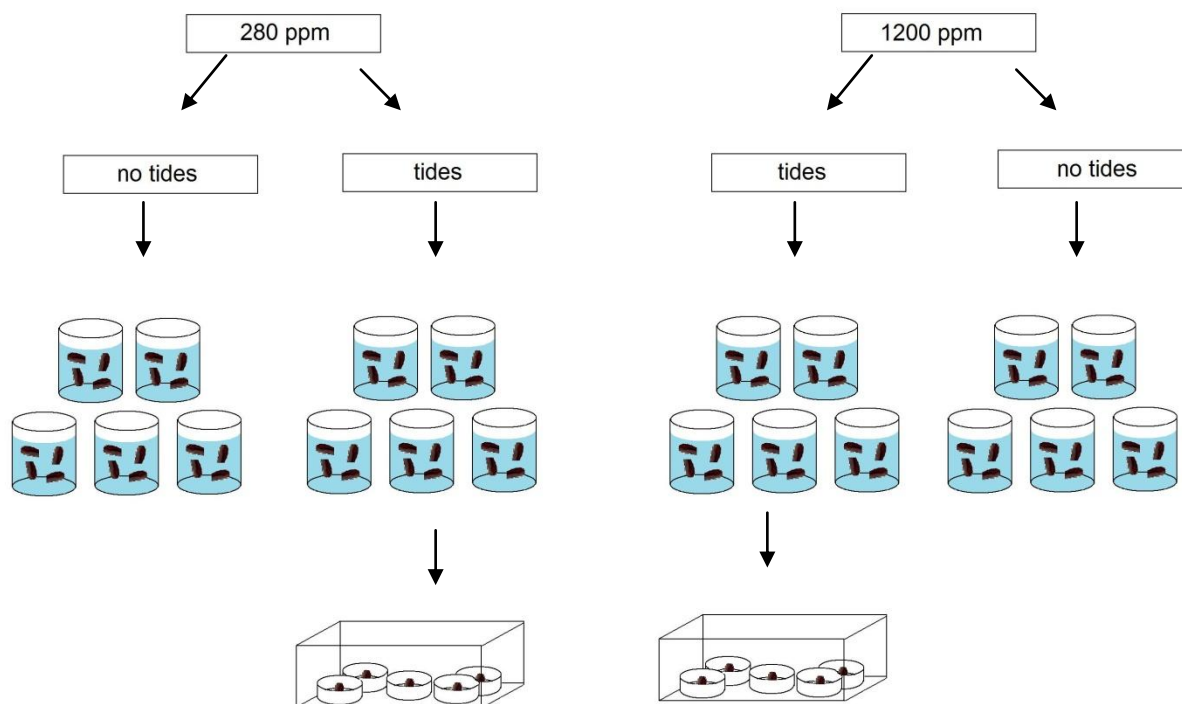
Fig. 5: Schematic experimental design for 5 replicates per treatment. A treatment consisted of a combination of two different CO_2 concentrations (280 and 1200 ppm CO_2) and two tidal regimes (tidal emergence and permanent submersion). For tidal emergence, the apical tips of *Fucus serratus* of the respective treatment were transferred into humid chambers with the respective CO_2 concentration for 3.5 h every day. Four apical tips of *F. serratus* were cultured at these conditions for 14 days

For the simulation of tides, algal pieces of the tidal treatments were transferred to one of two humid chambers for 3.5 h each day (09:30 a.m. – 13:00 p.m. local time). Humid chambers consisted of quadratic plastic boxes (33 x 22 cm) with five distinct Petri dishes (diameter: 10 cm). Each Petri dish was laid out with seawater-moistened filter paper to avoid extensive desiccation of the algal tips during periods of emergence. Filter papers were exchanged every day to avoid excessive bacterial growth that might influence the water chemistry. Each of the two humid chambers was continuously incubated with air of the respective CO_2 concentration and covered with a plastic lid to ensure a stable atmosphere. During tidal emergence of the algal pieces, substitutional algal tips were transferred into the 2 L beakers to ensure similar depletion of nutrients between permanently submersed and regularly emerged treatments. The substitutional algae pieces were cultured under the same conditions as the experimental apical tips.

The experiments were performed over two weeks under a constant temperature of 10 °C ± 2 °C and a photon fluence rate of ~ 100 µmol m^{-2} s^{-1} (± 10 µmol m^{-2} s^{-1}) of photosynthetically active radiation (PAR). These conditions were set to a 16:8 light:dark photoperiod. The high

light intensity was achieved by four daylight fluorescent lamps (OSRAM, 58W/965, Biolux, Munich, Germany) per CO_2 treatment. The first three days were used as acclimatization period for the algae after transferring them from field conditions to laboratory conditions. During this acclimatization, the temperature was set to 5 °C.

2.1.3 Biomass and growth

The biomass of the apical algal tips was measured as WW every three days throughout the entire experiment. Algal tips were removed from the beakers and carefully blotted with tissue paper to remove surface water. Afterwards, the WW was measured by an analytical balance (A 200S, Sartorius analytic GmbH, Göttingen, Germany). Growth of the algae was calculated as specific growth rate (SGR) as percent per day over the entire experimental duration as follows:

$$\text{SGR (\% d}^{-1}) = \frac{100 \ln W_2 W_1^{-1}}{t} \qquad \text{Equation 1}$$

with W_1 = algal WW [g] at the beginning of the experiment

       W_2 = algal WW [g] at the end of the experiment

        t = time interval (d)   (Lüning 1985)

Due to the required cutting of one apical tip per beaker on day 12 to a total length of 1.5 cm for photosynthetic measurements (see next section), the WW of the algae tips on day 14 was calculated as a mean of three of the four apical tips.

2.1.4 Photosynthesis

Apical tips of 1.5 cm length for photosynthetic measurements were cut off the algal pieces two days before the measurement started to allow for wound healing. The pieces were cut after tidal emergence to avoid additional stress for the algae. At the day of measurement, the algae did not experienced tidal emergence. For logistical reasons the measurements had to be extended over two days.

Photosynthetic activity and dark respiration were measured as oxygen production and depletion, respectively. The measurements were done by using a temperature compensated fibre-optics oxygen meter (Microx TX3, PreSens GmbH, Regensburg, Germany) equipped with needle type oxygen microsensors (quartz-quartz glass-fibers of 140 µm outer diameter, PreSens, Regensburg, Germany) (Fig. 6). The Microx TX3 was connected to a computer

with a measuring software (OxyView – TX3 – V6.02). Prior to each measurement the optodes were calibrated on a daily basis with a two-point-calibration in oxygen-free water (0% saturation) and completely oxygen-saturated water-vapoured air (100 % saturation). Oxygen-free water was produced by dissolving 1 g sodium sulfide (Na_2SO_3) in 100 mL water. Completely saturated water vapour was achieved by a moistened piece of cotton wool in a Schott beaker.

After calibration, a blank was measured to correct for potential bacterial oxygen consumption within the incubation chambers. For the measurements, the algal tips were weighed and transferred into incubation chambers (volume of chamber no. 7 = 0.027 L; volume of chamber no. 8 = 0.024 L) filled with seawater of the respective temperature and CO_2 concentration. Prior to each single measurement each incubation chambers received fresh seawater which had been incubated at the respective CO_2 concentration for ~ 24 hours. The algae (average WW = 0.17 ± 0.03 g, n = 20) were placed on a steel grid within the incubation chamber to fix the tissues. The incubation chambers were sealed by an acrylic glass lid. The medium inside the chambers was continuously mixed by an integrated magnetic stirrer. After inserting the micro optode, dark respiration of the algae was measured for 15 minutes after the chamber had been covered with a black plastic lid for 15 minutes. After 15 minutes the plastic lid was removed and oxygen production was measured for another 15 minutes. After each measurement the algae were transferred back to the respective beaker and the chambers were cleaned carefully.

Fig. 6: Experimental set-up for the measurement of photosynthetic activity. Apical tips of *Fucus serratus* were transferred into the white incubation chambers for 30 minutes (15 minutes each for measurement of respiration and gross photosynthesis). During this time, the oxygen consumption and/or production was measured via a needle type oxygen micro sensor (red arrow).

The recorded dataset by the OxyView software was analyzed by plotting the O_2 evolution or depletion [µmol/L] against time. For both, dark respiration and oxygen production, the first 5 minutes of the measurements, when the algae acclimate to the new light condition, were discarded. Accordingly, 10 minutes of dark respiration and gross photosynthesis were used from each measurement. Based on the curve fit equations of the linear regression line, the concentration of O_2 (cO_2) that was either consumed or produced was calculated. The measured values were first calculated as cO_2 per hour:

$$cO_2 \text{ [µmol h}^{-1}\text{]} = cO_2 \text{ [µmol/10 min] * 6} \qquad \text{Equation 2}$$

After that, the volume of the incubation was included into the calculation.

$$cO_2 \text{ [µmol L}^{-1}\text{ h}^{-1}\text{]} = (cO_2 \text{ [µmol/h]/1000)*(chamber volume [L]*1000)} \qquad \text{Equation 3}$$

Finally, the cO_2 was scaled to the individual WW of the algae after the following equation:

$$cO_2 \text{ [µmol h}^{-1}\text{ g}_{WW}^{-1}\text{]} = cO_2 \text{ [µmol/L h]/ WW [g]} \qquad \text{Equation 4}$$

Based on these calculations, the respiration (as oxygen consumption) and the gross photosynthetic activity (as oxygen production) were calculated. The net photosynthetic activity was calculated as the sum of respiration and gross photosynthetic activity. For the 280 ppm CO_2 and tidal emergence treatment, the net photosynthetic activity was only calculated for four replicates due to unrealistic respiration values for one replicate.

2.1.5 Chlorophyll *a* content

The chlorophyll *a* (Chl *a*) content was measured with the same apical algal tips as the photosynthetic activity to be able to correlate these two parameters. Since the photosynthetic measurements were split to two days, the Chl *a* content was measured after the photosynthetic measurements were complete (average WW = 0.18 ± 0.03 g, n = 20). Chl *a* content was determined for a total number of 5 replicates per treatment. Chl *a* pigments were extracted for three days in 5 mL 5% N,N-Dimethylformamide (DMF, K13563853, Darmstadt, Germany) (Inskeep and Bloom 1985) in a light proof test tube at 4°C. During the whole extraction, the samples were kept in darkness to avoid photodegradation of the pigments. To ensure even dissolution of the photopigments, the test tubes were shaken two times a day.

The absorption of Chl *a* was measured spectrophotometrically (U-3310 UV-vis, Hitachi High-Technologies Coopertion, Tokyo, Japan) in a quartz cuvette (Suprasil®, type: 104-Qs, thickness: 10.0 mm, volume: 1400 µl, application area: 200 – 2500 nm, Hellma Analytics,

Müllheim, Germany) at 664.5 nm against a blank of DMF. Each of the 20 replicates was measured in triplicates. The obtained absorption was used to calculate the amount of Chl *a* within each sample as follows:

mg Chl *a* / L = 12.7 · mean absorption from triplicates at 644.5 nm   Equation 5

The dilution factor was considered as:

mg Chl *a* = [mg Chl *a* / L] · 1000^{-1} / volume [mL] of DMF   Equation 6

Afterwards, the result of Equation 6 was divided by the WW [g] of the respective apical tip to calculate the amount of Chl *a* per 1 g WW.

2.1.6 Water chemistry

The carbonate chemistry of the seawater medium was monitored for each replicate beaker twice a week throughout the experiment. For this, the temperature of the seawater medium under experimental conditions was measured with a temperature sensor of a Profi Line conductometer (LF197-S, WTW GmbH, Weilheim, Germany). Subsequently, 250 mL of the medium from each replicate beaker was transferred into 250 mL borosilicate flasks and heated in a water bath (Type N4, Thermo Haake GmbH, Karlsruhe, Germany) to 25 °C. Salinity of subsamples was measured with the Profi Line conductometer and the pH and the electromotive force (e.m.f.) with a seven multi pH meter (Mettler Toledo AG, Schwerzenbach, Switzerland) equipped with an InLab® Routine pH electrode (Mettler Toledo AG, Schwerzenbach, Switzerland). The pH electrode was calibrated (2 point calibration) on the National Bureau of Standards (NBS) scale before each usage (technical buffer. pH 4.01 and 7.00, WTW GmbH, Weilheim, Germany).

To account for the relatively high ionic strength of seawater as compared to the buffer solutions, the pH and the e.m.f. were converted to the total scale by measuring pH and e.m.f. of a Tris buffer solution in synthetic seawater ("Dickson buffer": Batch # 6, bottle # 193, University of California, San Diego, A. Dickson) at 25°C and calculating the pH of the samples on the total pH scale by the following equation:

$$pH\ (X) = \ pH\ (S) + \ \frac{E_S - E_x}{RT \ln 10 \ /F}$$ Equation 7

To calculate the concentration of the different carbon species within the seawater medium it was necessary to determine the total alkalinity of the subsamples. This was done by potentiometric titration of 0.5 M HCl into 25 mL of the seawater subsample using a computer

controlled (Software: TitriSoft 2.6) automated titrating system (TitroLine®alpha plus; equipped with a Schott®Instruments IoLine-MICRO-pH-A-Din ph electrode, SI Analytics GmbH, Mainz, Germany). The total alkalinity was calculated automatically by the titration system. The concentrations of the carbon species were calculated by the MS Excel Macro CO2sys (Lewis and Wallace 1998) with the input parameters being the calculated pH (total scale), the salinity of the subsamples, the temperature of the water bath (25°C), the temperature of the medium inside the beakers in the temperature controlled culture room, and the determined total alkalinity. The constants for the calculation were chosen after Dickson and Millero (1987). The carbonate chemistry remained constant throughout the entire experimental period (Tab. 1).

Tab. 1: Parameters of the seawater chemistry. Water temperature [°C] inside the 2 L beakers in the culture room, salinity [PSU], pH (total scale after Equation 7), total alkalinity (calculated by the software TitriSoft 2.6), calculated pCO_2, and the concentration of the different carbon species (HCO_3^-, CO_3^{2-}, CO_2) of the seawater culture medium from two different CO_2 concentrations (280 and 1200 ppm) and two tidal regimes (tidal emergence and permanent submersion) over an experimental period of 14 days. Presented are the means ($\pm$ SD) (n = 5).

Treatment	Temperature [°C]	Salinity [PSU]	pH (total scale)	Total alkalinity	HCO_3^- [μmol kg^{-1}]	CO_3^{2-} [μmol kg^{-1}]	CO_2 [μmol kg^{-1}]	pCO_2 [ppm]
280 ppm tides	13.0 ($\pm$ 0.2)	31.1 ($\pm$ 0.4)	8.2 ($\pm$ 0.1)	2362.3 ($\pm$ 16.9)	1888.7 ($\pm$ 61.2)	195.5 ($\pm$ 25.4)	11.8 ($\pm$ 2.4)	291.2 ($\pm$ 58.9)
280 ppm no tides	13.3 ($\pm$ 0.1)	31.0 ($\pm$ 0.3)	8.2 ($\pm$ 0.1)	2359.3 ($\pm$ 19.2)	1871.3 ($\pm$ 52.2)	201.5 ($\pm$ 21.7)	11.2 ($\pm$ 2.0)	279.2 ($\pm$ 48.8)
1200 ppm tides	13.0 ($\pm$ 0.1)	31.5 ($\pm$ 0.8)	7.7 ($\pm$ 0.0)	2353.3 ($\pm$ 11.5)	2145.1 ($\pm$ 24.3)	85.6 ($\pm$ 10.8)	34.8 ($\pm$ 5.2)	857.8 ($\pm$ 130.4)
1200 ppm no tides	13.1 ($\pm$ 0.2)	31.5 ($\pm$ 0.8)	7.7 ($\pm$ 0.0)	2348.0 ($\pm$ 9.5)	2155.6 ($\pm$ 19.0)	79.1 ($\pm$ 7.0)	37.7 ($\pm$ 4.0)	935.3 ($\pm$ 102.8)

2.1.7 Statistics

The data were tested for deviation from normal distribution by a Kolmogorov-Smirnov test and for variance homogeneity by a Bartlett's test. If both criteria were fulfilled, the mean values of the response variables were tested for treatment effects and factor interactions by a two factorial analysis of variance (two-way ANOVA) with the parameters being "CO_2" and "tidal regime".

2.2 Molecular part

In this part of the study, the applicability of molecular methods in *Fucus serratus* was investigated. Furthermore, the expression patterns of selected genes of interest (GOIs), that are involved in photorespiration and carbon fixation processes have been investigated under different CO_2 conditions (280 and 1200 ppm) and different tidal regimes (tidal emergence and permanent submersion) in *F. serratus*. The chosen enzymes are listed in Tab. 2.

Tab. 2: Selected genes of interest (GOI). Listed are the names of the enzymes, the EC-number, the pathway in which they are involved (from KEGG), and the function of these enzymes.

Enzyme	EC-number	KEGG Pathway	Function
Phosphoenolpyruvate carboxykinase (PEPCK)	4.1.1.49	• Carbon fixation • Glycolysis	Phosphoenolpyruvate + CO_2 + ADP → oxalacetate + ATP
Ribulose-1,5-bisphosphate carboxynase oxygenase (RubisCO)	4.1.1.39	• Carbon fixation	**Carboxylase activity:** Ribulose-1,5-bisphosphate + CO_2 → 2 x 3 phophoglycerate **Oxygenase activity:** Ribulose-1,5-bisphosphate + O_2 → 3 phophoglycolate
Serine-glyoxylate transaminase	2.6.1.45	• Photorespiration	L-serine + glyoxylate ↔ 3-hydroxypyruvate + glycine
Phosphoglycolat phosphatase	3.1.3.18	• Glyoxylate and dicyrboxylate metabolism Photorespiration	2-phosphoglycolate + H_2O ↔ glycolate + phosphate
Phosphoenolpyruvate carboxylase (PEPC)	4.1.1.31	• Carbon fixation	Phosphoenolpyruvate + HCO_3^- ↔ phosphate + oxaloacetate
Malic enzyme	1.1.1.40	• Carbon fixation	Malate + $NADP^+$ → pyruvate + CO_2 + NADPH + H^+
Glycolat oxidase	1.1.3.15	• Glyoxylate and dicarboxylate metabolism • Photorespiration	Glycolate + O_2 → glyoxylate + H_2O_2
Carbonic anhydrase (CA)	4.2.1.1	• Nitrogen metabolism	Bicarbonate + H^+ ↔ CO_2 + H_2O
NAD^+- dependent glutamate synthase (GOGAT)	1.4.1.13 1.4.1.14	• Alanine, aspartate and glutamate metabolism • Nitrogen metabolism	Glutamine + α-ketoglutarate + NADPH + H^+ → glutamate + $NADP^+$

2.2.1 Primer testing

2.2.1.1 RNA extraction

After culturing, the apical tips of *F. serratus* were immediately cleaned from epibionts with ethanol. Subsequently, the tips were frozen in liquid nitrogen using a freeze clamp and stored at -80°C until further analyses. Frozen algal tips were ground three times in liquid nitrogen with a pre-cooled mortar and pistil and silica sand to receive a very fine algal powder. The powder was transferred into 2.0 mL Eppendorf cups. Care was taken to only fill up the tips of the cups. In previous test isolations of RNA from *F. serratus* it proved to be difficult to extract the RNA with a sufficient yield and low ranges of impurity from larger amounts of algal powder. RNA was extracted by a modified CTAB-extraction protocol after Heinrich (personal communication). 1 mL of extraction buffer (2% CTAB, 1 M NaCl, 100 mM Tris pH 8) and 20 µL 2 M DTT were added and immediately mixed well to prevent degradation of the RNA. The mixture was incubated for 15 minutes at 45°C in a thermomixer (Eppendorf, Hamburg, Germany). Occasional shaking during the incubation period ensured efficient cell lysis and sufficient yield of RNA. One volume of chloroform:isoamylalcohol (24:1) was added and mixed vigorously for 7 minutes. Subsequently, the extraction mixture was centrifuged for 20 minutes at 20°C and 12 000 rcf. During centrifugation, the chloroform denatured the proteins and the isoamylalcohol separated the phases. 750 µl of the aqueous supernatant, which contained the RNA, was transferred into a new 2.0 mL Eppendorf cup and 0.3 volumes of 100% ethanol (EtOH) were added and mixed gently by inverting the tube. A second chloroform extraction followed as described above. 500 µL of the supernatant containing RNA was transferred into a fresh test tube. Total RNA was further extracted with a Qiagen RNeasy® Plant Mini Kit (Qiagen, Hilden, Germany). This was done by following the respective manufactured protocol for RNA extraction including an additional DNase on column digestion (Qiagen, Hilden, Germany). Samples were eluted in 50 µL molecular grade water. Concentration and purity of the extracted RNA in the samples were determined by measuring the absorbance of 1 µL of each sample at 230, 260 and 280 nm with a NanoDrop ND-100 spectrometer (PeqLab, Erlangen, Germany; software: ND-1000, V3.7.0). Nucleic acids have an absorption maximum at 260 nm and proteins at 280 nm, whereas polysaccharides and EtOH have an absorption maximum at 230 nm. The ratios of A_{260}/A_{280} and A_{260}/A_{230} will give the rate of contamination with proteins and polysaccharides, respectively. Ratios below 1.8 would indicate a contamination by proteins or polysaccharides which might interfere with downstreaming molecular techniques. The integrity of the extracted RNA was verified by a RNA Nano Chip Assay with the 2100 Bioanalyzer device (Agilent Technologies, Böblingen, Germany). The RNA Nano chips were loaded with a gel-dye-mixture. 12 of the 13 wells were filled with the respective samples and one well was

loaded with a RNA 6000 ladder. During the measurement, the RNA fragments of each sample were separated by size within the gel matrix by gel electrophoresis. Simultaneously, the RNA intercalated with the fluorescent dye and the fragments were visualized by a gel electrophoresis picture and an electropherogram. The ND-1000 software automatically compared the peaks of the ribosomal RNA (first peak: 18S rRNA, second peak: 28S rRNA) with the RNA ladder and calculated the RNA concentration. Fig. 7a exemplarily shows an electropherogram of a RNA sample that is not degraded. The first peak represents the RNA ladder, the following two peaks are signals from the 18S and 28S rRNA, respectively. In Fig. 7b, an electropherogram of a degraded RNA sample is shown that cannot be used for further analysis.
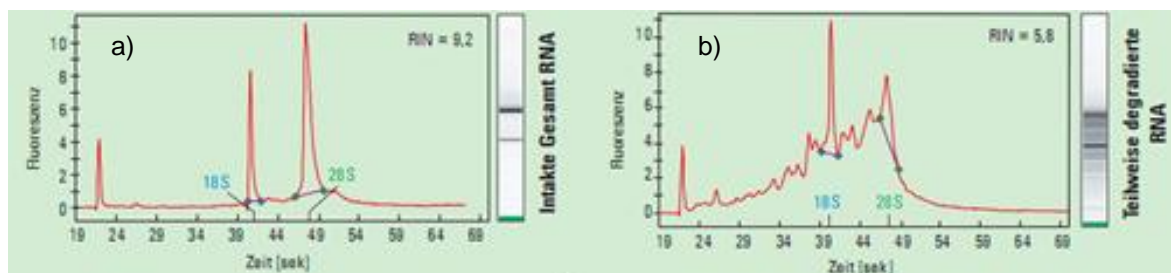
Fig. 7: Example for (a) intact and (b) degraded RNA loaded on a RNA Nano chip assay. Both, the 18S and the 28S rRNA should give two distinct peaks without any interfering peaks. (From: Agilent 2100 Bioanalyzer user´s information guide).

2.2.1.2 Primer design for GOIs

First, oligonucleotide primers had to be designed to amplify the GOIs. Because no species-specific sequences were accessible for the GOIs from *Fucus serratus*, it was necessary to find conserved regions for the respective genes. Thus, the protein sequences of the GOIs were taken from intensively investigated organisms (e.g. *Arabidopsis thaliana)* from the KEGG database (http://www.genome.jp/kegg/). These sequences were used as a target sequences for a Basic Local Alignment Search Tool (BLAST) search against the NCBI database (http://blast.ncbi.nlm.nih.gov/Blast.cgi; protein blast). This search algorithm compares a nucleic acid or amino acid sequence with a database containing already identified genes or proteins (Altschul et al. 1990). A multiple alignment was created with sequences of the same enzyme from differently related organisms (e.g. brown, green, and red algae, but also higher plants like tobacco and rice, or diatoms and cyanobacteria). By aligning sequences from different organisms, conserved regions of the GOIs are more accurate. If a region of a gene is conserved between different taxa, the likelihood that this region will be present in the study organism is higher. For the multiple alignment, only

sequences that had at least an overlap of 50 – 60% and an e-value between lower than e^{-20} – e^{-30} were chosen. At least 5 -6 sequences from different species per enzyme were taken.

The sequences were aligned with the freeware ClustalX (version: 1.81). The multiple alignments were observed manually for highly conserved regions within each protein sequence. These regions were chosen as preliminary primer sequences and should be at least about 6 – 7 amino acid sequences long. When the sequences were not conform between the different species, the sequence of the integrated brown algae *Ectocarpus siliculosus* was chosen due to the degree of relationship between *E. siliculosus* and *Fucus* sp. The amino acid sequences (in single letter code) were retranslated using the standard genetic code with a web-tool to generate degenerated oligonucleotide primers (http://www.vivo.colostate.edu/molkit/rtranslate/index.html

For each GOI, two sequences of the preliminary sequences were chosen. The forward sequence was copied from the web page and the reverse sequence had to be translated complementarily. Both primer sequences needed to be in 5' → 3' direction. The degenerated primers should be long enough to ensure a melting temperature of about 60 °C to ensure appropriate amplifying in a subsequent PCR by the respective *Taq* polymerase. The degenerated primers were synthesized by Eurofin MWG Operon (Ebersberg, Germany) (Tab. 3). The primer sequences for GOGAT were taken from the doctoral thesis of Silja Röttgers (2002), University of Gießen, Germany.

Tab. 3: Primer sequences (forward and reverse) in 5' – 3' direction, amplicon length and melting temperature of designed primers for chosen enzymes.

Gene	Sequence 5' - 3' (forward)	Sequence 5' - 3' (reverse)	Amplicon length	Tm [°C] (F - R)
PEPCK	GGKGGKGAGATGAAGAAGGG	TAKCCKSWKAGGAAGTGGTACAT	579 bp	61.4 - 59.8
RubisCO	TGGACKGTKGTKTGGACKGA	GCYTTGAAKCCGAAKACGTTKCC	405 bp	59.4 - 62.4
Serine-glyoxylate transaminase	ATGCKGAGACKKSKACKGG	CCKATKCKCAKATTTTKCC	630 bp	59.9 - 53.4
Phosphoglycolate phosphatase	GATGGKACKATKGCKGATAC	TTTCGTCKCCKACGTAKATKAC	603 bp	57.3 - 58.4
PEPC	TTKACKGCKCATCCKAGKGA	CKCKGACKCCKCCCATCCA	405 bp	58.3 - 63.1
Malic enzyme	TKGGKCTKGGKGATCAGGG	CCKGCTTCKCCKGCKCC	477 bp	61.0 - 62.4
Glycolate oxidase	GGKKSKGAGGGKACKTGG	AGGTTKCCGTCKCCKGCGTG	627 bp	61.7 - 64.5
Carboic anhydrase	TGTKSKGATKSKKGKATWGATCC	GGCAGTGKSWGAGKCCGCAKAC	198 bp	60.6 - 66.8
GOGAT	CCNCCNCCNCATCATGATTA	CCNCCNGTCATCTATTCGCA		58.3 - 59.4

2.2.1.3 cDNA synthesis from non-treatment algae

Extracted RNA from non-treated *Fucus serratus* taken from the field was used to synthesize single stranded cDNA with the First-Strand cDNA Synthesis SuperScript^{TM} III Reverse Transcriptase kit according to the manufactures protocol (Invitrogen, Darmstadt, Germany). This cDNA was needed to test the performance of the degenerated oligonucleotide primers in subsequent polymerase chain reactions (PCRs). 1000 ng of extracted RNA was mixed with 1 µl oligo dt primer (50 µM) and 1 µl dNTP mix (10 mM each). The solution was filled up with water to a total volume of 13 µl. The mixture was heated to 65°C for 5 minutes and incubated on ice for at least 1 minute. After a brief centrifugation, 4 µl 5x First-Strand buffer, 1 µl DTT (0.1 M), 1 µl RNaseOUT^{TM} Recombinant RNase Inhibitor (40 units/µl) and 1 µl SuperScript^{TM} III Reverse Transcriptase (200 units/µl) were added. The solution was mixed by gently pipetting up and down. Form this step onwards a modification of the manufactured protocol was used in order to obtain a higher yield of full lengths cDNA. The mixture was incubated for 45 minutes at 37 °C and subsequently for 45 minutes at 42 °C. Subsequently, 1 µl of fresh SuperScript^{TM} III RT was added to the mixture. The mixture was then incubated in two steps of 30 minutes each at 50 °C and 55 °C. After the incubation, an additional RNase H (2 U/µl) digestion for 20 minutes at 37 °C followed to remove RNA residues. The synthesized cDNA was purified with the MinElute$^®$ PCR Purification Kit (Qiagen, Hilden, Germany) according to the manufactured protocol. The quantity and purity of the samples were determined spectrophotometrically by measuring the absorption at 230, 260 and 280 nm and the ratio of A_{260}/A_{230} and A_{260}/A_{280} by a NanoDrop ND-1000 (PeqLab, Erlangen, Germany) (for details see 2.1.1.1).

2.2.1.4 Primer testing PCR

Synthesized cDNA of *Fucus serratus* from the field was used to test whether the designed oligonucleotide primers amplified the genes in question (GOIs). Because different oligonucleotide primers present in the mix of degenerate primers had different melting or annealing temperatures, a temperature gradient PCR was performed to test at which temperature the primers worked best. For each primer pair and enzyme, 12 different annealing temperatures were tested. For the PCR, 1 µl template cDNA (2 ng), 0.5 µl of the respective primers (forward and reverse, each), 0.1 µl HotMaster^{TM} *Taq* DNA polymerase (5 U/µl), 0.1 µl dNTP mix (10 mM each) and 1 µl 10x HotMaster^{TM} *Taq* buffer (with 25 mM Mg^{2+}) was mixed and filled up to a final volume of 10 µl. The PCR was performed following the HotMaster^{TM} *Taq* DNA polymerase kit (5 Prime, Hamburg, Germany) protocol for PCR products of 500 – 1000 base pairs (bp) length in a thermo PCR cycler (Mastercycler gradient, Eppendorf, Hamburg, Germany). The first step was an initial denaturation for 2 minutes at

94°C to separate all double stranded fragments that might have formed and to start the reaction, i.e. to initialize the HotMaster[TM] *Taq* DNA polymerase. The second step was a cycled template denaturation for 20 seconds at 94°C. Afterwards, the cycled primer annealing started for 15 seconds at 12 different annealing temperatures (53.0 °C, 53.2 °C, 53.7 °C, 54.6 °C, 55.8 °C, 57.1 °C, 58.4 °C, 59.8 °C, 61.1 °C, 62.2 °C, 63.0 °C, and 63.4 °C) with a deviation of 5°C from the mean annealing temperature of 58°C of the designed primers. The annealing period was followed by a cycled primer extension for 1 minute at 65°C, which represents the optimum temperature of the µl HotMaster[TM] *Taq* DNA polymerase to extent complementary nucleotides to the 3' end of the primer. The last three steps were repeated for 32 times. After 32 cycles, a last extension step was performed for 8 minutes at 65°C. During this period, the polymerase is able to fill potential gaps that might have occurred.

The efficiency of the PCR and the designed primers were tested by performing an agarose gel electrophoresis. A gel electrophoresis is used to separate nucleic acids by size (Mülhardt 2009). An agarose gel has pores that, depending on the applied concentration of agarose within the gel, can have different sizes. The negatively charged ribose-phosphate backbone of nucleic acids will migrate within the gel towards an anode when an electric field is applied. In general, smaller fragments will migrate further while large fragments will be retained in the pores of the agarose at the top of the gel. The speed of migration will depend on the electric field that is supplied. To visualize the nucleic acid fragments, the DNA staining dye ethidium bromide is added to the agarose gel. This dye intercalates into double stranded DNA between the aromatic residues. Ethidium bromide can be excited by ultra violet (UV) light.
4.5 g (1.5%) agarose were heated in 300 mL 1 X TAE buffer in a microwave until the agarose had completely dissolved. After cooling, ethidium bromide (1µl/100 mL buffer) was added into the liquid gel and mixed until the ethidium bromide was evenly distributed. The gel was poured into a gel-system (MWG Biotechnology, Ebersberg, Germany) and four 42 well combs were applied to the gel-system to form the wells for sample application. After cooling and solidifying of the gel, 1X TAE buffer was added until the cooled gel was completely covered and the combs were removed. 5 µl of the PCR-products were mixed with 1 µl 6x loading dye and loaded into the gel. For size determination of the fragments, 5 µl diluted DNA ladder mix (2 µl ladder stock (0.5 mg/ml) + 4 µl H_2O; peqGOLD DNA ladder) was applied to the gel. The gel was run at constant voltage of 140 V (Consort E143 power supply, Sigma-Aldrich[®], Schnelldorf, Germany) for ~ 40 minutes. Afterwards, the gel was analyzed under UV light with a gel documentation system (Vilber Lourmat, Eberhardzell, software: BioCapt).

Most distinct fragments, i.e. fragments that are darker and/or larger, show that oligonucleotide primers worked well at the respective annealing temperature. These annealing temperatures and oligonucleotide primers were chosen for another Hot Start PCR to produce higher concentrated fragments that can be excised out of the gel. The PCR was performed using 1 µl template cDNA (10 ng/µl), 0.25 µl primer (each forward and reverse), 0.1 µl µl HotMaster^{TM} *Taq* DNA polymerase (5 U/µl), 0.1 µl dNTP mix (10 mM each) and 1 µl 10x HotMaster^{TM} *Taq* buffer (with 25 mM Mg^{2+}). The mixture was filled up with water to a final volume of 10 µl. The PCR cycles were set as described above, but with the respective annealing temperature of the chosen enzymes and without a temperature gradient.

Again, the PCR products were analyzed with a 1% (0.7 g) agarose and 70 mL 1 x TAE buffer gel electrophoresis. Due to the fact, that the fragments were to be excised out of the gel for later cloning procedures, the less toxic DNA gel stain SYBR$^®$ Safe was used instead of ethidium bromide. The SYBR$^®$ Safe stained gel was visualized by a transilluminator DR-45M (Clare Chemical research, Göttingen, Germany). By this, it was possible to excise the correct fragments with a scalpel. The same gel was prepared a second time with ethidium bromide to visualize the fragments in this report.

The excised fragments were transferred into pre-weighted test tubes and the weight of the gel fragments was determined. The nucleic acids were extracted from the gel using a MinElute$^®$ Gel Extraction Kit (Qiagen, Hilden, Germany) following the respective manufactured protocol. Quantity and purity of the extracted nucleic acids were determined spectrophotometrically using a NanoDrop ND-1000 (PeqLab, Erlangen, Germany).

2.2.1.5 Cloning

The cloning procedure was performed by using a TOPO TA Cloning$^®$ Kit for Sequencing (Invitrogen, Darmstadt, Germany). The first step consisted of the insertion of the extracted sequences into a vector. This was done by the manufactured protocol for electro competent TOP10 *Escherichia coli* cells. In short, 4 µl of fresh excised PCR product, 1 µl of diluted salt solution (2 µl stock salt solution and 8 µl water) (1.2 M NaCl, 0.06 M MgCl$_2$) and 0.5 µl pCR$^®$ 4-TOPO$^®$ vector was mixed gently and incubated at room temperature for 15 minutes and stored at -20°C until further usage.

The pCR$^®$ 4-TOPO$^®$ vector (Fig. 8) was supplied in a linearized form with single 3' thymidine (T) overhangs. Due to the non-template dependent terminal transferase activity of the *Taq* polymerase during a PCR, the produced PCR products have a single deoxyadenosine (A) overhang at the 3' ends. The vector has bound a topoisomerase I isolated from *Vaccinia* viruses. The topoisomerase I is covalently bound to the vector through a covalent bond between a tyrosyl residue (Tyr-274) of the topoisomerase I and the terminal phosphate of the

linearized vector (Fig. 8b). This phosphotyrosylester "activates" the vector. This bond can be attacked by the 5'OH end of the PCR product and a new phosphodiester between the T and the A of the respective overhangs can be formed. The energy needed for this step is provided by the phosphotyrosylester and therefore, no further ligation step is needed to insert the PCR product into the vector.
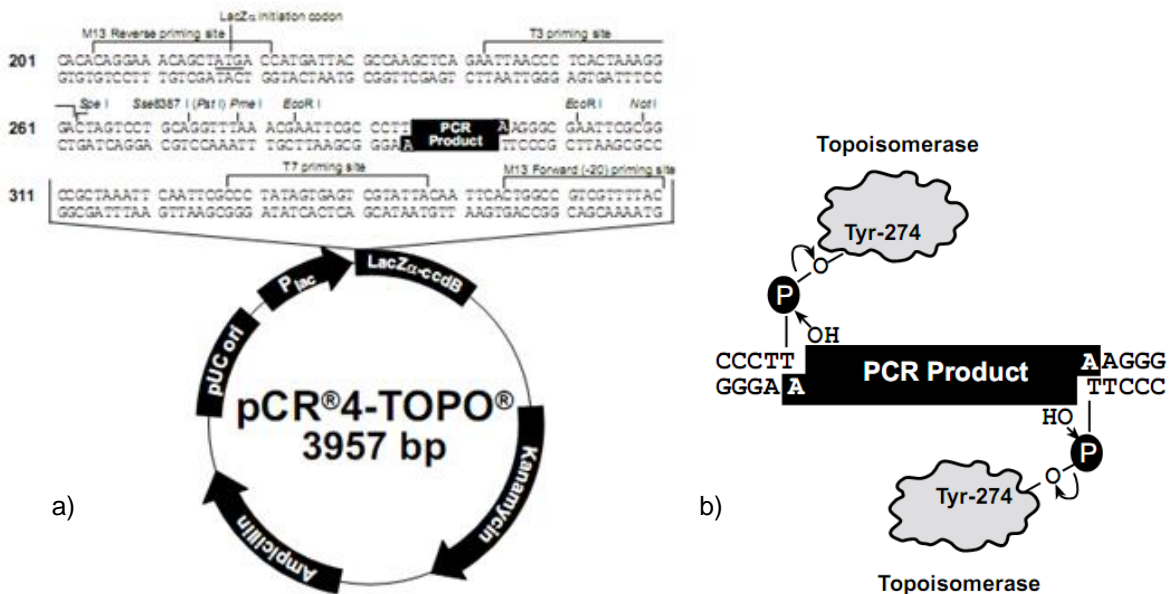
Fig. 8: a) Map of pCR®4-TOPO® vector and its associated features. b) Functionality of the ligation procedure of a PCR product into the linearized vector. By attacking the phosphotyrosylester of the covalently bound topoisomerase I by the hydroxyl lgroup of the PCR product, a new phosphodiester of the T and A overhangs will be formed. Source: TOPO TA Cloning® Kit for Sequencing (Invitrogen, Darmstadt, Germany).

The vector solution was desalted for 10 minutes through microdialysis by pipetting the solution on a membrane filter with 0.025 µm pore size (Millipore™, Billerica, MA, USA) placed on a large well that was filled with deionized water. Due to osmotic forces, the salt diffused through the membrane filter into the deionized water and the sample remained on the membrane filter and could be transferred back into a new test tube. This step is of great importance to avoid arcing during the following electroporation process.

The prepared vector was inserted into electro competent Top10 *E. coli* cells by One Shot ® electroporation using the manufactures protocol of TOPO TA® Cloning Kit for Sequencing (Invitrogen, Darmstadt, Germany). 2 µl of the vector solution was transferred into a vial on One Shot® electro competent *E. coli* and mixed gently. It is crucial not to mix the solution by pipetting up and down to avoid damage of the cells or the vectors. Afterwards, the cell-vector

mixture was transferred carefully into a 0.1 cm cuvette (Electroporation cuvette 0.1 cm gap, Sigma-Aldrich®, Schnelldorf, Germany) to avoid the formation of air bubbles that would cause arcing. The samples were electroporated (Gene Pulser Xcell™, Bio Rad, Hercules, CA, USA) and the following settings were used: voltage: 1800 V, capacitance: 25 µF; resistance: 200 Ω. Immediately after giving the electric pulse, 250 µl of room temperature S.O.C medium (Super Optimal Broth medium with glucose) was transferred into the cuvette and mixed well. The mixture was transferred into a falcon tube and was incubated and shaken for 250 rpm at 37°C in an incubator (Innova 4080 High-Temperature Benchtop Incubator Shaker, New Brunswick Scientific Co., Edison, NJ, USA) for 1 h. This incubation step allowed the expression of the ampicillin resistance gene for the later selection of transformed cells.

After the 1 h incubation, 10 µl of the transformed TOP10 *E. coli* cells were spread on pre-warmed LB (Luria-Bertani medium, see Tab. 16 in appendix for recipe) plates containing 50 µg/mL ampicillin and 40 µl X-Gal. The bacteria cells were allowed to grow within an incubator (Unimax 1010, Heidolph Instruments GmbH, Schwabach, Germany) for at least 24 h and up to 38 h if insufficient growth of the cultures was observed. Clones were selected with toothpicks under a clean bench through "blue-white screening". The "blue-white screening" is based on a special genetic feature of the vector allowing visual determination of clones containing vectors with inserts. Such vectors or plasmids contain a *lacZ* gene which encodes for the enzyme β-galactosidase. This enzyme is able to catalyze the breakdown of lactose that can be used as a food source for the bacteria. β-galactosidase is not only able to use lactose as a substrate, but also the chromogenic X-Gal. By cleaving X-Gal, a blue color will be formed (Sambrook and Russell 2001). The region in which the *lacZ* gene within the TOPO vector occurs will act as multiple cloning site. After a successful ligation, this will cause an interruption of a functional β-galactosidase. Thus, no blue color formation will occur as soon as the *E. coli* cells contain a vector with an insert. Blue colonies will only contain the vector without an insert.

The selected colonies were transferred individually into falcon tubes containing 1.5 mL of liquid LB-medium (see Tab. 16 in Appendix for recipe). The liquid cultures were allowed to incubate at 350 rpm and 37 °C for 22 h until the medium has obviously turned caliginous. Each colony was treated as a replicate of successful cloning procedure.

The cloned *E. coli* cells were collected by centrifugation. Subsequently, the plasmids of the selected colonies were isolated with the QuickLyse Miniprep Kit (Qiagen, Hilden, Germany) following the manufactures protocol. Quantity and purity of the extracted plasmid were determined spectrophotometrically by a NanoDrop ND-100 (PeqLab, Erlangen, Germany). The plasmids were stored on ice until further usage.

The isolated plasmids were amplified by a PCR to identify whether they contain the correct insert or not. For this, 1 µl template DNA (10 ng/µl),1 µl 10x HotMaster^{TM} *Taq* buffer, 0.1 µl dNTP mix (10 mM each), 0.2 µl M13 primer (forward and reverse, Invitrogen, Darmstadt, Germany), 0.2 µl HotMaster^{TM} *Taq* DNA polymerase and 7.3 µl H$_2$O were mixed. The PCR cycle is listed in Tab. 4. The PCR products were loaded on an 1.5% agarose gel (300 mL 1X TAE buffer) to inspect the sizes of the produced fragments.

Tab. 4: PCR program used for a hot start PCR.

Step	Time	Temperature	Cycles
Initial denaturation	2 minutes	94 °C	1 x
Denaturation	1 minute	94 °C	
Annealing	1 minute	55 °C	25 x
Extension	1 minute	72 °C	
Final extension	7 minutes	72 °C	1 x

2.2.1.6 Sequencing of cloned plasmids

Sequence analysis of the cloned plasmids was performed as chain-termination sequencing. This method was established by Sanger et al. 1977 and is also referred to as Sanger sequencing and is used to determine the genetic code of a certain sequence. The basic concept of this sequencing procedure is the controlled production of DNA fragments that terminate at specific points along the target sequence. This is achieved by incorporating fluorescent labeled dideoxynucleotide triphosphates (ddNTPs) into the synthesized DNA sequence by a DNA polymerase during a sequencing PCR. After incorporating ddNTPs, the chain elongation will terminate because ddNTPs do not contain a hydroxyl-group at the 3' end of the ribose (Sanger et al. 1977). Therefore, the polymerase is not able to form new phosphodiester bonds between the nucleotides which will cause the termination of the chain elongation. Within each reaction, all kinds of dNTPs and ddNTPs are present so that different fragments will be formed that differ in size and terminate at different nucleotides (Fig. 9a). Due to the different emission maxima of the different ddNTPs (Smith et al. 1986), the sequencing reaction can be performed within one single reaction.

After the sequencing PCR, the PCR products have to be purified and the DNA fragments will be heat-denatured and separated by size on a gel (Fig. 9b). Due to the fluorescent characteristics of the incorporated ddNTPs they can be detected by a fluorescence detector

(Fig. 9c). The sequence will be read from a produced chromatogram (Fig.9d) and can be used for further analyses.
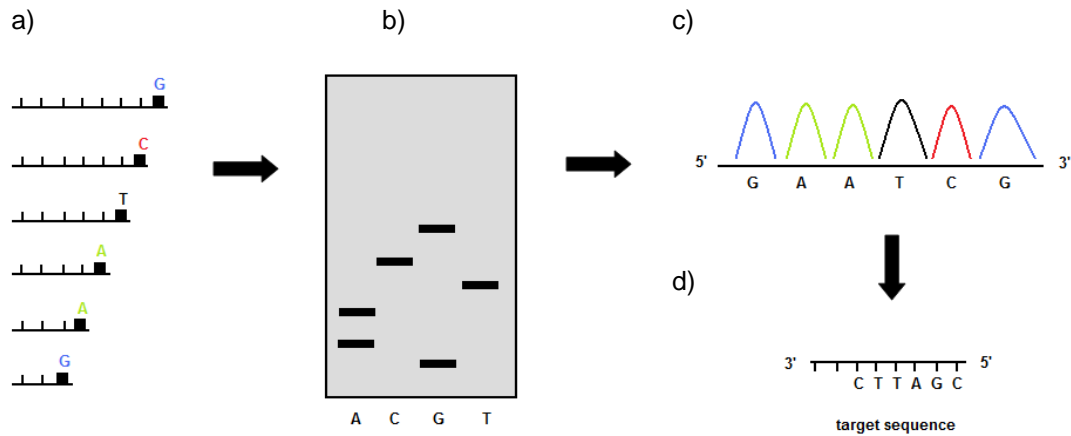
Fig. 9: Schematic overview of the chain termination sequencing method (i.e. Sanger sequencing). (a) DNA fragments produced within a PCR by a DNA polymerase that differ in size and terminate at different fluorescent dideoxynucleotide triphosphates (ddNTPs, black quadrates) will be size determined within a (b) gel electrophoresis. Due to the fluorescent characteristics of the ddNTPs, a fluorescence detector can detect these nucleotides and a (c) chromatogram can be produced. A specific software will back translate the sequence of the chromatogram into the (d) target sequence.

The sequencing reaction was performed using a BigDye® Terminator v3.1 Cycle sequencing kit (Applied Biosystems, Darmstadt, Germany) and the following protocol: 4.5 µl H$_2$O, 1.5 µl 5x sequencing buffer, 1.0 µl Premix BigDye® (including buffer, MgCl$_2$, dNTPs, ddNTPs), 1.0 µl M13 primer (forward or reverse) and 2.0 µl template DNA (10 ng/µl) were mixed. Forward and reverse primers were used to ensure complete sequencing of the entire fragments. The PCR reaction was performed as described in Tab. 5.

Tab. 5: PCR program used for sequencing PCR.

Step	Time	Temperature	Cycles
Initial denaturation	1 minute	96 °C	1 x
Denaturation	10 seconds	96 °C	
Annealing	5 seconds	55 °C	25 x
Extension	4 minutes	60 °C	

The PCR products were purified using the Agencourt® CleanSEQ® kit (Agencourt Bioscience Corporation, USA) according to the manufactures protocol. After purification, 35 µl of the samples were transferred into a MicroAmp® Optical 96-well reaction (Applied Biosystems, Darmstadt, Germany) plate and centrifuged to remove remaining air bubbles from the solution. The optical well-plate was loaded into the sequencer (3130*xl* Genetic Analyzer, ABI Prism, Applied Biosystems, Darmstadt, Germany) equipped with a 16 capillary array. The DNA fragments were separated in a POP 7 polymer (Applied Biosystems, Darmstadt, Germany) with a capillary length of 80 cm to allow the sequencing of sequences up to 1000 bp in size. After the first 16 samples, the remaining 12 samples were amplified using a modification of the PCR protocol. The signals of the first 16 samples were too low so that the determination the correct bases could be insecure. To ensure higher likelihood of determining the correct bases, the concentration of the template sequences was enhanced from 2 µl to 3 µl. Furthermore, only 3.5 µl H_2O was used in this approach.

For the analysis of the sequences, CLC Main Workbench (Muehltal, Germany, version: 6.0.2) was used. With this program it was possible to arrange and assemble the different replicate sequences and integrate them into contigs (assembled transcripts) that agree in most of the nucleotides. The best agreement of the contig-sequences were combined into a consensus sequence which only consisted of the nucleotide sequences of the most overlapping target sequences. This consensus sequence was used for a BLAST search against different databases (e.g. NCBI, swissprot). First, the sequences were used in a nucleotide BLAST (BLASTN) search to determine whether the sequence originate from the organism in question or not. With this search option, it is possible to characterize phylogenetic properties of the sequence in question by searching for similar nucleotide codes. After that, the search options were changed to translated nucleotide BLAST (BLASTX). By this, it was possible to explicitly search for the protein sequence (amino acid sequence) in question. Sequences that had at least an e-value of e^{-8} were expected to be confident and were chosen for further analysis.

2.2.2 Gene expression analysis of GOIs

2.2.2.1 cDNA synthesis of treatment algae

The isolated RNA from different treated algae had to be transcribed into cDNA, because the following quantitative real-time PCR (qRT-PCR) needed cDNA as a template. For analyses of the qRT-PCR, it is necessary to have genes integrated into the sample RNA which act as a reference (see also part 3.2.2 for more details). These are genes from the butterfly *Pieris rapae* ("small cabbage white") which show no sequence similarity to other genes outside of the Lepidoptera (Fischer et al. 2008). The first gene is the major allergen (MA) and the

second is the nitrile specifier protein (NSP) (Freitag et al. 2011). These spike-in genes were integrated into the sample RNA during the cDNA synthesis as mRNA. Previous cDNA syntheses of the non-treatment RNA showed that the amount of cDNA was too low when only oligo dt primers were used. The 3' ends of the RNA contain a poly-A-tail, after which brown algae contain long untranslated regions (3' UTR) (Apt et al. 1995; Pearson et al. 2010). Oligo dt primers will anneal at exactly such poly-A-tails. Since brown algal 3' UTRs are very long, the polymerase will not be able to synthesize the GOIs due to limitation of the amplicon size. This problem can be overcome by using a mixture of oligo dt primers and random hexamer primers. These random primers will anneal at random regions within the RNA, thus, acting as "stepping stones" for the polymerase. The probability that the regions of the RNA sequences, in which the coding region of the genes lay, will by synthesized into cDNA will be higher. Thus, 0.5 µl oligo dt primer, 0.5 µl random hexamer primer, 3 µl MA cRNA (spike-in gene, 1 ng/µl), 3 µl NSP cRNA (spike-in gene, 10 ng/µl), 2 µ 5mM dNTP mix and 7 µl template RNA (700 ng/µl) were mixed. The treatment RNA was diluted individually so that each sample contained 700 ng RNA per µl. This mixture was incubated at 65 °C for 5 minutes and immediately chilled on ice for at least one minute. Then, 6.4 µl of the following master mix was added: 2.4 µl 10x reaction buffer, 1 µl 0.1 M DTT, 1 µl RNase OUT[TM] (40 U/µl), 1 µl Omniscript[TM] reverse transcriptase and 1 µl SuperScript[TM] III Reverse Transcriptase (200 units/µl). The whole suspension was incubated for 1 h at 50 °C, 1 h at 42 °C and afterwards 1 h at 37 °C. At the end, an incubation step of 15 minutes at 75°C followed. The cDNA was aliquoted and stored at -20 °C to avoid damaging processes due to defrosting procedures.

2.2.2.2 Quantitative real-time PCR

qRT-PCR for GOIs of treatments

The qRT-PCR offers the opportunity to visually inspect amplification rates of different genes with unknown concentrations and therefore to quantify expression rates of genes during the amplification process (Pfaffl 2001). To determine the gene expression of GOIs in the different treated samples, primers (forward and reverse) had to be designed to amplify small sequences during the qRT-PCR (see Fig. 10a). These primers were designed using the program Primer Express (version: 2.0, http://www.appliedbiosystems.com) and were synthesized by Eurofins MWG Operon (Ebersberg, Germany). The amplicon sizes of these products were around 150 bp (Tab. 6). Due to the fact that some of the gene sequences provided by Gareth Pearson were assembled from different expressed sequence tags (ESTs) that might overlap in certain areas or were assembled incorrectly, such sequences

were tested by two distinct qRT-PCR primer sets (Fig. 10a). The following protocol for a 10 µl approach of the qRT-PCR was used: 3.8 µl water, 5 µl SYBR® Green power mix, 0.1 µl forward qRT-PCR primer, 0.1 µl reverse qRT-PCR primer, 1 µl template. As a template, cDNA from different treated *Fucus serratus* with an unknown concentration was used. The cDNA was diluted 1:2 with water.

a)

b)

Fig. 10: Schematic graphic showing the position of the two different primer types used for quantitative real-time polymerase chain reaction (qRT-PCR) approach. Outer primers will be used within a PCR reaction to produce larger sequences used for a standard curve for the qRT-PCR (indicated as yellow boxes). Smaller and inner primers will be used to quantify the gene expression of specific enzymes integrated into carbon fixation of *Fucus serratus* within the qRT-PCR (different coloured boxes). A) One outer primer pair (yellow) and two distinct inner primer pairs (blue) used for sequences reassembled from expressed sequence tags (ESTs). B) If sequences were too long, they were split (dashed line) into two distinct sequences with each one outer primer pair (yellow) and one inner primer pair (orange). Arrows indicate the length of the PCR and qRT-PCR products.

The cycles of the qRT-PCR were divided in three different stages. The first stage represented an initial denaturation step at 95 °C for 10 minutes. This step was repeated once. The second step was repeated for 40 times and included a denaturation step for 15 sec at 95 °C and a primer annealing period at 60 °C for 1 minute. The last step was the

production of a melt curve. For this, at 15 minutes denaturation at 95°C, a 10 minutes annealing at 60 °C and a final denaturation for 15 minutes was carried out. The last step of the qRT-PCR was the production of a melt curve for every reaction to ensure that each primer pair just amplified one target gene.

Additionally to the target gene analysis, the spike-in genes (MA and NSP) were amplified in a separate qRT-PCR reaction. This was done by using the qRT-PCR protocol as described above. Primers (forward and reverse) were provided as stock solutions. The spike-in genes function as (1) a normalization of the efficiency of the cDNA synthesis and (2) as reference expression rate, similar to those of housekeeping genes (Freitag et al. 2011). Therefore, it was possible to determine the amplification rate of highly concentrated genes (NSP) and low concentrated genes (MA) that will not be expressed by *Fucus serratus*, because they are not present in this organism.

Tab. 6: Primer sequences (forward and reverse) in 5' – 3' direction, amplicon length and melting temperature of designed primers to produce smaller fragments to detect the gene expression of selected enzymes within the qRT-PCR.

Gene name	Sequence 5' - 3' (forward)	Sequence 5' - 3' (reverse)	Amplicon length	Tm [°C] (F - R)
qRT-PCR				
MA	AAGAGTGGCCAGCACAGTAGACA	AGCTGCCTCCTTGGAAGCATA	100 bp	62.1 - 62.0
NSP	TTGACCACTACCCACGGATGA	ACGATCAATCCAGTATGCAACAA	100 bp	62.1 - 60.2
RubisCO 1	CCTTGCAGTTGATACCGACAAC	AGGCAATCAGTGCCCAATG	150 bp	60.3 - 56.7
RubisCO 2	CGGTATGTCCAGCCGTGTT	GCGCTGCGCGATGTAAG	150 bp	58.8 - 57.6
PEPCK 1	ATGCCGGAAGGCTCGTAGTT	CCGAGATCTACGATGCCATCA	66 bp	59.4 - 59.8
PEPCK 2	ACGGACGTCTCCAAGACAGAGA	GCTCGTAGTTATCGATGTGGTAGATG	150 bp	62.1 - 63.2
CA 1	TCAGTCATCTCGCGCTTGAA	AGCCATGCGTTACTCCCATAA	150 bp	57.3 - 57.9
CA 2	CAGAAGAGCCAGGCACAGAAC	CTGCGACCCAGCGAAGTC	152 bp	61.8 - 60.5

qRT-PCR for standard curves

For each gene expression analyses, it was necessary to perform a standard curve for each distinct primer pair (inner primer pair) that was used during the qRT-PCR of target genes and spike- in genes. By this standard curve it was possible (1) to detect the reaction efficiency of the primers and (2) to detect whether the amplified target genes of the samples have a concentration within the range of the standard curve (Freitag et al. 2011).

First, a set of primers had to be designed to produce larger PCR products of the GOIs during a normal PCR (Fig. 10). The primers were designed by the internet based program Primer 3 (http://frodo.wi.mit.edu/primer3/input.htm, version: 0.4.0) and synthesized by Eurofins MWG Operon (Ebersberg, Germany) (Tab. 7). The target sequences were uploaded and primer

sequences were chosen automatically by the program. It was important to choose primers at the beginning and the end of each gene to have amplicons of about 700 bp. By this, it will be assured that the used inner primers of the qRT-PCR are able to amplify fragments within the PCR products for the standard curve. If sequences were longer, they were split into two individual sequences with respective outer primer pairs (e.g. CA1 and CA2, Tab. 7, Fig. 10b). The amplicons for the standard curve were produced by running a PCR with 1 µl 10x µl HotMaster^{TM} *Taq* Buffer, 0.1 µl 10 mM dNTP mix, 0.2 µl primer (forward and reverse), 0.2 µl Hot Start *Taq* polymerase, 7.3 µl water and 1 µl template cDNA (10 ng/µl). After an initial denaturation for 2 minutes at 94 °C, a second denaturation for 1 minute at 94°C, a 1 minute primer annealing at the respective best mean annealing temperature of the respective designed primers (see Tab. 7) and a 1 minute primer extension at 65 °C followed. This cycle was repeated for 25 times in total. Afterwards, a final primer extension for 7 minutes at 65 °C followed. The PCR products were loaded on a 1% agarose gel containing 1 µl ethidium bromide to control whether they had amplified sequences or not. The remaining PCR products were purified using a MinElute$^{®}$ PCR Purification kit (Qiagen, Hilden, Germany) according to the manufactured protocol. The concentration and the purity of the cleaned PCR products were analyzed spectrophotometrically by a NanoDrop (ND-1000, PeqLab, Erlangen, Germany). It is important to know the exact concentration of the PCR products to perform a standard curve with the PCR products within the qRT-PCR. The PCR products were diluted in 1:10 steps to produce eight different concentrations of the GOIs for a standard curve. The qRT-PCR was performed as described above. A serial dilution of 1:10 with 8 steps of the PCR products was used as templates. The standard curve was performed in triplicates. qRT-PCR primers for MA and NSP were provided as stock solutions

Tab. 7: Primer sequences (forward and reverse) in 5' – 3' direction, amplicon length and melting temperature of designed primers to produce larger fragments used in a standard curve within a quantitative real-time PCT (qRT-PCR).

Gene name	Sequence 5' - 3' (forward)	Sequence 5' - 3' (reverse)	Amplicon length	Tm [°C] (F - R)
PCR products				
RubisCO	CTTCTCGTACATCCCCGGTA	TGCTTGTAGGCGACACACTC	780 bp	59.4 - 59.4
PEPCK (M13)	GTAAAACGACGGCCAG	CAGGAAACAGCTATGAC	712 bp	51.5 - 44.4
CA 1	TTTGAGCAGCAGACCCTTTC	TTTCCAACCCAGCCAGAAG	408 bp	57.3 - 56.7
CA 2	CGTCGTCTGGTTGAGTTGAA	CGTGTTCCGGGTTACTTCTC	237 bp	57.3 - 59.4

qRT-PCR result analysis

The resulting cycle threshold values (C_t values) of the standard curve for each GOI were analyzed using a relative expression software tool (REST 2009, Hilden, Germany; http://rest.gene-quantification.info/). This program calculated the reaction efficiency of the used primers (Tab. 8) from the slope of the best-fit standard curves (n = 3) of each primer set after the following equation 8:

$$E = 10^{-1/slope} - 1$$ Equation 8

The calculated reaction efficiency for each primer pair was further used by the REST software to correct for discrepancies in target gene amplification that could occur due differences in the performance of the primers when different target gene amounts are present (Pfaffl 2001; Pfaffl et al. 2002).

Tab. 8: Reaction efficiency of primers used within the standard curve of the quantitative real-time polymerase chain reaction (qRT-PCR) for different genes (MA = major allergen, PEPCK = Phosphoenol pyruvate carboxykinase, RubisCO = Ribulose-1,5- bisphosphate carboxylase oxidase, CA = carbonic anhydrase). MA will be the reference gene (REF) against which the data of the qRT-PCR will be normalized and the other genes are the target (TRG) genes. Numbers indicate that different primers were used for the same sequence.

Gene	Type	Reaction Efficiency
MA	REF	0.9952
PEPCK1	TRG	0.8813
PEPCK2	TRG	0.8943
RubisCO1	TRG	0.9415
RubisCO2	TRG	0.7876
CA1	TRG	0.8905
CA2	TRG	0.9345

The expression of target genes and the reference gene was calculated by REST 2009 based on the C_t values and the primer efficiencies of the standard curve (Pfaffl et al. 2002). REST 2009 allows comparing gene expression ratios between a control group (untreated) and a sample group (treated). For this, the respective C_t values of the control and the sample group were included into the software. The expression ratios of MA were used as a reference. Relative quantification enables the estimation of the gene expression of target genes but does not provide statistical information to compare the gene expression between control and

sample groups in a proper and robust way. Therefore, REST 2009 simultaneously uses an integrated randomization and bootstrapping method which tests for statistical significance of the calculated expression ratios (see REST 2009 Software User Guide (2009), Qiagen, Hilden, Germany). Unlike standard statistical tests (such as ANOVAs of *t*-tests), randomization tests avoid making distributional assumptions about the data (e.g. normality of distribution). Instead, they are based on the fact that the treatments were randomly allocated. The randomization test reallocates the observed values from the control and the treatment group and notes the expression ratio. If, after e.g. 2000 randomizations, the resulted values are similar to the observed values from the qRT-PCR, the observed effect is created by change and the p-value is > 0.05 (Pfaffl et al. 2002). Thus, this statistical test is a powerful tool that tests the stability of the observed expression ratios even when outliers were included (REST 2009 Software User Guide (2009), Qiagen, Hilden, Germany). Expression ratios >1 represent an up-regulation, whereas expression ratios < 1 indicate a down-regulation of the sample group against the control group.

3. Results

3.1 Physiological part

3.1.1 Biomass and growth

Growth of the apical *Fucus serratus* tips followed an exponential regression model (Fig. 11). The model described 84 – 96 % of the variation of the total biomass (R^2, Tab. 9). Apical tips grown at 280 ppm CO_2 had a slightly higher biomass production than algae tips cultured at 1200 ppm CO_2. *F. serratus* grown at 280 ppm CO_2 without tidal emergence had the highest final biomass of 0.40 (± 0.06 g) which represents a biomass increment of 0.23 (± 0.05 g) in 14 days (Tab. 10). The lowest biomass increment was found in algae grown at 280 ppm CO_2 and regular tidal emergence (0.20 ± 0.03 g). However, the pCO_2, (df = 1, F = 0.01, p = 0.93) and the tidal emergence (df = 1, F = 0.42, p = 0.52) had no statistically significant influence on the final WW of apical *F. serratus* tips. The interaction between the pCO_2 and the tidal regime was statistical insignificant (df = 1, F = 0.27, p = 0.61).
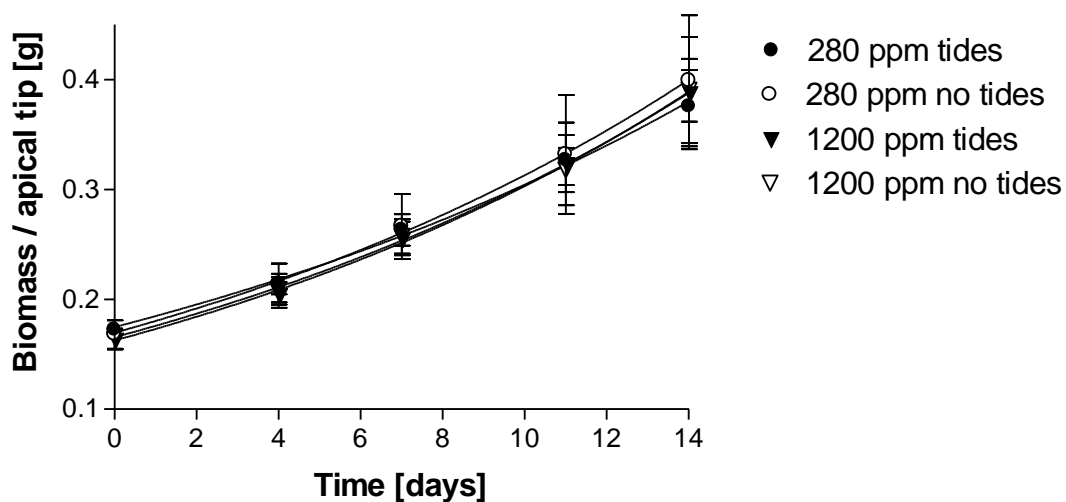
Fig. 11: Growth of apical tips of *Fucus serratus* cultured at a combination of two CO_2 concentrations (280 and 1200 ppm) and two tidal regimes (tidal emersion and permanent submersion) over a period of 14 days. Symbols give mean biomass [g_{WW}] of the three to four algal tips per 2L beaker for all replicates ± standard deviation (n = 5).

Tab. 9: Exponential growth equations and correlation coefficient (R^2) of the best fit model ($N(t) = N_0$ e^{kt}) explaining growth of *Fucus serratus* under two different CO_2 concentrations (280 and 1200 ppm) and two tidal regimes (tidal emergence and permanent submersion) (n = 5).

Treatment		Equation	R^2
280 ppm CO_2	tides	$N(t) = 0.17\ e^{\ 0.06\ \cdot 12.49}$	0.94
	no tides	$N(t) = 0.17\ e^{\ 0.06\ \cdot 11.31}$	0.84
1200 ppm CO_2	tides	$N(t) = 0.16\ e^{\ 0.06\ \cdot 11.13}$	0.90
	no tides	$N(t) = 0.17\ e^{\ 0.06\ \cdot 11.40}$	0.96

Tab. 10: Initial fresh weight (WW) [g] of field-grown apical tips of *Fucus serratus,* SGR [% d^{-1}], final WW [g] and increase of growth [g] of apical tips of *F. serratus* cultured at two different CO_2 concentrations (280 and 1200 ppm) and two different tidal regimes (tidal emergence and permanent submersion). Presented are the means per treatment (± standard deviation) (n = 5).

Treatment		Initial WW [g]	SGR [% d^{-1}]	Final WW [g]	Increase of growth [g]
280 ppm CO_2	tides	0.17 (± 0.00)	5.53 (± 0.54)	0.38 (± 0.03)	0.20 (± 0.03)
	no tides	0.17 (± 0.01)	6.13 (± 0.80)	0.40 (± 0.06)	0.23 (± 0.05)
1200 ppm CO_2	tides	0.16 (± 0.01)	6.14 (± 0.83)	0.39 (± 0.05)	0.22 (± 0.05)
	no tides	0.17 (± 0.01)	6.06 (± 0.33)	0.39 (± 0.03)	0.22 (± 0.02)

The specific growth rate (SGR) of apical algae tips was lowest in algae grown at 280 ppm CO_2 and tidal emergence (5.53 ± 0.54 % d^{-1}) and highest in apical tips cultured at 1200 ppm CO_2 and tidal emergence (6.14 ± 0.83 % d^{-1}) (Fig. 12, Tab. 10). However, these differences were statistically insignificant. The different CO_2 concentrations and the tidal emergence, both showed no effect on the SGR of apical tips of *Fucus serratus* (df = 1, F = 0.84, p = 0.37 and df = 1, F = 0.79, p = 0.39, respectively). Additionally, both factors did not interact (df =1, F = 1.3,1 p = 0.27).
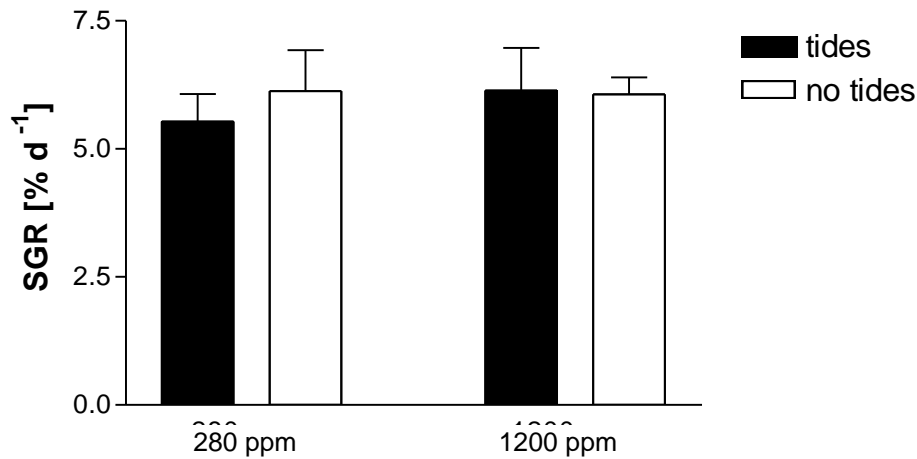
Fig. 12: Specific growth rate (SGR) [% d^{-1}] of apical tips of *Fucus serratus* cultured at two different CO_2 concentrations (280 and 1200 ppm) and two tidal regimes (tidal emergence and permanent submersion). The SGR was calculated over an experimental period of 14 days. Bars give mean values ± standard deviation (n = 5).

3.1.2 Photosynthetic activity

Mean dark respiration of cultured algal tips was highest in apical tips grown at 1200 ppm CO_2 without tidal emergence with -2.78 ± 1.94 µmol O_2 h^{-1} $g_{WW}$$^{-1}$ and lowest in apical tips cultured at 280 ppm CO_2 and tidal emergence with an oxygen consumption of -1.90 ± 1.34 µmol O_2 h^{-1} $g_{WW}$$^{-1}$ (Fig. 13, Tab 14 in appendix). Both factors did not affect the dark respiration of apical tips statistically (pCO_2: df = 1, F = 2.35, p = 0.31; tidal emergence: df = 1, F = 0.14, p = 0.80), neither did both factors interact (df = 1, F = 0.04, p =0.90).
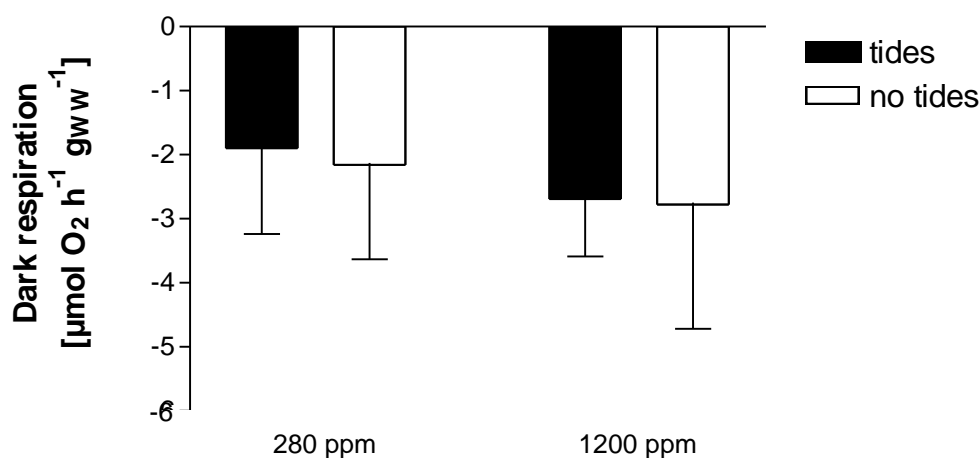
Fig. 13: Dark respiration as oxygen consumption [μmol O_2 h^{-1} g$_{WW}$$^{-1}$] of apical tips of *Fucus serratus* cultured at two different CO_2 concentrations (280 and 1200 ppm) and two different tidal regimes (with and without the simulation of tides). Bars give means ± standard deviation (n = 4 - 5).

Gross photosynthetic activity, i.e. photosynthetic oxygen production, was highest in algae cultured at 280 ppm CO_2 and tidal emergence (24.98 ± 3.83 μmol O_2 h^{-1} g$_{WW}$$^{-1}$) and lowest in apical tips that experienced 280 ppm CO_2 without tidal emergence (23.23 ± 4.96 μmol O_2 h^{-1} g$_{WW}$$^{-1}$) (Fig. 14, Tab. 14 in Appendix). Irrespective of the CO_2 concentration, algal tips cultured with regular desiccation had a slightly higher oxygen production. However, this tidal effect was statistically insignificant (df = 1, F = 0.55, p = 0.47). The CO_2 concentration did not affect the gross photosynthetic activity (df = 1, F = 0.01, p = 0.93). Both factors did not interact (df = 1, F = 0.07, p = 0.80).

Fig. 14: Gross photosynthetic activity as oxygen production [μmol O_2 h^{-1} g$_{WW}$$^{-1}$] of apical tips of *Fucus serratus* cultured at two different CO_2 concentrations (280 and 1200 ppm) and two different tidal regimes (with and without the simulation of tides). Bars give means ± standard deviation (n = 5).
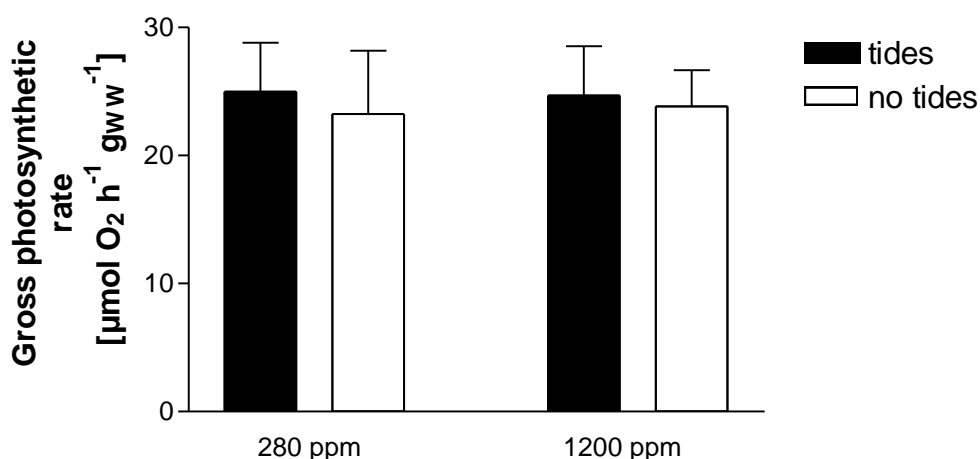
Similar to the gross photosynthetic activity, net photosynthetic activity in algae that experienced tidal emergence was higher, irrespective of the CO_2 concentration, with algae cultured at 1200 ppm CO_2 and tides having an oxygen production of 21.98 ± 3.41 μmol O_2 h^{-1} g$_{WW}$$^{-1}$ (Fig. 15, Tab. 14 in Appendix). Apical tips grown under permanently submersed conditions had almost the same photosynthetic oxygen production at 280 ppm CO_2 (21.07 ± 6.12 μmol O_2 h^{-1} g$_{WW}$$^{-1}$) and 1200 ppm CO_2 (21.05 ± 3.73 μmol O_2 h^{-1} g$_{WW}$$^{-1}$). Again, these differences between the different CO_2 concentrations (df = 1, F = 0.12, p = 0.94) and the two tidal regimes (df = 1, F = 2.89, p = 0.69) were statistically not significant. The two factors did not interact (df = 1, F = 0.1, p = 0.93).
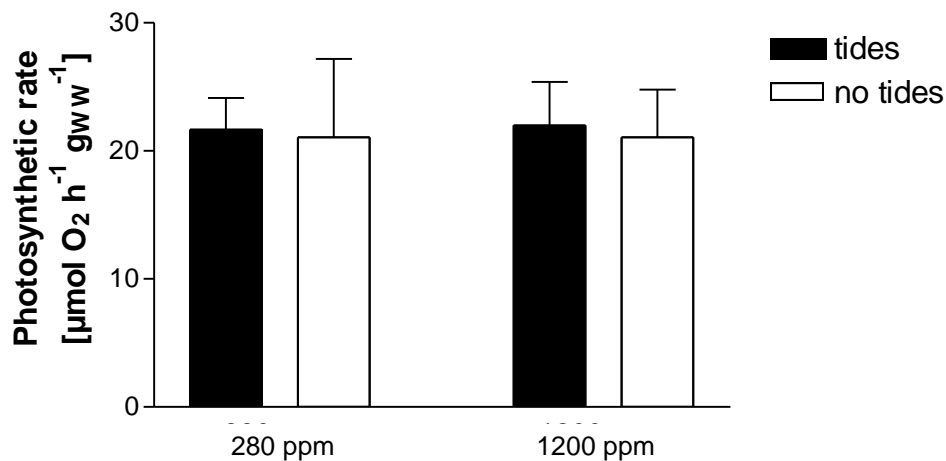
Fig. 15: Net photosynthetic activity as oxygen production [μmol O_2 h^{-1} g_{WW}^{-1}] of apical tips of *Fucus serratus* cultured at two different CO_2 concentrations (280 and 1200 ppm) and two different tidal regimes (with and without the simulation of tides). Bars give means ± standard deviation (n = 5).

3.1.3 Chlorophyll *a* content

Chlorophyll *a* (Chl *a*) content of tissues of apical tips of *Fucus serratus* was higher in algae cultured with a regular tidal emergence than in algae cultured at permanently submersed conditions, irrespective of the CO_2 concentration (Fig. 16, Tab. 15 in Appendix). Furthermore, algae grown at 280 ppm CO_2 and tidal emergence showed the highest content of Chl *a* (0.27 ± 0.03 mg Chl *a* g_{WW}^{-1}) and algae grown at 280 ppm without tidal emergence the lowest Chl *a* content of 0.22 (± 0.03 mg Chl *a* g_{WW}^{-1}). These patterns were statistically insignificant (pCO_2: df = 1, F = 1.44, p = 0.25; tidal emergence: df = 1, F = 4.07, p = 0.06) and both factors did not interact (df = 1, F = 1.81, p = 0.20).
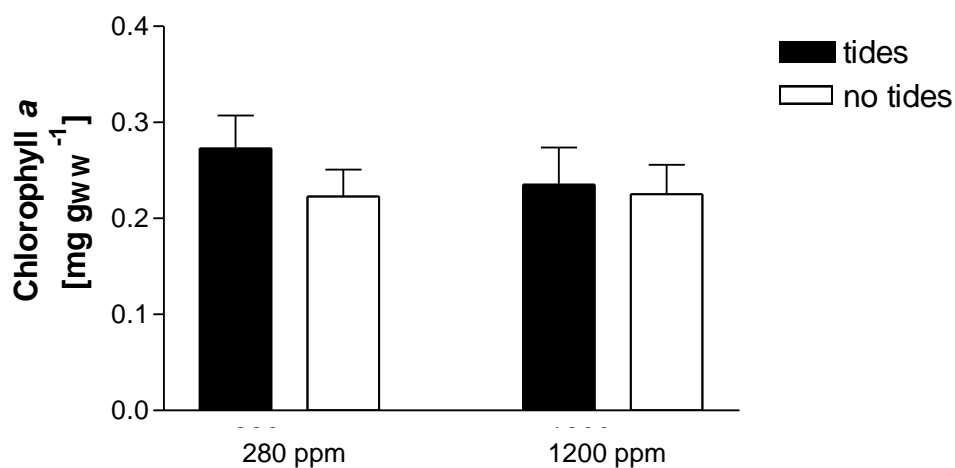
Fig. 16: Chlorophyll *a* (Chl *a*) content [mg g_{WW}^{-1}] of apical tips of *Fucus serratus* cultured at two different CO_2 concentrations (280 and 1200 ppm) and two different tidal regimes (with and without the simulation of tides). Bars give means ± standard deviation (n = 5).

3.2 Molecular part

3.2.1 Testing of molecular methods

3.2.1.1 RNA extraction and quality determination

RNA extraction of the different treated algae (combination of two CO_2 concentrations and two tidal regimes) resulted in sufficient yield of total RNA for further analysis (Tab. 17 in appendix). In general, the sample RNA was of excellent purity accept the samples 3, 5 and 15 (Tab. 17). The absorption ratios of these samples were below 2, which indicate that the samples were contaminated by e.g. polysaccharides or ethanol. Therefore, these samples were purified using a Qiagen RNeasy® MinElute® Cleanup Kit (Hilden, Germany). Afterwards, the yield of total RNA within these three samples was slightly less, but the A_{260}/A_{230} nm absorption ratio was above the critical threshold. Nevertheless, despite purification, sample no. 5 was still slightly contaminated, but in a range that was acceptable for further analysis.

Samples 1 – 12 and samples 13 – 20 were investigated in two distinct RNA Nano chips. The gel electrophoresis pictures of both chips show that for each of the investigated sample, two distinct fragments, the 18S and the 28S rRNA, have separated. Samples loaded on chip 1 showed light smeared bands, whereas chip 2 showed fragments that are not smeared (Fig. 17). The electropherograms of the different samples showed that the samples were not degraded and show clear and distinct peaks for the 18S and 28S rRNA (Fig. 18). The ratios between the two types of rRNA were in a sufficient range as well as the yield of total RNA. The negative control (water) showed no signal.
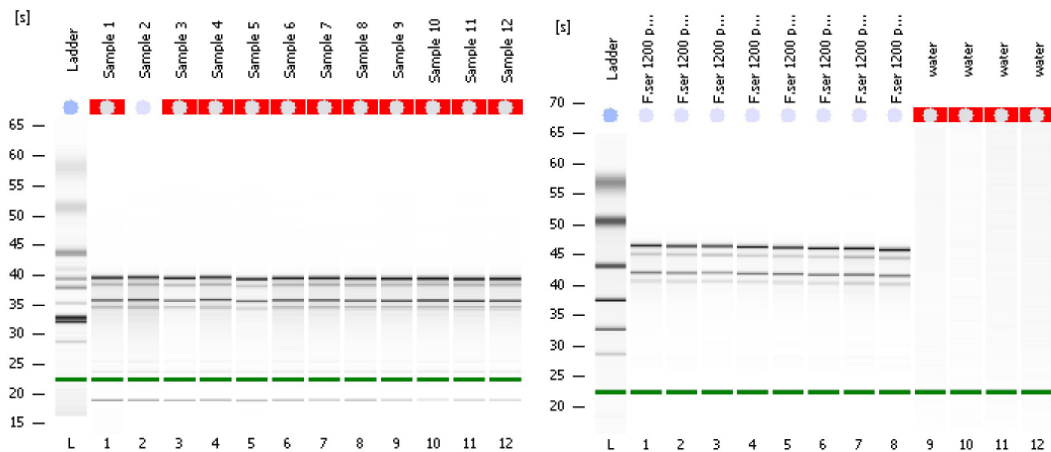
Fig. 17: Electrophoretical separation of the isolated RNA samples from different treated *Fucus serratus*. From left to right: sample 1 to 20, plus negative controls (water).
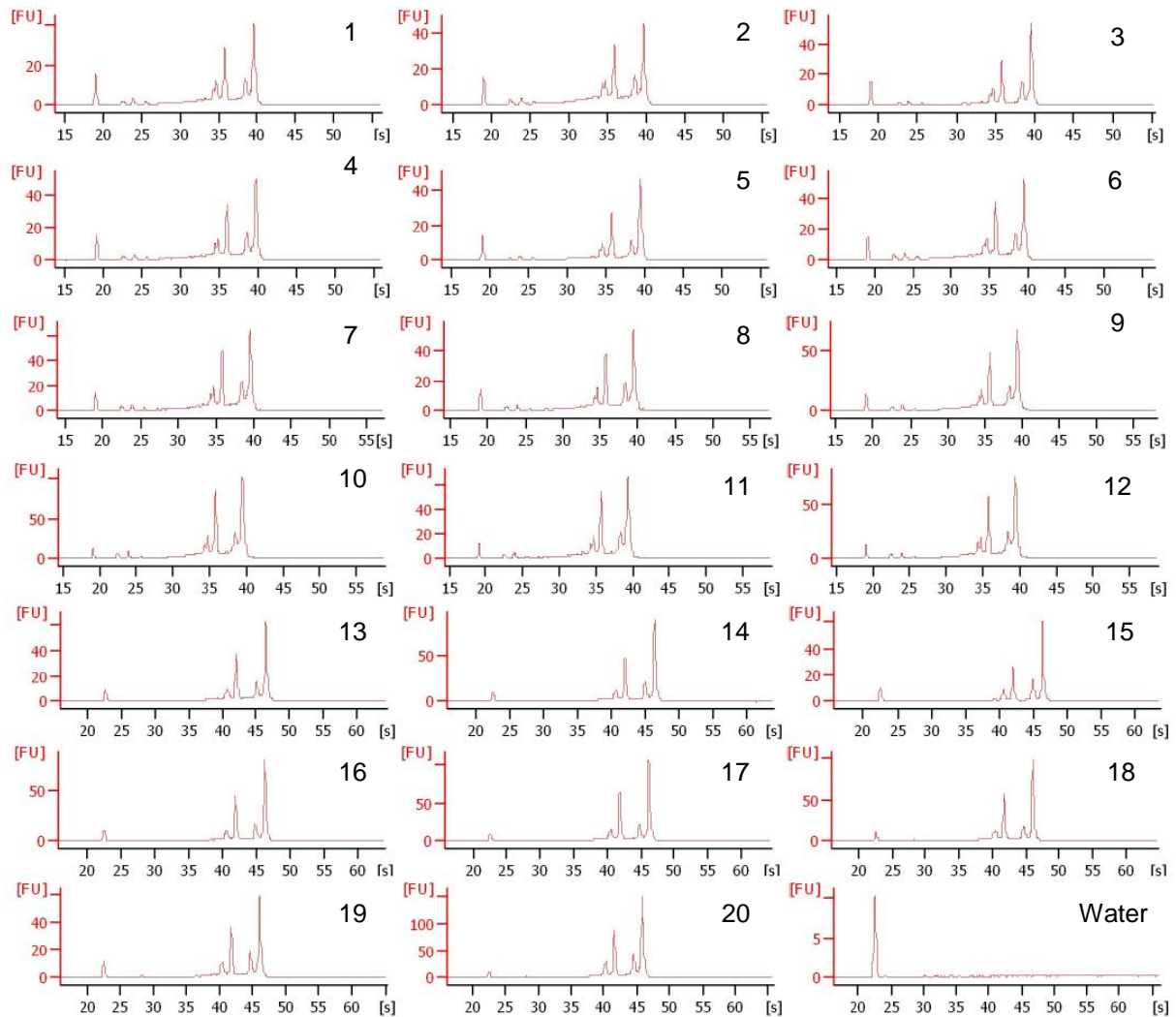
Fig. 18: Electropherograms of the isolated RNA samples from different treated *Fucus serratus*. Numbers indicate the different treated samples: 1 – 5 : 280 ppm CO_2 tides, 6 – 10: 280 ppm CO_2 no

tides; 11 – 15: 1200 ppm CO_2 tides; 16 – 20: 1200 ppm CO_2 no tides. The last electropherogram represents a negative control were water was used instead of RNA.

3.2.1.2 Primer testing PCRs

The temperature gradient PCR was run with designed oligonucleotide primers for 9 different candidate enzymes (see Tab. 2) and with different annealing temperatures (see Tab. 3) to determine the most efficient conditions for each the primer pair.

The gel electrophoresis picture is shown in Fig. 19. Most of the performed PCRs produced fragments with the predicted sizes of the respective genes. Genes encoding for PEPCK were amplified using the designed oligonucleotide primers at each of the tested temperatures. Every annealing temperature yielded in dark and distinct fragments of around 550 bp (Fig. 19 a - f). For further analysis, the mean of the annealing temperatures of 61.1 and 62.2°C was chosen based on the best fragments at these temperatures (Fig. 19 e). Most of the GOIs were amplified at 53.7 – 54.6 °C (RubisCO, serine-glyoxylate transaminase, malic enzyme and carbonic anhydrase, Fig. 19 b). Amplified RubisCO, serine-glyoxylate transaminase and malic enzyme sequences showed light but distinct fragments at around 400 bp. Amplified CA sequences showed darker, distinct fragments of 500 bp. Primers designed for glycolate oxidase genes worked most efficiently at the highest annealing temperatures of 63.0 – 63.4 °C (Fig. 19 f). At these temperatures, the fragments were most distinct and had a size of ~ 400 bp but the amplified genes showed multiple fragments. With the designed oligonucleotide primers for phosphoglycolate phosphatase and PEPC, it was not possible to amplify any sequences at any temperature and thus, was not further analyzed. The primers designed for GOGAT did not amplified in any product at any temperature (Fig. 20).
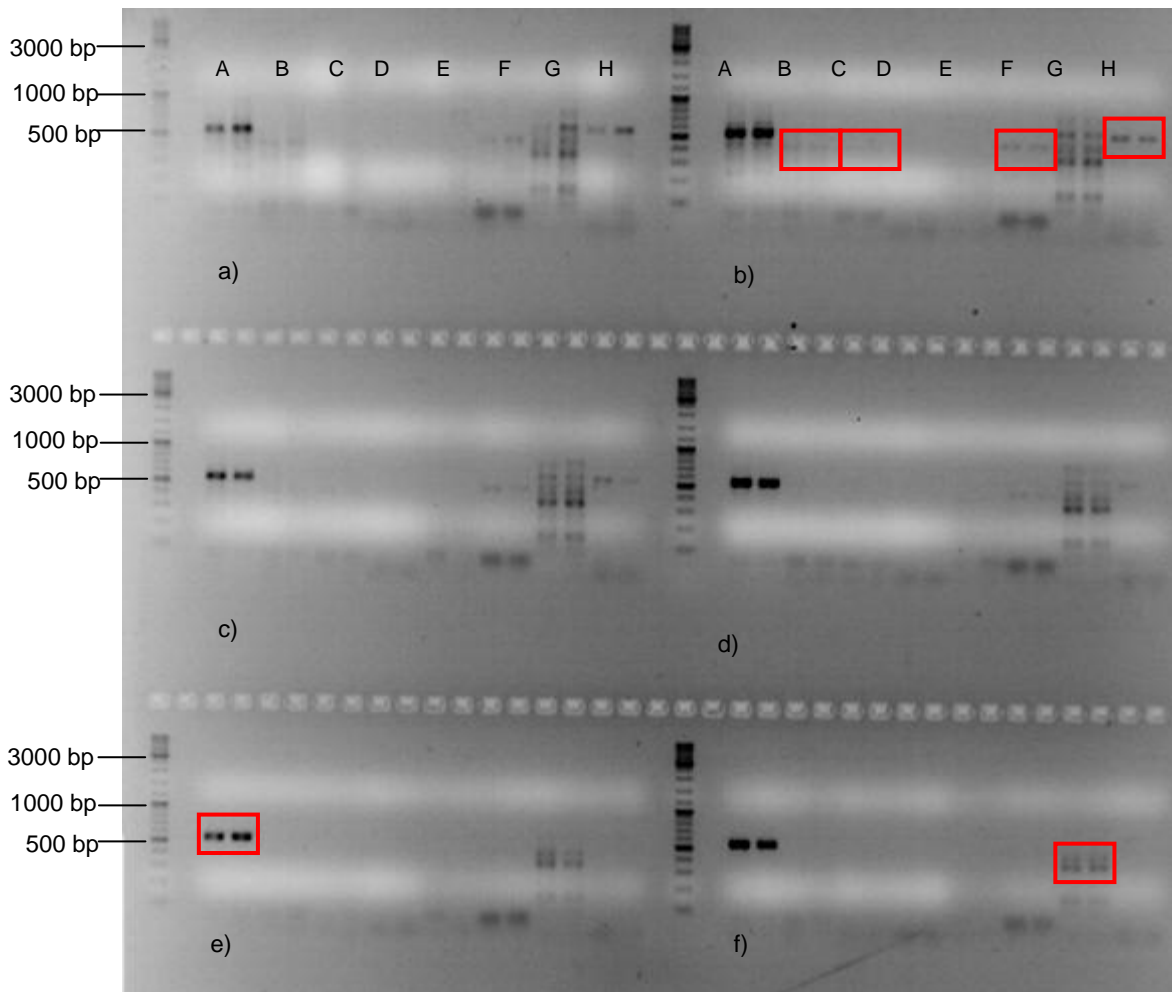
Fig. 19: 1.5 % agarose gel elceltrophoresis picture stained with 3 µl ethidium bromide of temperature gradient PCR products of the genes of interest (GOIs) (A = PEPCK, B = RubisCO, C = Serine-glyoxylate transaminase, D = Phosphoglycolate phosphatase, E = PEPC, F = Malic enzyme, G = Glycolate oxidase, H = CA). a) 53.0 and 53.2 °C, b) 53.7 and 54.6 °C, c) 55.8 and 57.1 °C, d) 58.4 and 59.8 °C, e) 61.1 and 62.2 °C, f) 63.0 and 63.4 °C. Red quadrates indicate fragments that were chosen for an additional PCR with the best annealing temperature of the designed oligonucleotide primers needed for excising these fragments. DNA ladder: peqGOLD ladder-mix (0.5 mg DNA/ µl; PeqLab, Erlangen, Germany).
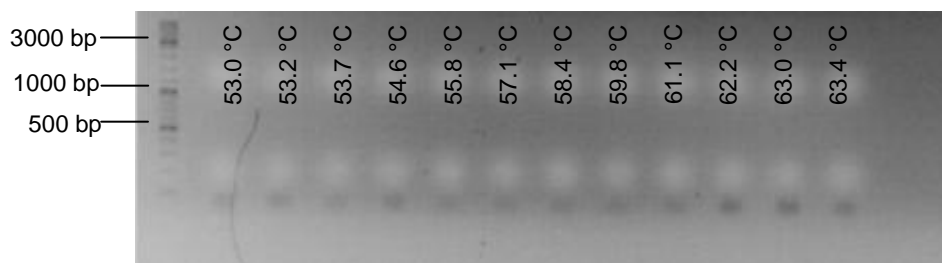
Fig. 20: 1.5 % agarose gel elceltrophoresis picture stained with 3 µl ethidium bromide of temperature gradient PCR products of GOGAT genes for different annealing temperatures of the designed ologinucleotides. DNA ladder: peqGOLD ladder-mix (0.5 mg DNA/ µl; PeqLab, Erlangen, Germany).

The additional PCR amplified the sequences of PEPCK, RubisCO, malic enzyme, serine-glyoxylate transaminase, CA and glycolate oxidase at the mean annealing temperatures at which the primers worked the best to get distinct fragments for subsequent excision processes. RubisCO had a very light and smeared fragment of around 500 bp (Fig. 21 a). Malic enzyme had a distinct fragment of around 500 bp (Fig 21 b) and CA a distinct fragment of ~ 600 bp (Fig. 21 c). The darkest and most distinct fragment showed PEPCK with a size of around 550 bp (Fig. 21 e). Glycolate oxidase had a very light and smeared fragment of around 450 - 500 bp (Fig. 21 f). The PCR with the designed oligonucleotide primers for serine-glyoxylate transaminase did not amplify any product at the best annealing temperature (Fig 21. d). Serine-glyoxylate transaminase, thus, was not analyzed any further.
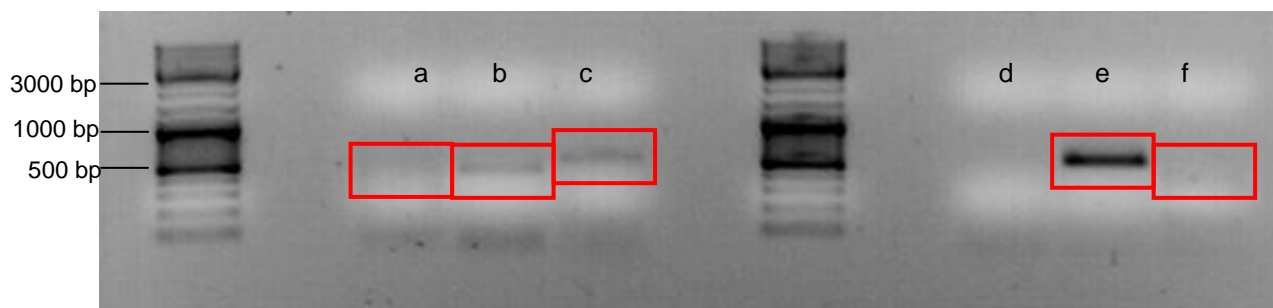
Fig. 21: 1 % agarose gel electrophoresis stained with 1 µl ethidium bromide of PCR products of genes of interest (GOIs) amplified at best mean annealing temperature of the oligonucleotide primers. Red boxes indicate fragments that were used for further analysis. A = RubisCO 54.1 °C, b = Malic enzyme 54.1 °C, c = CA 54.1°C, d = serine –glyoxylate transaminase 54.1 °C, e = PEPCK 61.7 °C, glycolate oxidase 63.4 °C. DNA ladder: peqGOLD ladder-mix (0.5 mg DNA/ µl; PeqLab, Erlangen, Germany).

3.2.1.3 Cloning

The transformed *E. coli* cells containing the GOIs were plated on an LB plate and incubated. After 25 h of incubation at 37 °C only a few colonies containing the GOIs were grown sufficiently. Only transformed cells containing inserts of RubisCO (2), PEPCK and glycolate oxidase have produced several blue and white colonies (example in Fig. 22) and were transferred to cool conditions to avoid an over growth of ready-to-pick colonies. *E. coli* cells transformed with malic enzyme, CA and RubisCO (1) gene inserts were allowed to incubate for 36 h in total. After the incubation RubisCO and CA formed several blue and white colonies. *E. coli* cells that should contain the gene sequence of malic enzyme did not form any colonies and were not analyzed any further. The numbers of white colonies containing the GOIs that can be used for further analysis are listed in Tab. 11.
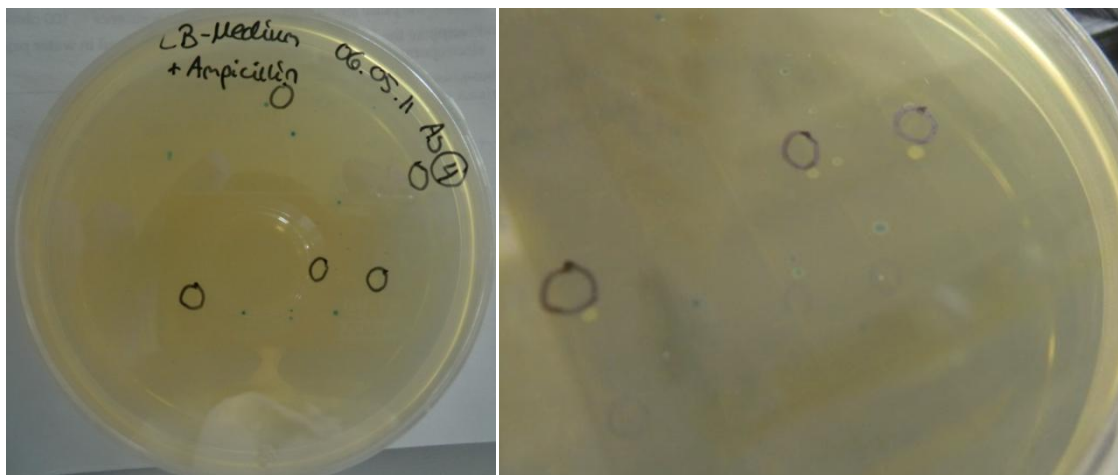
Fig. 22: Exemplary agar plate containing positive (white) and negative (blue) colonies of transformed *E. coli* cells with respective gene sequences. Black circles indicate white colonies that were selected for further analysis.

Tab. 11: Number of chosen white colonies of transformed *E. coli* cells with inserts of the genes RubisCO, malic enzyme, CA, PEPCK, glycolate oxidase from solid LB agar plates and number of colonies that were grown in liquid LB medium for 19 h.

Enyzme	Selected colonied from the LB agar plates	Grown colonies in liquid LB medium
RubisCO1	8	2
Malic enzyme	none	none
CA	12	7
RubisCO2	5	5
PEPCK	10	10
Glycolate oxidase	8	6

After selecting the positive colonies, they were incubated a second time in liquid LB medium for 12 h. After these 12 h, some of the colonies achieved the required density and were used to isolate the plasmids containing the GOI sequences (Tab. 11).

The determination of the quantity and the purity of the extracted plasmids yielded in high concentrations of plasmids and mostly acceptable degrees of purity (Tab. 18 in Appendix). Some samples (A8, D2, E1) had a A_{260}/A_{230} nm ratio that was below 1.4, which represents the purity threshold to perform a PCR. Nevertheless, these samples were used without any purification due to the large amount of replicate colonies.

Successful transformation of the desired gene sequences into TOP10 *E. coli* cells is shown in Fig. 23. Transformation of electro competent TOP10 *E. coli* cells with vectors containing RubisCO gene sequences was done two times to ensure sufficient colonies of clones containing the RubisCO gene. The first plate of transformed TOP10 *E. coli* cells with RubisCO genes is shown in Fig. 23 a. The first fragment has an approximate size of ~ 600 bp, which is conform to the size of the vector containing an insert. The second well shows a fragment of the size of the vector without an insert; thus, this sample was not used for the subsequent sequencing reaction. TOP10 *E. coli* cells containing the gene sequence of the CA are shown in Fig. 23 b. It is obvious that almost all fragments have the same size of around 750 – 800 bp. Only one fragment has a total size of ~ 500 bp. However, these sizes do not fit to the expected size of the vector including a CA insert. The second run of RubisCO colonies is shown in Fig. 23 c. The plasmids containing RubisCO genes are very heterogeneous referring to the size. Only the first and the last well contained fragments that had the predicted length of around 500 bp. In Fig. 23 d plasmids with PEPCK gene inserts are shown. Accept the fragment in the first well, the fragments are very homogenous and are conform to the predicted size of the plasmid of around 700 bp. The first well of PEPCK transformants shows a fragment of the predicted size and a fragment of a vector without an insert. This sample was not analyzed in the subsequent sequencing reaction. The last plasmids with inserted glycolate oxidase genes are shown in Fig. 23 e. These fragments differ in sizes from around 450 bp to almost 650 bp and none of them are conform to the predicted size of 760 bp.

Accept of the PCR products of the extracted plasmid in which a vector without an insert was determined (red circle Fig. 23); all extracted plasmids were used for subsequent sequencing analysis.
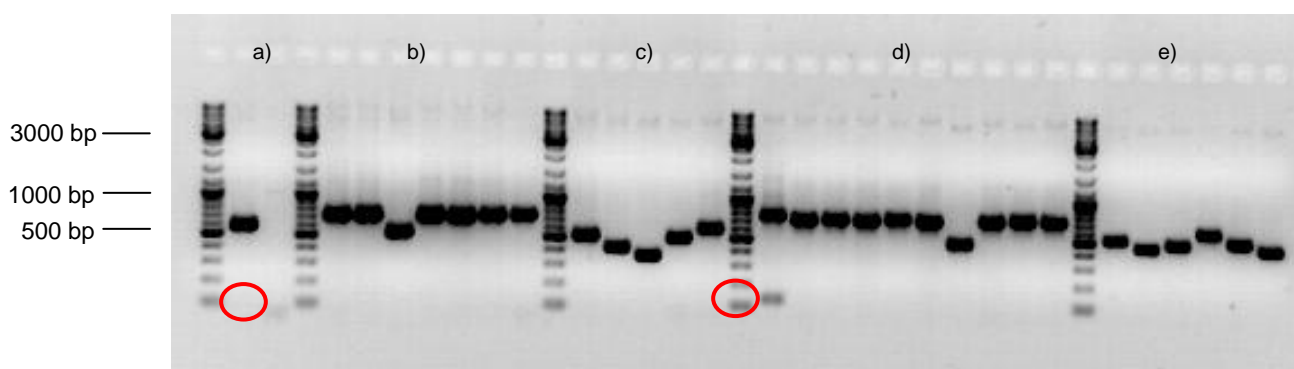
Fig. 23: 1.5 % agarose gel electrophoresis stained with 3 µl ethidium bromide of amplified PCR products of extracted cloned *E. coli* plasmids for four different genes (a = RubisCO 1, b = CA, c = RubisCO 2, d = PEPCK, e = Glycolate oxidase). Red circles indicate fragments that only consist of vectors without insert that were not used for further analysis. DNA ladder: peqGOLD ladder-mix (0.5 mg DNA/ µl; PeqLab, Erlangen, Germany).

3.2.1.4 Sequencing of cloned plasmids

Sequencing of the first 16 samples yielded in light signals concerning to low template concentration. After enhancing the concentration of the template cDNA, the signals became more intense and therefore more appropriate. Every sequence that yielded in signals was analysed and blasted. For sequence annotation two different BLAST searches, BLASTN and BLASTX were performed. During the BLASTN search, the target nucleotide sequence is compared to a nucleotide database; the BLASTX search implies the translation of the target sequence to a protein sequence, which is compared to a protein database.

RubisCO gene sequencing yielded in four different contigs. None of them showed significant results when BLASTX search was performed (e-values > 0.04). During a BLASTN search, the RubisCO sequence was characterized as a large SU rRNA gene of *Fucus gardneri* (e-value e^{-81}). This sequence could not be used for qRT-PCR due to the fact that the sequence could not have been characterized as a RubisCO gene.

Sequencing of cloned CA genes yielded in one contig. BLASTN search yielded in only non-significant results (e-value: 0.17) and BLASTX search only resulted in a sequence of *Rhodopirellula baltica* (e-value: e^{-51}). Thus, these sequences were excluded from further analysis.

Cloning of glycolate oxidase genes yielded in six different colonies, i.e. replicates. After assembling these sequences, six different contigs were formed. This indicates very heterogeneous replicates. The sequence could not have been indicated as the sequence coding for glycolate oxidase in a BLASTX search. BLASTN search resulted in a very high likelihood (e-value: e^{-131}) that this sequences stems from *Fucus vesiculosus* or *Ectocarpus siliculosus*. However, this sequence could not be used for qRT-PCR, since it could not have been identified as glycolate oxidase gene.

The sequencing reaction of PEPCK resulted in sequences that could have been assembled in two distinct contigs. The BLASTX search yielded in a high probability (e-value: e^{-97}) that the sequences are genes coding for PEPCK. Thus, this sequence was used for subsequent qRT-PCR.

The qRT-PCR was performed with the sequence of PEPCK and with the sequences of CA and the gene incorporated in the expression of RubisCO (*cbbX*) provided by annotation data from *Fucus serratus* by Gareth Pearson.

3.2.2 Gene expression analysis by a quantitative real-time PCR

Amplification of the larger target sequences by a PCR yielded in distinct fragments of predicted sizes for each of the GOIs (Fig. 24). PCR products of PEPCK genes were not loaded on a gel due to the fact that M13 primers were used which amplified the correct sequences in previous reactions (see part 3.2.1.3 and Fig. 23d). The CA gene was split into two sequences to have rather two smaller sequences than one long sequence, thus two different primer sets for the PCR were used. The first CA fragment (CA1) (Fig. 24a) had a size of ~ 400 bp (predicted size: 408 bp). The purified PCR products of CA1 had a concentration of 12.78 ng/µl. Fragments of the second part of the CA sequence had a size of ~ 250 bp (predicted size: 237 bp) (Fig. 24b) and a concentration of 41.13 ng/µl. Amplified PCR products of the RubisCO gene were the largest with a length of 800 bp (predicted size: 780 bp) (Fig. 24c) and a concentration of 40.27 ng/µl. Thus, each of the designed primer pairs amplified products of the predicted sizes.
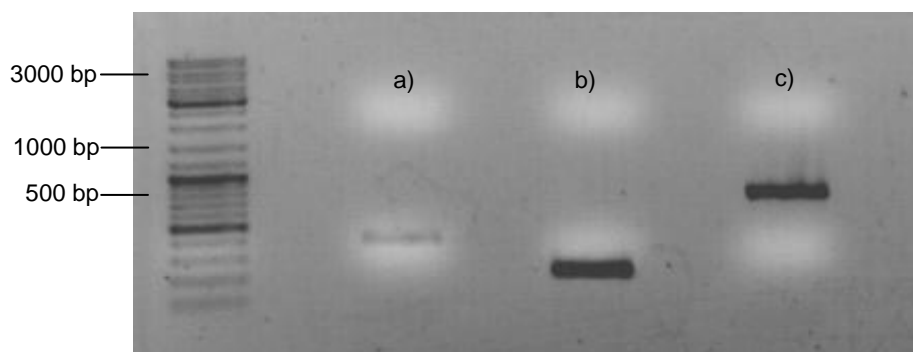
Fig. 24: PCR products amplified by specific designed primers to obtain large sequence used within the standard curve of the quantitative real-time PCR (a = CA1, b = CA2, c = RubisCO). DNA ladder: peqGOLD ladder-mix (0.5 mg DNA/ µl; PeqLab, Erlangen, Germany).

To detect differences in gene expression by a qRT-PCR approach it is required to normalize the data set against a reference gene. Within this study, this was done by incorporating two different genes of *Pieris rapae* as spike-in genes into the sample cDNA in two different concentrations. The low concentrated (1 ng/µl) spike-in gene MA was detected in all samples (n = 20) at a mean C_t value of around 30.3 (± 1.1) (Tab. 19 in appendix) and the high concentrated (10 ng/ µl) NSP spike-in gene at a mean C_t value of around 30.0 (± 1.1). Due to the fact that the NSP gene was incorporated into the cDNA in a higher concentration, the C_t value should have been lower (at around 17). The Ct values of the different treated samples were more similar to the Ct values of MA, thus the data were normalized against the MA

spike-in mRNA. Differences in expression ratios of the GOIs cannot be determined solely by the given C_t values. Thus, relative gene expression ratios were calculated and analyzed statistically by the program REST 2009. The different treatment effects were investigated individually and in a combination of both tested parameters (CO_2 and tidal emergence). For every tested combination of parameters the relative gene expression ratios of CA1 were excluded due to unusable high variations.

The CO_2 effect

Algae cultured at two different CO_2 concentrations without tidal emergence showed no significant difference in gene expression between the control group (280 ppm CO_2 no tides) and the sample group (1200 ppm CO_2 no tides) within any of the tested genes (Tab. 12). The two discrete sequences of PEPCK were differently regulated. The first sequence PEPCK1 was up-regulated by a mean factor of 1.191 (p = 0.660) whereas the second part of the sequence was down-regulated a mean factor of 0.702 (p = 0.674). Expression ratios above 1 indicate a potential up-regulation, whereas expression ratios below 1 represent a potential down-regulation. The same pattern was found for RubisCO gene sequences with an expression ratio of 1.055 (p = 0.810) for RubisCO1 gene sequence and an expression ratio of 0.976 (p = 0.992) for RubisCO2 gene sequences. The CA2 gene was down-regulated by a mean factor of 0.469 (p = 0.270). However, these regulations were statistically not significant (p > 0.05) (Tab. 12).

The tidal effect

To test for the effect of regular tidal emergence, the effect of desiccation on the gene expression of the GOIs was tested for both CO_2 concentrations separately. Apical tips of *Fucus serratus* cultured at regular tidal emergence showed no statistical significant difference in gene regulation of the GOIs, irrespective of the CO_2 concentration (Tab. 12). PEPCK genes, RubisCO genes and CA2 genes were down-regulated when experiencing tidal emergence at 280 ppm CO_2 compared to permanently submersed algal tips at 280 ppm CO_2 (expression ratios 0.624 (p = 0.175), 0.305 (p = 0.053), 0.716 (p = 0.212), 0.325 (p = 0.054) and 0.420 (p = 0.093), respectively (Tab. 12)). There is a tendency that the expression of PEPCK2 and RubisCO2 is repressed during tidal emergence and 280 ppm CO_2. Even though the p-values indicate a strong tendency, these regulations patterns were not statistically significant (p > 0.05). Algal tips that were cultured at regular tidal emergence at high CO_2 concentrations showed no significant changes in gene expression compared to the control group (1200 ppm no tides, Tab. 12). PEPCK, RubisCO1 and CA2 genes were up-regulated by a mean factor of 1.656 (p = 0.170), 1.373 (p = 0.455), 1.754 (p = 0.074) and

1.973 (p = 0.054), respectively. Only RubisCO2 genes were down-regulated in the sample group (1200 ppm and tides) compared to the control group by mean factor of 0.848 (p = 0.813). Although gene expression is higher in algae that exhibit tidal emergence in a high CO_2 regime and especially CA2 showed a strong tendency for up-regulation, none of the described expression patterns of the GOIs were statistically significant (p > 0.05).

The combined effects of enhanced CO_2 and tidal emergence

Gene expression analysis of the GOIs in algae cultured in a combination of different CO_2 concentrations and tidal emergence was significantly affected by the tested parameters. Only the combination of the tested parameters significantly altered the gene expression of the GOIs (Tab. 12). Algae cultured at 1200 ppm CO_2 and regular emergence (sample group) showed differences in their gene expression of the investigated gene when compared to algae cultured at 280 ppm CO_2 and regular tidal emergence (control group). PEPCK genes were up-regulated by mean factor of 3.163 (p = 0.012) and 3.158 (p = 0.001), respectively. RubisCO1 and 2 were up-regulated by mean factor of 2.585 (p = 0.009) and 2.548 (p = 0.009) and the expression of CA2 genes was induced by a mean factor of 2.205 (p = 0.026). Accordingly, all investigated genes were significantly up-regulated by a combination of enhanced CO_2 and tidal emergence.

Tab. 12: Result table of the statistical analysis of the nested real-time quantitative polymerase chain reaction (qRT-PCR) for the tested genes (TRG = target). The given expression values as fold changes are normalized against the reference MA gene (REF). Different combinations of treatments were tested. Highlighted values (yellow) indicate significant up-regulations of the tested genes.

Gene	Type	Expression ratio	Std. Error	95% C.I.	p-value
280 ppm no tides vs. 1200 ppm no tides					
MA	REF	1			
PEPCK1	TRG	1.191	0,563 - 2,265	0,390 - 4,009	0.660
PEPCK2	TRG	0.702	0,195 - 2,230	0,037 - 7,736	0.674
RubisCO1	TRG	1.055	0,644 - 1,714	0,494 - 2,315	0.810
RubisCO2	TRG	0.976	0,287 - 5,404	0,034 - 10,086	0.992
CA2	TRG	0.469	0,072 - 1,194	0,036 - 1,838	0.270
280 ppm no tides vs. 280 ppm tides					
MA	REF	1			
PEPCK1	TRG	0.624	0,314 - 1,224	0,198 - 2,148	0.175
PEPCK2	TRG	0.305	0,037 - 0,939	0,021 - 1,347	0.053
RubisCO1	TRG	0.716	0,409 - 1,181	0,307 - 1,725	0.212
RubisCO2	TRG	0.325	0,041 - 0,909	0,021 - 1,454	0.054
CA2	TRG	0.42	0,059 - 0,982	0,033 - 1,469	0.093
1200 ppm no tides vs. 1200 ppm tides					
MA	REF	1			
PEPCK1	TRG	1.656	0,872 - 3,662	0,541 - 5,552	0.170
PEPCK2	TRG	1.373	0,774 - 3,151	0,246 - 5,948	0.455
RubisCO1	TRG	1.754	1,039 - 3,650	0,697 - 6,612	0.074
RubisCO2	TRG	0.848	0,223 - 2,450	0,141 - 5,248	0.813
CA2	TRG	1.973	1,014 - 3,632	0,795 - 7,267	0.054
280 ppm tides vs. 1200 ppm tides					
MA	REF	1			
PEPCK1	TRG	3.163	1.653 - 5.675	1.029 - 10.561	0.012
PEPCK2	TRG	3.158	1.928 - 5.817	1.438 - 9.966	0.001
RubisCO1	TRG	2.585	1.433 - 4.864	0.938 - 10.759	0.009
RubisCO2	TRG	2.548	1.500 - 4.239	1.004 - 8.453	0.009
CA2	TRG	2.205	1.267 - 4.268	0.884 - 7.594	0.026

4. Discussion

The present study showed no effect of enhanced CO_2 concentration and tidal emergence on growth and photosynthetic traits of the intertidal brown seaweed *Fucus serratus*. In contrast to the physiological traits, expression rates of specific genes involved in carbon fixation processes were affected by a combination of elevated CO_2 concentration and tidal emergence. All investigated genes were up-regulated during enhanced CO_2 concentrations and tidal emergence. Both factors alone did not affect the gene expression selected genes of *F. serratus*.

4.1 Physiology

4.1.1 Effects of CO_2 on permanently submersed *Fucus serratus*

Enhanced CO_2 concentrations alone did not affect growth and photosynthesis of permanently submersed *Fucus serratus*. No differences were observed in growth rate and photosynthetic oxygen evolution between the control group (280 ppm CO_2) and the sample group (1200 ppm CO_2). Other studies on the effect of high CO_2 concentrations on permanently submersed macroalgae showed similar results (Israel and Beer 2000; Israel and Hophy 2002). Israel and Hophy (2002) investigated the effect of enhanced CO_2 concentrations (700 ppm) on numerous algae species belonging to the Chlorophyta, the Rhodophyta and the Phaeophyta. None of those species showed an enhanced photosynthetic rate at elevated CO_2 concentrations. Similarly, the brown algae *Saccharina latissima*, *Laminaria digitata* and *Pylaiella littoralis* were unaffected by enhanced CO_2 concentrations of 700 ppm (Stecher 2009). This insensitivity of algal photosynthesis against variations in the CO_2 availability might be explained by the existence of an efficient CCM in many marine seaweeds (see part 1.2 for more details), which enhance the CO_2 availability within the algal thallus although external CO_2 concentrations are low (Giordano et al. 2005). Accordingly, photosynthesis and growth of permanently submersed seaweeds might be unaffected by rising CO_2 concentrations, as it was shown for the investigated *F. serratus* in the present study.

The effects of CO_2 on submersed algae can be very heterogeneous. Several seaweeds benefit from enhanced CO_2 concentration by an increment in photosynthesis or growth, since their photosynthesis is unsaturated at present CO_2 concentrations (Andría et al. 2001; Gao et al. 1991; Rivers and Peckol 1995). However, some macroalgal species appear to be negatively affected by enhanced CO_2 concentrations by a decrease in photosynthesis and growth (García-Sánchez et al. 1994; Mercado et al. 1999). Such a down-regulation of photosynthesis might be explained by an enhanced amount of carbohydrates that might

repress photosynthetic enzymes and thus photosynthesis (Webber et al. 1994). Together, all these divers results (see Wu et al. 2008 for review) indicate that even closely related algal species from the same genus (e.g. *Gracilaria* species) can be influenced differently by enhanced CO_2 concentrations. As a result, the effects of ocean acidification on growth and photosynthesis of submersed marine macroalgae appear to be heterogeneous and no general predictions can be taken.

The Chl *a* content of apical tips of *Fucus serratus* did not change with the CO_2 concentration. This finding is supported by other studies on the effects of enhanced CO_2 on the Chl *a* content in marine photoautotrophs. The eelgrass *Zostera marina* (Zimmerman et al. 1997), the brown algae *Hizikia fusiforme* (Zou 2005) and the green microalga *Scenedesmus obtusiusculus* (Larsson et al. 1985) showed no changes in their Chl *a* content when cultured at enhanced CO_2 concentrations. Johnston and Raven (1990) found that *F. serratus* did not exhibit any change in Chl *a* content at very high CO_2 concentration of 5 kPa (~ 50.000 ppm) but a decreased photosynthetic rate. However, this is not in accordance with the results of the present study. Other studies showed that enhanced CO_2 concentrations led to reduced Chl *a* contents in tissues of *Gracilaria* sp. (Andría et al. 2001), *G. tenuistipitata* (García-Sánchez et al. 1994), *Spirulina platensis* (Gordillo et al. 1999) and *Porphyra leucosticta* (Mercado et al. 1999). In a previous study, I found that the Chl *a* content of *F. vesiculosus* decreased with increasing CO_2 concentration. Surprisingly, the photosynthetic activity of *F. vesiculosus* remained unaffected by elevated CO_2 concentrations while somatic growth increased. Similar results were found in other studies (Gordillo et al. 2003; Gordillo et al. 2001). Gordillo et al. (1999) proposed that a non-photosynthetic growth enhancement might be explained by a degradation of molecules that do not contribute to the light-capturing procedure. The energy conserved by the degradation of molecules could be used for other physiological process, e.g. growth. However, this effect was not observed in *F. serratus*.

4.1.2 Effect of enhanced CO_2 on regularly emerged *Fucus serratus*

Photosynthetic activity, growth and Chl *a* content of *Fucus serratus* remained unaffected by enhanced CO_2 concentrations and tidal emergence. However, many macroalgae which grow in the intertidal zone have to cope not only with increased CO_2 concentrations in a changing ocean but also with other abiotic stress like desiccation and exposure to atmospheric conditions (Davison and Pearson 1996). Nevertheless, several studies showed that photosynthesis of some intertidal seaweeds is enhanced at the beginning of a desiccation event. An enhanced photosynthesis at moderate desiccation has been observed in several intertidal macroalgae from different taxa (Ji and Tanaka 2002), in *Porphyra yezoensis* (Gao and Aruga 1987) and in different fucoid species (Dring and Brown 1982). *Fucus spiralis* from

the upper eulittoral is able to photosynthesize more rapidly during periods of emergence. However, photosynthesis of this species is reduced in the field for a large proportion of the day due to severe desiccation (Maberly and Madsen 1990). For this reason, it has been hypothesized that photosynthesis is more limited during emersion than during submersion (Zou and Gao 2002; Zou et al. 2007). Furthermore, other studies showed that the CO_2 concentration required to saturate photosynthesis increased with desiccation, indicating that the CO_2 affinity of the alga is lowered by desiccation and that photosynthesis is limited during emersion at present CO_2 concentrations (Gao et al. 1999; Johnston and Raven 1990). These constraints might be overcome with increasing atmospheric CO_2 concentrations. At moderate desiccation and enhanced CO_2 concentrations several marine macroalgae are able to enhance photosynthesis during emergence. For instance, the green alga *Ulva lactuca* (Zou et al. 2007), the red alga *Gloiopeltis furcata* and the brown alga *Petalonia fascia* (Zou and Gao 2005) increased their photosynthetic activity at elevated CO_2 concentrations and moderate desiccation. Gao et al. (1999) observed an increase of photosynthesis of 25 – 40 % at a CO_2 concentration of 700 ppm in the green alga *Enteromorpha linza*, the red alga *G. furcata* and the brown seaweed *Ishige okamurae*. Zou and Gao (2002) detected an even greater increase in photosynthesis of 31 – 89 % in *Porphyra haitanensis* at 700 ppm CO_2 and moderate desiccation. However, such an increase was not detected in *F. serratus* in this study. In marine macroalgae which are able to efficiently drive photosynthesis during low tide, increasing atmospheric CO_2 concentrations under future climate conditions might intensify this effect. This might lead to a competitive advantage over algae that are not able to use the additional CO_2.

Tidal emergence and elevated CO_2 concentrations did not alter growth, photosynthetic rate or Chl *a* content of *Fucus serratus* in the present study. In a previous study, the closely related species *Fucus vesiculosus* showed a growth enhancement when cultured at 700 ppm CO_2 and regular tidal emergence (Stecher 2011). Both congeners experience regular exposure to atmospheric conditions in the intertidal zone, although the exposure times differ between the two seaweeds due to a different vertical distribution. *F. vesiculosus* inhabits the upper to mid eulittoral zone (Kornmann and Sahling 1977) with a daily emergence of 5 – 7 hours (Stocker and Holdheide 1937). *F. serratus* occurs in the lower eulittoral zone (Kornmann and Sahling 1977) with a daily emergence of 4 – 5 hours (Stocker and Holdheide 1937). Apparently, the zonation and thus the exposure to air has an impact on the photosynthetic rate during emergence (Einav et al. 1995; Quadir et al. 1979; Zou and Gao 2005). Zou and Gao (2005) investigated four different intertidal macroalgae, two red algae (*Gloiopeltis furcata* and *Gigartina intermedia*) and two brown algal species (*Petalonia fascia* and *Sargassum hemiphyllum*). *G. furcata* and *P. fascia* inhabit the upper intertidal zone while *G. intermedia* and *S. hemiphyllum* occur in the lower intertidal area. It was shown that the net

photosynthetic rate of the algae from the upper intertidal zone increased by an initial water loss whereas this increase was not detected in the algae from the lower intertidal zone (Zou and Gao 2005). Another study conducted by Quadir et al. (1979) revealed that species of the upper intertidal zone had a maximum photosynthesis during emersion at a 20% water loss. These authors also showed that the low intertidal alga *Iridaea cordata* had a maximum photosynthesis during submersion and a negative photosynthesis during emersion, whereas *Fucus distichus* from the upper intertidal benefitted from desiccation up to a water loss of 50 % (Quadir et al. 1979). This ecophysiological adaptation to the intertidal zone (Einav et al. 1995) might be one reason for the observed differences between *F. vesiculosus* and *F. serratus* grown at enhanced CO_2 and tidal emergence. *F. vesiculosus* is adapted to mid-intertidal conditions by a higher photosynthetic rate during desiccation, whereas the photosynthesis of *F. serratus* from lower eulittoral zone did not benefit from emergence. Since *F. serratus* does not spend as much time under atmospheric conditions as *F. vesiculosus* (Stocker and Holdheide 1937), *F. vesiculosus* is apparently able to use atmospheric CO_2 more efficiently than species from the lower intertidal and thus might have an adaptive advantage when the atmospheric CO_2 concentrations increase. However, these assumptions have to be further investigated and more studies are needed to understand the adaptive ecophysiological mechanisms of species in the intertidal zone at enhanced CO_2 concentrations.

4.1.3 General considerations concerning measurements of physiological parameters and experimental design

Some of the used methods to determine physiological differences due to CO_2 exposure and tidal emergence should be improved with regard to further investigations. For instance, it is questionable if the photosynthetic measurements properly reveal the natural situation. First, photosynthetic measurements were not conducted during a tidal event. Results might be more accurately when oxygen/CO_2 evolution would be measured during aerial exposure, e.g. via infrared gas analysis, as it was done in other studies (Gordillo et al. 1999; Zou and Gao 2005). Secondly, during emersion, the algae were exposed to identical light conditions during emergence in the humid chambers and during submersion. The light intensity in the humid chambers might have been too low in comparison to natural light intensities during low tide in the field (Stocker and Holdheide 1937). Other studies which investigated the effect of tides on photosynthesis used higher light intensities during the simulation of low tide. Johnston and Raven (1990) found that photosynthesis of *Fucus serratus* was saturated during emersion at light intensities of 500 µmol m^{-2} s^{-1} without causing photoinhibition. According to Stocker and Holdheide (1938) intertidal light exposure can be much higher, depending on the

position of the alga. It would be helpful to apply higher light intensities than in the present study, without, however, exceeding the alga's tolerance level for light. Maybe, the effect of CO_2 and tidal emergence would have been more pronounced at higher light intensities during emersion. Since the aim of this study was to investigate the effect of desiccation and not the effect of high radiation in the alga, a slight increase in light intensity would have been sufficient. Furthermore, the amount of desiccation (i.e. evaporation) could have been measured to correlate the effect of water loss to photosynthetic activity.

Photosynthetic performance was only measured at the end of the experiment. It would have been interesting to measure the photosynthesis of freshly collected algae to have a baseline of photosynthesis in the field. For this, a pulse amplitude modulation (PAM) fluorometry measurement would be appropriate. Additionally, the photosynthetic performance could have been controlled during the course of the experiment to identify probable acclimation processes and stress responses.

Furthermore, it should be mentioned that the high CO_2 concentration was lower than the predicted 1200 ppm. After measuring the carbonate chemistry it appeared that the CO_2 concentration of the seawater medium was ~ 900 ppm (Tab. 1). This, however, might further led to an attenuation of the effect of enhanced CO_2 on physiological parameters.

4.2 Molecular analyses

4.2.1 Applicability of molecular tool in a fucoid alga

Amplification of target sequences

The sequences of the genes of interest (GOIs) were chosen by a BLAST search with different organisms. The sequences were aligned and conserved regions were chosen as primer sequences. It would have been better to directly design species-specific primers. However, due to unavailability of a database for *Fucus serratus*, the primers were designed by multiple alignments of amino acid sequences of differently related species. The amino acid codes of these sequences were used and back-translated into nucleotide sequences. Due to the discrepancy of the genetic code, a specific amino acid might be encoded by different triplet codons ("wobbles"), thus some of the positions are encoded by several bases (Kwok et al. 1994), which was the reason why the used primers were degenerated. As soon as a wobble occurred, the respective base based on the IUPAC (International Union of Pure and Applied Chemistry) letter code (http://www.bioinformatics.org/sms/iupac.html) was integrated into the primers. Degenerated primers are advantageous if one is interested in the

screening of a genomic/cDNA database for a corresponding gene (Linhart and Shamir 2005). Whenever possible, the primers should be designed with the least degeneracy, leading to high specificity (Kwok et al. 1994). In the present study, a high proportion of degeneracy was integrated into the primers, leading to high error rates during amplification of the initially chosen genes (accept of PEPCK). After designing oligonucleotide primers based on *Fucus serratus* specific sequences provided by Gareth Pearson, amplification of the target sequences was successful, pointing out the disadvantage of using degenerate primers in this study.

The present study proved that molecular tools are applicable for *Fucus serratus*. Although some difficulties in RNA extraction occurred which led to a modification of the RNA extraction procedure, the RNA extraction was successful and yielded in a high amount of RNA. Another issue concerning brown algae in molecular genetics is the long 3' UTR (Apt et al. 1995; Pearson et al. 2010). In the present study, these 3'UTRs hampered cDNA synthesis. However, this was overcome by the usage of different primers. Pearson et al. (2010) showed, that the long brown algal 3' UTRs led to low annotation rates in their study. In general, the investigation of gene expression in brown fucoid macroalgae is possible and led to a successful gene expression analysis in the present study.

4.2.2 Gene expression analysis of GOIs at enhanced CO_2 concentration and tidal emergence

Transcription profile analyses of the enzymes RubisCO, CA and PEPCK at different CO_2 concentrations or tidal regimes resulted in an unchanged expression of mRNA coding for those genes under high CO_2 concentrations (compared to low CO_2) and regular tidal emergence (compared to permanently submersed algae). Enhanced CO_2 concentrations or regular short time desiccation did not affect transcription of the GOIs involved in carbon fixation processes. These results are in accordance with the observed insensitivity of physiological traits (growth, photosynthesis and Chl *a* content) to enhanced CO_2 concentrations and tidal emergence. However, a combination of the two factors implemented an induction of the GOIs. Expression ratios of the transcripts coding for GOIs were up-regulated under enhanced CO_2 concentrations and combined regular tidal emergence. Due to a lack of molecular investigations including a combination of those two parameters, the gene expression results of this study cannot be supported by other studies and will be discussed separately for each tested parameter.

The effect of enhanced CO_2 on selected GOIs

RubisCO is the most abundant enzyme and is involved in photosynthetic carbon fixation (Calvin cycle) and thus was intensively studied in the past (Bowes 1991). RubisCO either catalyzes the carboxylation of CO_2 or the oxidation of O_2 to ribulose-1,5-bisphosphate (RuBP). During its carboxylation activity, CO_2 is added to RuBP and two molecules of 3-phosphoglycerate (3-PGA) are formed (Fujita et al. 2008), which are subsequently used by other enzymes of the Calvin cycle to produce carbohydrates. RubisCO consists of a large subunit octamer (encoded by the *rbcL* gene) and a small subunit octamer (encoded by the *rbcS* gene) (Fujita et al. 2008; Webber et al. 1994). In Rhodophyta and some heterokont species, different than higher plants, both *rbcL* and *rbcS* are located in the plastid genome. In addition to those two genes encoding for the large and the small subunit of RubisCO, another RubisCO related gene coevolved in Rhodophyta, Heterokontophyta and Cryptophyta (Fujita et al. 2008; Maier et al. 2000). The *cbbX* gene is presumed to be involved in RubisCO expression (Maier et al. 2000) as a transcriptional regulator of RubisCO (Grzebyk et al. 2003). Due to difficulties to investigate the *rbcL* and/or the *rcbS* gene in the isolated *Fucus serratus* RNA in the present study, the sequence coding for *cbbX* provided by Gareth Pearson was used for expression analysis.

The present study showed an unchanged transcript abundance of *cbbX* at enhanced CO_2 concentrations. A study of Fujita et al. (2008) focused on the expression of *cbbX* at enhanced CO_2 concentration in the unicellular red algae *Cyanidioschyzon merolae* (Fujita et al. 2008). *C. merolae* contains a set of *rbcL-rbcS-cbbX* genes in the plastid genome and additionally a *cbbX* homologue in the cell nucleus (Matsuzaki et al. 2004). The transcription of *cbbX* (nuc) at 5% CO_2 concentration (50.000 ppm) in *C. merolae* was enhanced, while the expression of *cbbX* (pt) was not affected (Fujita et al. 2008). Fujita et al. (2008) argued that the induction of *cbbX* transcription could be explained by the different roles of the two *cbbX* genes. They state that during evolution of the red algal linage, the *cbbX* (nuc) gene evolved to be the responder to environmental CO_2 concentration instead of *cbbX* (pt). Thus, *cbbX* (nuc) is differently regulated by enhanced CO_2 than *cbbX* (pt) (Fujita et al. 2008). If *cbbX* of *F. serratus* is encoded in the plastid as well, the results agree with the results of the present study and *cbbX* is not regulated by CO_2. Another study investigating the effect of enhanced CO_2 concentration on photosynthesis, found that several marine macroalgae did not experienced a change in RubisCO content, activity and CO_2 affinity when cultured under enhanced CO_2 concentrations (Israel and Hophy 2002). However, they did not examine the transcript abundance of RubisCO expression correlated genes. The unicellular green algae *Chlorococcum littorale* only increased the expression level of RubisCO activase when grown under extremely high CO_2 concentrations of 20% CO_2 (Beuf et al. 1999). Interestingly, the algae did not show any difference in gene expression between air grown (0.04% CO_2) and

5% CO_2 concentration. The authors explain this observation by the actively operating CCM of this species. This explanation might be applicable for the present study as well. Even at high CO_2 concentrations (1200 ppm) the half saturation of RubisCO for CO_2 was not reached, thus *F. serratus* still seems to concentrate carbon at the active site of RubisCO, leading to neither an increase nor a decrease in photosynthetic activity. Although some authors state that high CO_2 concentrations (1 % CO_2 ~ 10.000 ppm) will cause a deactivation or down-regulation of the CCM (Gordillo et al. 2001), this might not be the case for *F. serratus* at 1200 ppm CO_2 leading to an unchanged transcript abundance of the GOIs between low and high CO_2 concentrations.

Contrastingly, other studies showed different results. On the one hand, a few studies observed an induction of RubisCO related genes in the green microalgae *Chlamydomonas reinhardtii* (Winder et al. 1992) or an increase in RubisCO activity/content in *Chlorococcum littorale* (Pesheva et al. 1994) at enhanced CO_2 concentrations. On the other hand, several studies observed a repression of RubisCO transcripts, activity and/or content in several higher plants (Cheng et al. 1998; Gesch et al. 1998; Majeau and Coleman 1996; Nie et al. 1995; Van Oosten and Besford 1995). The RubisCO content of the red macrolagae *Gracilaria* sp. (Andría et al. 2001) and *Gracilaria tenuistipitata* (García-Sánchez et al. 1994) decreased when cultured under enhanced CO_2 concentrations.

All these different results indicate that the effect of enhanced CO_2 concentrations on the gene expression in marine macroalgae is very species-specific and heterogeneous.

Another important enzyme concerning photosynthetic efficiency of marine macroalgae is the carbonic anhydrase (CA), which is a zinc-containing metalloenzyme that catalyzes the bi-directional conversion of CO_2 to HCO_3^- and vice versa (Fabre et al. 2007). The primary role of the external CA is the enhancement of the conversion of HCO_3^- to CO_2 (Zhang et al. 2010), whereas the internal CA is responsible for mobilizing the internal HCO_3^- pool to the carboxylating site of RubisCO (Mercado and Niell 2000; Zhang et al. 2010). Several higher plants showed a decrease in CA activities under enhanced CO_2 conditions (Cervigni et al. 1971; Peet et al. 1986; Porter and Grodzinski 1984). Gárcia-Sanchez et al. (1994) and Andría et al. (1999) detected reduced CA activity in the red macroalgae *Gracilaria tenuistipitata* and *Gracilaria* sp. and an accompanied reduction of photosynthesis at high CO_2 conditions. Few studies have investigated the effect of enhanced CO_2 on CA on the expression level. Majeau and Coleman (1996) found that both, CA transcript abundance and activity decreased when pea was cultured at 1000 ppm CO_2. Szabo and Colman (2007) focused on the characterization and localization of CA in the marine diatom *Phaeodactylum tricornutum*. They found that internal and external CA were differently regulated by CO_2. The external CA appeared to be up-regulated at low CO_2 concentrations, whereas at high CO_2

concentrations, only internal CA could have been detected in the diatom (Szabo and Colman 2007). Similar results were found in *Chlamydomonas reinhardtii,* in which two genes were observed, *Cah1* and *Cah2* that encode for the external α-CA (Fujiwara et al. 1990). Resultant proteins are similar but differentially regulated. *Cah1* encodes for an external CA that is up-regulated at low CO_2 concentrations, whereas *Cah2* encodes for an external CA, which is expressed at high CO_2 concentrations (Fujiwara et al. 1990). However, in the present study, no effects of enhanced CO_2 concentrations on CA gene expression in *F. serratus* could have been observed. This result could be attributed to the CCM which is still operating at enhanced CO_2 concentrations and requires a continuous demand for CA between the two tested CO_2 concentrations. Thus, the transcription of CA was not affected by enhanced CO_2 concentrations. Additionally, the investigation of CA might be difficult since several different isoforms of this enzyme were observed (Fabre et al. 2007). Furthermore, it was not possible to detect which type of CA was used in the present study. Thus, the results of the present study concerning the CA remain preliminary and more studies are needed addressing this issue.

Phosphoenolpyruvate carboxykinase (PEPCK) is an important enzyme of light-independent carbon fixation in marine algae (Kremer 1981). A high PEPCK activity was observed in brown seaweeds, especially in laminarians and fucoids (Giordano et al. 2005). PEPCK catalyzes the reversible carboxylation of phosphoenolpyruvate (PEP) to oxaloacetic acid (OAA) by the use of Mg^{2+} and ADP (Akagawa et al. 1972; Cabello-Pasini et al. 2000; Kremer 1981). By this, CO_2 is incorporated into OAA, which can be used in other metabolic pathways such as amino acid synthesis. An important feature of PEPCK is that it reduces the loss of CO_2 during glycolysis by incorporating CO_2 into a C_3 molecule by producing ATP. There is still a high carbon loss by respiration, but PEPCK can conserve some of the carbon lost from dark respiration (Lobban and Harrison 1994). PEPCK has a low affinity for CO_2 (Chen et al. 2002). Thus, with increasing CO_2 concentrations the activity of PEPCK might be enhanced, leading to a faster conversion of its substrate. However, since PEPCK is involved in glycolysis, it remains questionable if enhanced CO_2 concentrations might affect this enzyme. Thus, it could be that PEPCK remains unaffected by enhanced CO_2 concentrations, leading to the unchanged transcript abundance investigated in *Fucus serratus*.

The effect of desiccation on selected GOIs

Desiccation, induced by tidal emergence, can severely impact intertidal organisms (Davison and Pearson 1996). Nevertheless, in the present study regular tidal emergence did not lead to a significant change in the transcript level for the investigated GOIs, which is in accordance to the obtained physiological data. Such unchanged RubisCO transcription was

shown for two higher terrestrial plants that experienced desiccation (Dreesmann et al. 1994; Pelloux et al. 2001). Both studies concluded that the detected decrease in photosynthesis could be explained by stomatal limitations rather than by negative effects on photosynthetic enzymes caused by desiccation stress. A similar pattern was observed in the C_4 grasses *Paspalum dilatatum* and *Zoysia japonica* when experiencing desiccation stress (Carmo-Silva et al. 2008).

In marine macroalgae the unchanged transcription of the GOIs might be caused by other factors. During desiccation, atmospheric CO_2 has to diffuse (1) through the water layer that surrounds the algal tissue and (2) from the water film into the cell interior (Mercado and Niell 2000). The CO_2 flux can be enhanced by an increase in the concentration gradient between the atmosphere and the water layer (Portielje and Lijklema 1995). Such a gradient might be achieved by the bi-directional function of the CA and the hydration of CO_2 to HCO_3^- observed in several macroalgae during emergence (Bidwell and McLachlan 1985; Giordano and Maberly 1989; Mercado and Niell 2000). The CA allows the rapid conversion of atmospheric CO_2 to HCO_3^- within the boundary layer, which then is taken up by the algal thallus. This conversion will cause a CO_2 gradient leading to a diffusion of external CO_2 into the water layer (Portielje and Lijklema 1995). HCO_3^-, which might be actively transported into the algal thallus, will be transported to the chloroplast where an internal CA will dehydrate it to CO_2 available for RubisCO (Badger and Price 1994). Zou and Gao (2004b) reported that the external CA facilitates the atmospheric CO_2 acquisition during emersion in *Hizikia fusiforme*. The activity of CA during desiccation might indicate that the CCM is still active during tidal emergence and inorganic carbon is still concentrated within the algae. This would explain that no transcriptional changes of CA and RubisCO were observed in *F. serratus* in the present study.

There was an insignificant tendency for PEPCK2 and RubisCO2 to be repressed during tidal emergence and low CO_2 concentrations. Negative effects of desiccation were observed in two red and two brown algae, which showed a sharply increased CO_2 compensation point, indicating that severe desiccation might affect photochemical properties and the carboxylase activity of RubisCO (Zou and Gao 2005). However, it remains unclear what triggers the repression of these two enzymes during desiccation at 280 ppm CO_2 in the present study. Furthermore, CA2 showed a tendency to be up-regulated during desiccation and enhanced CO_2 concentrations. This result might indicate, that the CA is able to catalyze its substrate during emersion as well, which was shown by several studies as well (Bidwell and McLachlan 1985; Giordano and Maberly 1989; Mercado and Niell 2000). The p-values of these three genes indicate a very strong tendency of regulation of these genes by the tested parameters. However, since the statistical randomization and bootstrapping method is a test for stability (REST 2009 Software User Guide (2009), Qiagen, Hilden, Germany) and in the

present study a randomization of 2000 steps was performed, it appears that regulation patterns of these genes remain insignificant, irrespective of the tendency.

Only a few studies were conducted on the activity of PEPCK in response to drought stress. The PEPCK activity in three C_4 grasses is unaffected by drought, except of *Cynodon dactylon* in which PEPCK activity declined with leaf desiccation (Carmo-Silva et al. 2008). However, because literature on the effect of desiccation on the expression of PEPCK in marine macrolagae is scarce, further studies are needed to investigate the regulation of PEPCK by abiotic factors. Thus, the effect of enhanced CO_2 and tidal emergence on PEPCK expression remains unclear.

Most of the studies investigating the effect of desiccation on marine macroalgae found that during moderate desiccation photosynthesis is enhanced (Dring and Brown 1982; Gao and Aruga 1987; Ji and Tanaka 2002). Literature concerning the transcriptional abundance during desiccation stress in marine brown macroalgae is scarce. A recent molecular study focused on the effect of desiccation on transcription profiles. Pearson et al. (2010) found that the two related species *F. vesiculosus* and *F. serratus* responded differently to desiccation stress. In *F. serratus*, which is sensitive to desiccation, genes involved in light-harvesting and electron transport were up-regulated, whereas in the desiccation-tolerant *F. vesiculosus* mainly translation and protein degradation pathways were up-regulated. The different responses to desiccation at the gene expression level might explain the ability of related species to differentially adapt to environments (Pearson et al. 2010). Further investigations are needed to identify genes which are involved in desiccation stress and might lead to ecophysiological adaptations and zonation patterns.

Combined abiotic parameters affecting gene expression of GOIs

Based on the results of the present study, it appears that desiccation and enhanced CO_2 concentrations do not individually affect gene expression of the GOIs in *F. serratus*. However, the combination of both factors induced an up-regulation of all investigated GOIs. A similar combined effect of enhanced CO_2 concentrations and desiccation was found in the higher plant *Larrea tridentata* (Huxman et al. 1998). When grown at enhanced CO_2 concentrations, *L. tridentata* exhibited a repression of the carboxylation efficiency of RubisCO and thus of photosynthesis. This down-regulation of photosynthesis might be a response to high levels of carbohydrates (Van Oosten and Besford 1996), which might cause a depression of photosynthetic enzymes (Webber et al. 1994). Drought, however, might reduce the accumulation of carbohydrates at high CO_2 concentrations and thus repress the down-regulation of photosynthesis. The photosynthetic rate and the carboxylating activity of RubisCO was higher when the two parameters were combined compared to enhanced CO_2 concentrations alone, indicating interactive effects of enhanced CO_2 and desiccation

(Huxman et al. 1998). In how far such a regulatory signaling might be present in *Fucus serratus* as well remains unclear. The present study does not provide information about the carbohydrate content of the algal thallus. RubisCO transcripts, however, did not vary with respect to CO_2 concentration as it is predicted by Huxman et al. (1998).

The results of the present study indicate an interaction of the tested abiotic parameters. However, it was not possible to explain the enhanced expression of the GOIs at high CO_2 and tidal emergence. One possible explanation, derived from studies on higher plants, is the feedback regulation of photosynthetic gene expression under conditions of desiccation and enhanced CO_2 concentrations (Huxman et al. 1998). Furthermore, it might be possible that an enhanced CO_2 concentration during moderate desiccation might cause a higher reaction rate of CCM related enzymes, leading to a higher transcription of CCM related genes, such as CA in this study. Many marine macroalgae are able to enhance photosynthesis under conditions of moderate desiccation (Dring and Brown 1982). This enhancement might be even greater if the CO_2 concentration increases. More CO_2 might diffuse into the water layer during desiccation, needing more CA for conversion reactions in the remaining water layer (external CA) and allocation reaction within the cells (internal CA). However, it was not possible to discriminate between different types of CA in this study. Contrastingly, it might be that the uptake of atmospheric CO_2 into the surrounding water layer by diffusion is high enough so that no enhancement of the expression of this gene is needed. It remains to be further investigated how the different types of CAs are affected by enhanced CO_2 concentrations during desiccation in marine macroalgae. Therefore, the reason for the increased CA expression in algal tips that had experienced regular tidal emergence and high CO_2 remain speculative. Since the higher availability of carbon during the combined effects of high CO_2 and desiccation might lead to a higher carboxylation rate of RubisCO, i.e. a higher activity of the enzyme, it is contra intuitive why these parameters caused an up-regulation of RubisCO. If the combination of high CO_2 and tidal effect will increase the availability of carbon to a higher concentration than the half saturation of RubisCO, this might lead to a higher activity of RubisCO enzymes present in the cells but might not cause a higher expression of RubisCO. Since the enzyme activity and content was not measured in the present study, the observed regulation pattern of the GOIs cannot be explained.

Interactive effects of abiotic parameters appear to be common, especially in the intertidal zone. Pearson et al. (2001) showed that the transcript abundance of RubisCO was higher in desiccated *F. vesiculosus* than in *F. vesiculosus* that had been grown in seawater under high light conditions. Desiccation alone did not induce the expression of RubisCO, but did the combination of desiccation and high light. The transcript level in algae during desiccation under high light conditions was higher compared to algae cultured under high light conditions

in sea water. In the latter treatment, the RubisCO level declined whereas it remained stable during desiccation under high light conditions (Pearson et al. 2001).

4.3 Conclusion

The observed changes in the expression of the GOIs were not in accordance with the observations from the physiological investigations. The investigated parameters led to a change in carbon fixation on the molecular level, even though no changes in physiological parameters were observed. Besides methodological failures (see section 4.1.3), it might be possible, that the increase of transcripts does not necessarily lead to a higher amount of the respective enzyme or an increase in enzyme activity. Although gene expression often indicates an active metabolic pattern, in some cases transcription of mRNA and enzyme activity are uncoupled (see López 2007). Thus, it is not always possible to directly extrapolate the enzyme activity or enzyme content from the transcript level (Levitan et al. 2010) due to translational and post-translational modifications (López 2007). Similar uncoupling of gene activity and transcript level was found for CA in the diatom *Thalassiosira pseudonana* (McGinn and Morel 2008). Furthermore, compared to other enzymes involved in the Calvin cycle, RubisCO has a low turnover number. This indicates that relatively large amounts of the enzyme are required to sustain a sufficient photosynthetic rate (Parry et al. 2008). Based on an unknown factor, higher quantities of RubisCO might be required to obtain the same rate of photosynthesis when the alga is exposed to the combined effects of CO_2 and tidal emergence. This might induce higher expression rates but not changes in physiological parameters indicating that *F. serratus* is able to adapt to changing conditions without a reduction in the measured fitness parameters. The results of the present study indicate that *F. serratus* is well adapted to abiotic stress of the intertidal zone and it will not be affected by changing atmospheric CO_2 concentrations.

4.4 Outlook

In this study, the effect of enhanced CO_2 concentrations and tidal emergence on the brown macroalga *Fucus serratus* was investigated for the first time by simultaneously investigating the physiological performance and the gene expression of this species. Thus, this study will act as a first opportunity to investigate the effects of combined abiotic parameters not only on physiological traits but also on the transcriptional level. Since this study was not able to explain the observed patterns, more studies are needed to be able to understand the impacts of ocean acidification on important species. Future studies should include proteomic (protein-based) approaches additionally to genomic (nucleic acid-based) analyses used in this study. Proteomics provides not only information about the gene expression but also about different

regulation patterns of certain proteins. By analyzing the transcription without the proteomics, one might not be able to investigate regulatory steps at the level of mRNA translation (such as post-translational modifications and alternate gene splicing). Thus, the amount of mRNA transcript during two different situations or treatments might be the same, but differences in the phosphorylation state of a protein might result in a significant increase in the protein activity (López 2007). By considering proteomics in future studies, one would be able to gain a more comprehensive understanding about the effects of ocean acidification on this important intertidal species and thus, might be able to extrapolate effects on the whole ecosystem. Furthermore, the CCM is a very complex process not only including CA but also several ion channels which transporting, amongst other, HCO_3^- into the algal thallus (Giordano et al. 2005). Thus, future studies should focus not only on CA but also on such ion channels incorporated into CCMs. Since, as the present study proved, the effects of different abiotic factors are heterogeneous and interacting, it might be advisable to first investigate the effects of one abiotic parameter in detail before including several different parameters. Additionally, it has to be mentioned, that most previous studies on the effect of stress on algae had a short experimental duration ranging from hours to one day at maximum (e.g. Pearson et al. 2001). These studies were able to investigate the short term response of the algae (acclimation processes). The present study was conducted over a longer period (2 weeks). Furthermore, studies that intended to investigate the molecular response are often performed under severe stresses (e.g. Beuf et al.1999) that provoke clear physiological stress responses.

5. References

Akagawa, H., Ikawa, T., & Nisizawa, K. (1972). The enzyme system for the entrance of $^{14}CO_2$ in the dark-fixation of brown algae. *Plant and Cell Physiology, 13*, 999-1016.

Altschul, S. F., Gish, W., Miller, W., Myers, E. W., & Lipman, D. J. (1990). Basic local alignment search tool. *Journal of Molecular Biology, 215*, 403 - 410.

Andría, J. R., Brun, F. G., Pérez-Lloréns, J. L., & Vergara, J. J. (2001). Acclimation responses of *Gracilaria* sp (Rhodophyta) and *Enteromorpha intestinalis* (Chlorophyta) to changes in the external inorganic carbon concentration. [Article]. *Botanica Marina, 44*(4), 361-370.

Apt, K., Clendennen, S., Powers, D., & Grossman, A. (1995). The gene family encoding the fucoxanthin chlorophyll proteins from the brown alga *Macrocystis pyrifera*. *Molecular & General Genetics, 246*(4), 455-464.

Badger, M. R., Andrews, T. J., Whitney, S. M., Ludwig, M., Yellowlees, D. C., Leggat, W., & Price, G. D. (1998). The diversity and coevolution of Rubisco, plastids, pyrenoids, and chloroplast-based CO_2-concentrating mechanisms in algae. *Canadian Journal of Botany-Revue Canadienne De Botanique, 76*(6), 1052-1071.

Badger, M. R., & Price, G. D. (1994). The role of carbonic anhydrase in photosynthesis. *Annual Review of Plant Physiology and Plant Molecular Biology, 45*, 369 - 392.

Beuf, L., Kurano, N., & Miyachi, S. (1999). Rubisco activase transcript (*rca*) abundance increases when the marine unicellular green alga *Chlorococcum littorale* is grown under high-CO_2 stress. *Plant Molecular Biology, 41*(5), 627-635.

Bidwell, R. G. S., & McLachlan, J. (1985). Carbon nutrition of seaweeds - photosynthesis, photorespiration and respiration. *Journal of Experimental Marine Biology and Ecology, 86*(1), 15-46.

Bischof, K., G√≥mez, I., Molis, M., Hanelt, D., Karsten, U., L√ºder, U., Roleda, M., Zacher, K., & Wiencke, C. (2006). Ultraviolet radiation shapes seaweed communities. *Reviews in Environmental Science and Biotechnology, 5*(2-3), 141-166.

Bowes, G. (1991). Growth at elevated CO_2: photosynthetic responses mediated through RubisCO. *Plant Cell and Environment, 14*(8), 795-806.

Brinkhuis, B. H., Tempel, N. R., & Jones, R. F. (1976). Photosynthesis and respiration of exposed salt-marsh fucoids. *Marine Biology, 34*, 349 - 359.

Cabello-Pasini, A., Smith, G. J., & Alberte, R. S. (2000). Phosphoenolpyruvate carboxykinase from the marine diatom *Skeletonema costatum* and the phaeophyte *Laminaria setchellii*. I. Isolation and biochemical characterization. *Botanica Marina, 43*(6), 559-568.

Caldeira, K., & Wickett, M. E. (2005). Ocean model predictions of chemistry changes from carbon dioxide emissions to the atmosphere and ocean. *Journal of Geophysical Research-Oceans, 110*(C9).

Carlsen, B., Johnsen, G., Berge, J., & Kuklinski, P. (2007). Biodiversity patterns of macro-epifauna on different lamina parts of *Laminaria digitata* and *Saccharina latissima* collected during spring and summer 2004 in Kongsfjorden, Svalbard. *Polar Biology, 30*(7), 939-943.

Carmo-Silva, A. E., da Silva, A. B., Keys, A. J., Parry, M. A. J., & Arrabaca, M. C. (2008). The activities of PEP carboxylase and the C-4 acid decarboxylases are little changed by drought stress in three C-4 grasses of different subtypes. *Photosynthesis Research, 97*(3), 223-233.

Cervigni, T., Teofani, F., & Bassanel.C. (1971). Effect of CO_2 on carbonic anhydrase in *Avena sativa* and *Zea mays. Phytochemistry, 10*(12), 2991-&.

Chapman, A. R. O. (1995). Fuctional ecology of fucoid algae: twenty-three years of progress. *Phycologia, 34*(1), 1-32.

Chen, Z. H., Walker, R. P., Acheson, R. M., & Leegood, R. C. (2002). Phosphoenolpyruvate carboxykinase assayed at physiological concentrations of metal ions has a high affinity for CO_2. *Plant Physiology, 128*(1), 160-164.

Cheng, S. H., Moore, B. D., & Seemann, J. R. (1998). Effects of short- and long-term elevated CO_2 on the expression of ribulose-1,5-bisphosphate carboxylase/oxygenase genes and carbohydrate accumulation in leaves of *Arabidopsis thaliana* (L) Heynh. *Plant Physiology, 116*(2), 715-723.

Cock, J., Sterck, L., Rouze, P., Scornet, D., Allen, A., Amoutzias, G., Anthouard, V., Artiguenave, F., Aury, J.-M., Badger, J., Beszteri, B., Billiau, K., Bonnet, E., Bothwell, J., Bowler, C., Boyen, C., Brownlee, C., Carrano, C., Charrier, B., Cho, G., Coelho, S., Collen, J., Corre, E., Da Silva, C., Delage, L., Delaroque, N., Dittami, S., Doulbeau, S., Elias, M., Farnham, G., Gachon, C., Gschloessl, B., Heesch, S., Jabbari, K., Jubin, C., Kawai, H., Kimura, K., Kloareg, B., Kupper, F., Lang, D., Le Bail, A., Leblanc, C., Lerouge, P., Lohr, M., Lopez, P., Martens, C., Maumus, F., Michel, G., Miranda-Saavedra, D., Morales, J., Moreau, H., Motomura, T., Nagasato, C., Napoli, C., Nelson, D., Nyvall-Collen, P., Peters, A., Pommier, C., Potin, P., Poulain, J., Quesneville, H., Read, B., Rensing, S., Ritter, A., Rousvoal, S., Samanta, M., Samson, G., Schroeder, D., Segurens, B., Strittmatter, M., Tonon, T., Tregear, J., Valentin, K., von Dassow, P., Yamagishi, T., Van de Peer, Y., & Wincker, P. (2010). The *Ectocarpus* genome and the independent evolution of multicellularity in brown algae. *Nature, 465*(7298), 617-621.

Cooper, T. G., Filmer, D., Wishnick, M., & Lane, M. D. (1969). The active species of "CO_2" utilized by ribulose diphosphate carboxylase. *The Journal of Biological Chemistry, 244*(4), 1081 - 1083.

Davison, I. R., & Pearson, G. A. (1996). Stress tolerance in intertidal seaweeds. *Journal of Phycology, 32*(2), 197-211.

Delille, B., Harlay, J., Zondervan, I., Jacquet, S., Chou, L., Wollast, R., Bellerby, R. G. J., Frankignoulle, M., Borges, A. V., Riebesell, U., & Gattuso, J. P. (2005). Response of primary production and calcification to changes of pCO_2 during experimental blooms of the coccolithophorid *Emiliania huxleyi*. *Global Biogeochemical Cycles, 19*(2).

Dickson, A. G., & Millero, F. J. (1987). A comparison of the equilibrium constants for the dissociation of carbonic-acid in seawater media. *Deep-Sea Research Part a-Oceanographic Research Papers, 34*(10), 1733-1743.

Dreesmann, D. C., Harn, C., & Daie, J. (1994). Expression of genes encoding RubisCO in suger-beet (*Beta vulgaris* L.) plants subjected to gradual desiccation *Plant and Cell Physiology, 35*(4), 645-653.

Dring, M. J., & Brown, F. A. (1982). Photosynthesis of intertidal brown algae during and after periods of emersion: a renewed search for physiological causes of zonation. *Marine Ecology-Progress Series, 8*, 301 - 308.

Dupont, S., Wilson, K., Obst, M., Skold, H., Nakano, H., & Thorndyke, M. (2007). Marine ecological genomics: when genomics meets marine ecology. *Marine Ecology-Progress Series, 332*, 257-273.

Einav, R., Breckle, S., & Beer, S. (1995). Ecophysiological adaptation strategies of some intertidal marine macroalgae of the Israeli Mediterranean coast. *Marine Ecology-Progress Series, 125*(1-3), 219-228.

Fabre, N., Reiter, I. M., Becuwe-Linka, N., Genty, B., & Rumeau, D. (2007). Characterization and expression analysis of genes encoding alpha and beta carbonic anhydrases in *Arabidopsis*. *Plant Cell and Environment, 30*(5), 617-629.

Feely, R. A., Sabine, C. L., Lee, K., Berelson, W., Kleypas, J. A., Fabry, V. J., & Millero, F. J. (2004). Impact of anthropogenic CO_2 on the $CaCO_3$ system in the oceans. *Science, 305*(5682), 362-366.

Fischer, H. M., Wheat, C. W., Heckel, D. G., & Vogel, H. (2008). Evolutionary origins of a novel host plant detoxification gene in butterflies. *Molecular Biology and Evolution, 25*(5), 809-820.

Freitag, M., Beszteri, S., Vogel, H., & John, U. (2011). Effects of physiological shock treatments on toxicity and polyketide synthase gene expression in *Prymnesium parvum* (Prymnesiophyceae). *European Journal of Phycology, 46*(3), 193 - 201.

Fujita, K., Ehira, S., Tanaka, K., Asai, K., & Ohta, N. (2008). Molecular phylogeny and evolution of the plastid and nuclear encoded *cbbX* genes in the unicellular red alga *Cyanidioschyzon merolae. Genes & Genetic Systems, 83*(2), 127-133.

Fujiwara, S., Fukuzawa, H., Tachiki, A., & Miyachi, S. (1990). Structure and differential expression of two genes necoding carbonic anhydrase in Chlamydomonas reinhardtii. *Proceedings of the National Academy of Sciences of the United States of America, 87*, 9779 - 9783.

Gao, K., Aruga, Y., Asada, K., Ishihara, T., Akano, T., & Kiyohara, M. (1991). Enhanced growth of the red alga *Porphyra yezoensis* Ueda in high CO_2 concentrations. *Journal of Applied Phycology, 3*(4), 355-362.

Gao, K. S., & Aruga, Y. (1987). Preliminary studies on the photosynthesis and respiration of *Porphyra yezoensis* under emersed conditions. *Journal of the Tokyo University of Fisheries, 47*(1), 51 - 65.

Gao, K. S., Ji, Y., & Aruga, Y. (1999). Relationship of CO_2 concentrations to photosynthesis of intertidal macroalgae during emersion. *Hydrobiologia, 399*, 355-359.

García-Sánchez, M. J., Fernández, J. A., & Niell, X. (1994). Effect of inorganic carbon supply on the photosynthetic physiology of *Gracilaria tenuistipitata. Planta, 194*(1), 55-61.

Gazeau, F., Quiblier, C., Jansen, J. M., Gattuso, J. P., Middelburg, J. J., & Heip, C. H. R. (2007). Impact of elevated CO_2 on shellfish calcification. *Geophysical Research Letters, 34*(7).

Gesch, R. W., Boote, K. J., Vu, J. C. V., Allen, L. H., & Bowes, G. (1998). Changes in growth CO_2 result in rapid adjustments of ribulose-1,5-bisphosphate carboxylase/oxygenase small subunit gene expression in expanding and mature leaves of rice. *Plant Physiology, 118*(2), 521-529.

Giordano, M., Beardall, J., & Raven, J. A. (2005). CO_2 concentrating mechanisms in algae: Mechanisms, environmental modulation, and evolution. *Annual Review of Plant Biology, 56*, 99-131.

Giordano, M., & Maberly, S. C. (1989). Distribution of carbonic anhydrase in British marine macroalgae. *Oecologia, 81*(4), 534-539.

Gordillo, F. J. L., Figueroa, F. L., & Niell, F. X. (2003). Photon- and carbon-use efficiency in *Ulva rigida* at different CO_2 and N levels. *Planta, 218*(2), 315-322.

Gordillo, F. J. L., Jimenez, C., Figueroa, F. L., & Niell, F. X. (1999). Effects of increased atmospheric CO_2 and N supply on photosynthesis, growth and cell composition of the cyanobacterium *Spirulina platensis* (Arthrospira). *Journal of Applied Phycology, 10*(5), 461-469.

Gordillo, F. J. L., Niell, F. X., & Figueroa, F. L. (2001). Non-photosynthetic enhancement of growth by high CO_2 level irm the nitrophilic seaweed *Ulva rigida* C. Agardh (Chlorophyta). *Planta, 213*(1), 64-70.

Grzebyk, D., Schofield, O., Vetriani, C., & Falkowski, P. G. (2003). The mesozoic radiation of eukaryotic algae: The portable plastid hypothesis. *Journal of Phycology, 39*(2), 259-267.

Huxman, T. E., Hamerlynck, E. P., Moore, B. D., Smith, S. D., Jordan, D. N., Zitzer, S. F., Nowak, R. S., Coleman, J. S., & Seemann, J. R. (1998). Photosynthetic down-regulation in *Larrea tridentata* exposed to elevated atmospheric CO_2: interaction with drought under glasshouse and field (FACE) exposure. *Plant Cell and Environment, 21*(11), 1153-1161.

Inskeep, W. P., & Bloom, P. R. (1985). Extinction coeffiencts of chlorophyll-a and chlorophyll-b in N,N-Dimethylformamide and 80% acetone. *Plant Physiology, 77*(2), 483-485.

IPCC. (2007). Climate Change 2007: Synthesis Report. An assessment of the Intergovernmental Panel on Climate Change (IPCC). Cambridge University Press, Cambridge, UK and New York, USA.

Israel, A., & Beer, S. (2000). Photosynthetic and growth responses of macroalgae to globally changing CO_2 concentrations. *First Mediterranean Symposium on Marine Vegetation. Ajaccio, Corsica., 3 - 4 October 2000*.

Israel, A., & Hophy, M. (2002). Growth, photosynthetic properties and Rubisco activities and amounts of marine macroalgae grown under current and elevated seawater CO_2 concentrations. *Global Change Biology, 8*(9), 831-840.

Ji, Y., & Tanaka, J. (2002). Effect of desiccation on the photosynthesis of seaweeds from the intertidal zone in Honshu, Japan. *Phycological Research, 50*, 145 - 153.

Johnston, A. M., & Raven, J. A. (1990). Effects of culture in high CO_2 on the photosynthetic physiology of *Fucus serratus. British Phycological Journal, 25*(1), 75-82.

Kawamitsu, Y., & Boyer, J. S. (1999). Photosynthesis and carbon storage between tides in a brown alga, Fucus vesiculosus. *Marine Biology, 133*(2), 361-369.

Kawamitsu, Y., Driscoll, T., & Boyer, J. S. (2000). Photosynthesis during desiccation in an intertidal alga and a land plant. *Plant and Cell Physiology, 41*(3), 344-353.

Kleypas, J. A., Feely, R. A., Fabry, V. J., Langdon, C., Sabine, C. L., & Robbins, L. L. (2006). Impacts of ocean acidification on coral reefs and other marine calcifiers: A guide for future research. Workshop report 18 - 20. April 2005, St. Petersburg, Florida.

Kornmann, P., & Sahling, P.-H. (1977). Meeresalgen von Helgoland. Benthische Grün-, Braun- und Rotalgen. *Helgoländer wissenschaftliche Meeresuntersuchungen, 29*, 1 - 289.

Kremer, B. P. (1981). Metabolic implications on non-photosynthetic carbon fixation in brown macroalgae. *Phycologia, 20*(3), 242-250.

Kurihara, H., Kato, S., & Ishimatsu, A. (2007). Effects of increased seawater pCO_2 on early development of the oyster *Crassostrea gigas. Aquatic Biology, 1*(1), 91-98.

Kwok, S., Chang, S. Y., Sninsky, J. J., & Wang, A. (1994). A guide to the design and use of mismatched and degenerate primers *Pcr-Methods and Applications, 3*(4), S39-S47.

Larsson, C., & Axelsson, L. (1999). Bicarbonate uptake and utilization in marine macroalgae. *European Journal of Phycology, 34*(1), 79-86.

Larsson, M., Larsson, C. M., & Guerrero, M. G. (1985). Photosynthetic nitrogen metabolism in high and low CO_2-adapted *Scenedesmus.* I. Inorganic carbon-dependent O_2 evolution, nitrate utilization and nitrogen recycling. *Journal of Experimental Botany, 36*(170), 1373-1386.

Levitan, O., Sudhaus, S., LaRoche, J., & Berman-Frank, I. (2010). The influence of pCO_2 and temperature on gene expression of carbon and nitrogen pathways in *Trichodesmium* IMS101. *Plos One, 5*(12).

Lewis, E., & Wallace, D. W. R. (1998). Program developed for CO_2 system calculations. ORNL/CDIAC-105. Carbon dioxide informantion analysis center, Oak Ridge National Laboratory, U.S. Department of Energy, Oak Ridge, Tennessee.

Linhart, C., & Shamir, R. (2005). The degenerate primer design problem: Theory and applications. *Journal of Computational Biology, 12*(4), 431-456.

Lobban, C. S., & Harrison, P. J. (1994). Seaweed ecology and physiology. *Cambridge University Press, Cambridge, UK and New York, USA*.

López, J. L. (2007). Applications of proteomics in marine ecology. *Marine Ecology-Progress Series, 332*, 275-279.

Lüning, K. (1985). Meeresbotanik. Verbreitung, Ökophysiologie und Nutzung der marinen Makroalgen. Georg Thieme Verlag Stuttgart, New York.

Maberly, S. C., & Madsen, T. V. (1990). Contribution of air and water to the carbon balance of *Fucus spiralis. Marine Ecology-Progress Series, 62*(1-2), 175-183.

Maier, U. G., Fraunholz, M., Zauner, S., Penny, S., & Douglas, S. (2000). A nucleomorph-encoded *cbbX* and the phylogeny of RuBisCo regulators. *Molecular Biology and Evolution, 17*(4), 576-583.

Majeau, N., & Coleman, J. R. (1996). Effect of CO_2 concentration on carbonic anhydrase and ribulose-1,5-biphosphate carboxylase/oxygenase expression in pea. *Plant Physiology, 112*(2), 569-574.

Matsuzaki, M., Misumi, O., Shin-I, T., Maruyama, S., Takahara, M., Miyagishima, S. Y., Mori, T., Nishida, K., Yagisawa, F., Yoshida, Y., Nishimura, Y., Nakao, S., Kobayashi, T., Momoyama, Y., Higashiyama, T., Minoda, A., Sano, M., Nomoto, H., Oishi, K.,

Hayashi, H., Ohta, F., Nishizaka, S., Haga, S., Miura, S., Morishita, T., Kabeya, Y., Terasawa, K., Suzuki, Y., Ishii, Y., Asakawa, S., Takano, H., Ohta, N., Kuroiwa, H., Tanaka, K., Shimizu, N., Sugano, S., Sato, N., Nozaki, H., Ogasawara, N., Kohara, Y., & Kuroiwa, T. (2004). Genome sequence of the ultrasmall unicellular red alga *Cyanidioschyzon merolae* 10D. *Nature, 428*(6983), 653-657.

McGinn, P. J., & Morel, F. M. M. (2008). Expression and regulation of carbonic anhydrases in the marine diatom *Thalassiosira pseudonana* and in natural phytoplankton assemblages from Great Bay, New Jersey. *Physiologia Plantarum, 133*(1), 78-91.

Mercado, J. M., Gordillo, F. J. L., Figueroa, F. L., & Niell, F. X. (1998). External carbonic anhydrase and affinity for inorganic carbon in intertidal macroalgae. *Journal of Experimental Marine Biology and Ecology, 221*(2), 209-220.

Mercado, J. M., Javier, F., Gordillo, L., Niell, F. X., & Figueroa, F. L. (1999). Effects of different levels of CO_2 on photosynthesis and cell components of the red alga *Porphyra leucosticta*. *Journal of Applied Phycology, 11*(5), 455-461.

Mercado, J. M., & Niell, F. X. (2000). Carbon dioxide uptake by *Bostrychia scorpioides* (Rhodophyceae) under emersed conditions. *European Journal of Phycology, 35*(1), 45-51.

Mülhardt, G. (2009). Der Experimentator: Molekularbiologie/Genomics, 6th edition. Spektrum Akademischer Verlag, Heidelberg.

Nie, G. Y., Hendrix, D. L., Webber, A. N., Kimball, B. A., & Long, S. P. (1995). Increased accumulation of carbohydrates and decreased photosynthetic gene transcript levels in wheat grown at an elevated CO_2 concentration in the field. *Plant Physiology, 108*(3), 975-983.

Parry, M. A. J., Keys, A. J., Madgwick, P. J., Carmo-Silva, A. E., & Andralojc, P. J. (2008). Rubisco regulation: a role for inhibitors *Journal of Experimental Botany* (Vol. 59, pp. 1569-1580).

Pearson, G., Hoarau, G., Lago-Leston, A., Coyer, J., Kube, M., Reinhardt, R., Henckel, K., Serr√£o, E., Corre, E., & Olsen, J. (2010). An expressed sequence tag analysis of the intertidal brown seaweeds *Fucus serratus* (L.) and *F. vesiculosus* (L.) (Heterokontophyta, Phaeophyceae) in response to abiotic stressors. *Marine Biotechnology, 12*(2), 195-213.

Pearson, G., Serrao, E. A., & Cancela, M. L. (2001). Suppression subtractive hybridization for studying gene expression during aerial exposure and desiccation in fucoid algae. *European Journal of Phycology, 36*(4), 359-366.

Peet, M. M., Huber, S. C., & Patterson, D. T. (1986). Acclimation to high CO_2 in monoecios cucumbers. II Carbon exchange rates, enzyme activities, and starch and nutrient concentrations. *Plant Physiology, 80*(1), 63-67.

Pelloux, J., Jolivet, Y., Fontaine, V., Banvoy, J., & Dizengremel, P. (2001). Changes in Rubisco and Rubisco activase gene expression and polypeptide content in *Pinus halepensis* M. subjected to ozone and drought. *Plant Cell and Environment, 24*(1), 123-131.

Pesheva, I., Kodama, M., Dionisiosese, M. L., & Miyachi, S. (1994). Changes in photosynthetic characteristics induced by transferring air-grown cells of *Chlorococcum littorale* in high-CO_2 conditions. *Plant and Cell Physiology, 35*(3), 379-387.

Pfaffl, M. W. (2001). A new mathematical model for relative quantification in real-time RT-PCR. *Nucleic Acids Research, 29*(9).

Pfaffl, M. W., Horgan, G. W., & Dempfle, L. (2002). Relative expression software tool (REST) for group-wise comparison and statistical analysis of relative expression results in real-time PCR. *Nucleic Acids Research, 30*(9).

Porter, M. A., & Grodzinski, B. (1984). Acclimation to high CO_2 in bean. Carbonic anhydrase and ribulose bisphosphate carboxylase. *Plant Physiology, 74*(2), 413-416.

Portielje, R., & Lijklema, L. (1995). Carbon-dioxide fluxes across the air-water interface and its impacts on carbon availability in aquatic systems *Limnology and Oceanography, 40*(4), 690-699.

Pörtner, H.-O. (2008). Ecosystem effects of ocean acidification in times of ocean warming: a physiologist´s view. *Marine Ecology Progress Series, 373*, 203 - 217.

Quadir, A., Harrison, P. J., & DeWreede, R. E. (1979). The effects of emergence and submergence on the photosynthesis and respiration of marine macrophytes. *Phycologia, 18*(1), 83 -88.

Rivers, J. S., & Peckol, P. (1995). Interactive effects of nitrogen and dissolved inorganic carbon on photosynthesis, growth, and ammonium uptake of the macroalga *Cladophora vagabunda* and *Gracilaria tikvahiae*. *Marine Biology, 121*(4), 747-753.

Rost, B., Zondervan, I., & Wolf-Gladrow, D. A. (2008). Sensitivity of phytoplankton to future changes in ocean carbonate chemistry: current knowledge, contradictions and research directions. *Marine Ecology Progress Series, 373*, 227 - 237.

Röttgers, S. (2002). Phylogenie und Genexpression der Glutamat-Synthase (GOGAT) in verschiedenen Algengruppen. Doctoral thesis, Justus-Liebig University Gießen, Germany

Sabine, C. L., Feely, R. A., Gruber, N., Key, R. M., Lee, K., Bullister, J. L., Wanninkhof, R., Wong, C. S., Wallace, D. W. R., Tilbrook, B., Millero, F. J., Peng, T. H., Kozyr, A., Ono, T., & Rios, A. F. (2004). The oceanic sink for anthropogenic CO_2. *Science, 305*(5682), 367-371.

Sambrook, J., & Russell, D. W. (2001). Molecular cloning: A lab manual, third edition. Cold Spring Harbor Laboratory Press, Cold Spring Harbor, NY, USA.

Sanger, F., Nicklen, S., & Coulson, A. R. (1977). DNA sequencing with chain-terminating inhibitors. *Proceedings of the National Academy of Sciences of the United States of America, 74*(12), 5463-5467.

Sciandra, A., Harlay, J., Lefevre, D., Lemee, R., Rimmelin, P., Denis, M., & Gattuso, J. P. (2003). Response of coccolithophorid *Emiliania huxleyi* to elevated partial pressure of CO_2 under nitrogen limitation. *Marine Ecology-Progress Series, 261*, 111-122.

Smith, L. M., Sanders, J. Z., Kaiser, R. J., Hughes, P., Dodd, C., Connell, C. R., Heiner, C., Kent, S. B. H., & Hood, L. E. (1986). Fluorescence detection in automated DNA-sequence analysis. *Nature, 321*(6071), 674-679.

Stecher, A. (2009). Effekte unterschiedlicher CO_2-Konzentrationen und Temperaturen auf die Primärproduktion von Braunalgen der Nordsee. Bachelor thesis, University of Bremen, Germany.

Stecher, A. (2011). Combined effects of CO_2 and tides on growth and photosynthetic performance of *Fucus vesiculosus*. Research Project, University of Bremen, Germany.

Stocker, O., & Holdheide, W. (1937). Die Assimilation Helgoländer Gezeitenalgen während der Ebbezeit. *Zeitschrift für Botanik, 32*, 1 - 59.

Swanson, A. K., & Fox, C. H. (2007). Altered kelp (Laminariales) phlorotannins and growth under elevated carbon dioxide and ultraviolet-B treatments can influence associated intertidal food webs. *Global Change Biology, 13*(8), 1696-1709.

Szabo, E., & Colman, B. (2007). Isolation and characterization of carbonic anhydrases from the marine diatom *Phaeodactylum tricomutum*. *Physiologia Plantarum, 129*(3), 484-492.

Tait, L. W., & Schiel, D. R. (2010). Primary productivity of intertidal macroalgal assemblages: comparison of laboratory and in situ photorespirometry. *Marine Ecology-Progress Series, 416*, 115-125.

The Royal Society (2005). Ocean acidification due to increasing atmospheric carbon dioxide. Policy document 12/05, the Clyvedon Press Ltd, Cardiff, UK.

Thoms, S., Pahlow, M., & Wolf-Gladrow, D. A. (2001). Model of the carbon concentrating mechanism in chloroplasts of eukaryotic algae. *Journal of Theoretical Biology, 208*(3), 295-313.

Van Oosten, J. J., & Besford, R. T. (1995). Some relationships between gas-exchange, biochemistry and molecular-biology of photosynthesis during leaf development of tomato plants after transder to different carbon dioxide concentrations. *Plant Cell and Environment, 18*(11), 1253-1266.

Van Oosten, J. J., & Besford, R. T. (1996). Acclimation of photosynthesis to elevated CO_2 through feedback regulation of gene expression: Climate of opinion. *Photosynthesis Research, 48*(3), 353-365.

Webber, A. N., Nie, G. Y., & Long, S. P. (1994). Acclimation of photosynthetic proteins to rising atmospheric CO_2. *Photosynthesis Research, 39*(3), 413-425.

Wiencke, C., Clayton, M., Gómez, I., Iken, K., Lüder, U., Amsler, C., Karsten, U., Hanelt, D., Bischof, K., & Dunton, K. (2007). Life strategy, ecophysiology and ecology of seaweeds in polar waters. *Reviews in Environmental Science and Biotechnology, 6*(1-3), 95-126.

Winder, T. L., Anderson, J. C., & Spalding, M. H. (1992). Translational regulation of the large and small subunits of ribulose bisphosphate carboxylase oxygenase during induction of the CO_2 concentrating meachnism in *Chlamydomonas reinhardtii. Plant Physiology, 98*(4), 1409-1414.

Wolf-Gladrow, D. A., Riebesell, U., Burkhardt, S., & Bijma, J. (1999). Direct effects of CO_2 concentration on growth and isotopic composition of marine plankton. *Tellus Series B-Chemical and Physical Meteorology, 51*(2), 461-476.

Wu, H. Y., Zou, D. H., & Gao, K. S. (2008). Impacts of increased atmospheric CO_2 concentration on photosynthesis and growth of micro- and macro-algae. *Science in China Series C-Life Sciences, 51*(12), 1144-1150.

Xu, Z. G., Zou, D. H., & Gao, K. S. (2010). Effects of elevated CO_2 and phosphorus supply on growth, photosynthesis and nutrient uptake in the marine macroalga *Gracilaria lemaneiformis* (Rhodophyta). *Botanica Marina, 53*, 123 - 129.

Zhang, B. Y., Yang, F., Wang, G. C., & Peng, G. (2010). Cloning and quantitative analysis of the carbonic anhydrase gene from *Porphyra yezoensis. Journal of Phycology, 46*(2), 290-296.

Zimmerman, R. C., Kohrs, D. G., Steller, D. L., & Alberte, R. S. (1997). Impacts of CO_2 enrichment on productivity and light requirements of eelgrass. *Plant Physiology, 115*(2), 599-607.

Zou, D. H. (2005). Effects of elevated atmospheric CO_2 on growth, photosynthesis and nitrogen metabolism in the economic brown seaweed, *Hizikia fusiforme* (Sargassaceae, Phaeophyta). *Aquaculture, 250*(3-4), 726-735.

Zou, D. H., & Gao, K. S. (2002). Effects of desiccation and CO_2 concentrations on emersed photosynthesis in *Porphyra haitanensis* (Bangiales, Rhodophyta), a species farmed in China. *European Journal of Phycology, 37*(4), 587-592.

Zou, D. H., & Gao, K. S. (2004). Comparative mechanisms of photosynthetic carbon acquisition in *Hizikia fusiforme* under submersed and emersed conditions. *Acta Botanica Sinica, 46*(10), 1178-1185.

Zou, D. H., & Gao, K. S. (2005). Ecophysiological characteristics of four intertidal marine macroalgae during emersion along Shantou coast of China, with a special reference to the relationship of photosynthesis and CO2. *Acta Oceanologica Sinica, 24*(3), 105-113.

Zou, D. H., Gao, K. S., & Ruan, Z. X. (2007). Daily timing of emersion and elevated atmospheric CO2 concentration affect photosynthetic performance of the intertidal macroalga Ulva lactuca (Chlorophyta) in sunlight. *Botanica Marina, 50*(5-6), 275-279.

Internet sources:

5 Prime HotMasterTM Taq DNA Polymerase Manual (2007)
http://www.5prime.com/media/3388/hotmaster%20taq%20dna%20polymerase%20manual_5prime_1044359_032007.pdf

Agencourt® CleanSEQ® for ABI BigDye Terminator (2006)
https://products.appliedbiosystems.com/ab/en/US/adirect/ab?cmd=ABGenSearch

Agilent Bioanalyzer User´s Information Guide (2007)
http://www.chem.agilent.com/Library/brochures/Agilent%202100%20Bioanalyzer_lores_052785.pdf

Agilent RNA 6000 Nano Kit Guide (2006)
http://icob.sinica.edu.tw/pubweb/Core%20Facilities/Data/R401-core/RNA6000Nanomanual.pdf

Applied Biosystems BigDye® Terminatore v3.1 Cycle Sequencing Kit (2002)
http://www.ibt.lt/sc/files/BDTv3.1_Protocol_04337035.pdf

Invitrogen SuperScriptTM III Reverse Transcriptase manual (2004)
http://tools.invitrogen.com/content/sfs/manuals/superscriptIII_man.pdf

Invitrogen TOPO TA Cloning® Kit for Sequencing (2002)
http://130.15.90.245/methods/handbooks%20and%20manuals/PCR-4%20TOPO%20kit.pdf

KEGG database
http://www.genome.jp/kegg/

Primer 3 software
https://frodo.wi.mit.edu/primer3/input.htm

Primer Express Version: 2.0
http://www.appliedbiosystems.com

NCBI BLAST search
http://blast.ncbi.nlm.nih.gov/Blast.cgi

Qiagen MinElute® Gel Extraction Handbook (2008)
www.qiagen.com/literature/render.aspx?id=160

Qiagen MinElute® PCR Purification Handbook (2008)
www.qiagen.com/literature/render.aspx?id=160

Qiagen REST 2009 software
http://rest.gene-quantification.info/

Qiagen REST 2009 Software User Guide (2009)
http://www.gene-quantification.de/REST_2009_Software_User_Guide.pdf

Qiagen RNeasy® MinElute® Cleanup Kit (2007)
www.qiagen.com/literature/render.aspx?id=351

Qiagen RNeasy® Plant Mini Kit Handbook (2006)
www.qiagen.com/hb/rneasymini

Qiagen QuickLyse Miniprep Kit manual (2006)
www.qiagen.com/literature/render.aspx?id=194

Web-tool to generate degenerated oligonucleotide primers
http://www.vivo.colostate.edu/molkit/rtranslate/index.html

6. Appendix

Tab. 13: List of used chemicals, the supplier and the location.

Chemical	Supplier	Location
2% CTAB	Carl Roth GmbH	Karlsruhe, Germany
Agarose	AppliChem	Darmstadt, Germany
ampicillin	Sigma-Aldrich®	Schnelldorf, Germany
Beta mercaptoethanol	AppliChem	Darmstadt, Germany
Chloroform:isoamylalcohol (24:1)	AppliChem	Darmstadt, Germany
dNTP mix	5 Prime	Hamburg, Germany
DTT	AppliChem	Darmstadt, Germany
Ethanol	Merck GmbH	Darmstadt, Germany
Ethidium bromide	Sigma-Aldrich®	Schnelldorf, Germany
Fist-Strand buffer	Invitrogen	Darmstadt, Germany
HotMasterTM *Taq* buffer	5 Prime	Hamburg, Germany
HotMasterTM *Taq* polymerase	5 Prime	Hamburg, Germany
Molecular grade water	Eppendorf	Hamburg, Germany
NaCl	Fluka BioChemika	Buchs, Switzerland
Omniscript reverse transcriptase	Qiagen	Hilden, Germany
peqGOLD DNA ladder	PeqLab	Erlangen, Germany
Premix BigDye®	Applied Biosystems	Darmstadt, Germany
RNase H	Invitrogen	Darmstadt, Germany
RNase OUT™	Invitrogen	Darmstadt, Germany
S.O.C. medium	Invirtogen	Darmstadt, Germany
Salt solution (1.2 M NaCl, 0.06 M $MgCl_2$)	Invitrogen	Darmstadt, Germany
SuperScriptTM III reverse transcriptase	Invitrogen	Darmstadt, Germany
SYBR© Safe	Invitrogen	Darmstadt, Germany
Tris	Invitrogen	Darmstadt, Germany
X-Gal	Invitrogen	Darmstadt, Germany

Tab. 14: Respiration, gross photosynthesis (PS), and net PS in [μmol O_2 h^{-1} g_{WW}^{-1}] of apical tips of *Fucus serratus* cultured at two different CO_2 concentrations (280 and 1200 ppm) and two different tidal regimes (tidal emergence and permanent submersion). Presented are the means per treatment (± standard deviation) (n = 5). Bold values indicate n = 4.

Treatment		Respiration [μmol O_2 h^{-1} g_{FW}^{-1}]	Gross PS [μmol O_2 h^{-1} g_{FW}^{-1}]	Netto PS [μmol O_2 h^{-1} g_{FW}^{-1}]
280 ppm CO_2	tides	-1.90 (± 1.34)	24.98 (± 3.83)	**21.67 (± 2.48)**
	no tides	-2.16 (± 1.48)	23.23 (± 4.96)	21.07 (± 6.12)
1200 ppm CO_2	tides	-2.69 (± 0.89)	24.68 (± 3.85)	21.98 (± 3.41)
	no tides	-2.78 (± 1.94)	23.83 (± 2.84)	21.05 (± 3.73)

Tab. 15: Chlorophyll (Chl) *a* content [mg g_{WW}^{-1}] of apical tips of *Fucus serratus* cultured at two different CO_2 concentrations (280 and 1200 ppm) and two different tidal regimes (tidal emergence and permanent submersion). Presented are the means per treatment (± standard deviation) (n = 5).

Treatment		Chl *a* content [mg g_{WW}^{-1}]
280 ppm CO_2	tides	0.27 (± 0.03)
	no tides	0.25 (± 0.03)
1200 ppm CO_2	tides	0.24 (± 0.04)
	no tides	0.23 (± 0.03)

Tab 16: Recipe for Luria-Bertani (LB) medium used in cloning procedure to grow bacterial colonies.

	Component	Quantity
liquid (for 300 mL)		
	1.0% Tryptone	3 g
	0.5 % Yeast extract	1.5 g
	1.0% NaCl	3 g
	H_2O	250 mL
agar plates		
	1.0% Tryptone	3 g
	0.5 % Yeast extract	1.5 g
	1.0% NaCl	3 g
	agar	4.5 g
	H_2O	250 mL

Tab. 17: RNA concentration [ng/µl] and its absorption at 260/280 and 260/230 nm extracted from *Fucus serratus* cultured at two different CO_2 concentrations (280 and 1200 ppm) and two different tidal regimes (tidal emergence and permanent submersion) for each of the used replicates (left side of the table). The right side of the table presents the RNA concentration and its absorption of sample 3,5 and 15 after purification.

					After purification		
Treatment	No.	RNA concentration [ng/µl]	Absorption ratio 260/280 nm	Absorption ratio 260/230 nm	RNA concentration [ng/µl]	Absorption ratio 260/280 nm	Absorption ratio 260/230 nm
280 ppm CO_2 — tides	1	120.03	2.15	2.00			
	2	150.65	2.15	2.11			
	3	144.95	2.15	1.09	105.69	2.12	1.73
	4	144.96	2.15	2.23			
	5	126.13	2.15	1.46	107.64	2.06	2.27
280 ppm CO_2 — no tides	6	159.18	2.13	2.1			
	7	169.74	2.18	2.03			
	8	136.51	2.15	2.03			
	9	149.70	2.18	2.18			
	10	264.04	2.18	2.33			
1200 ppm CO_2 — tides	11	184.78	2.18	2.28			
	12	180.25	2.16	2.25			
	13	172.84	2.12	1.99			
	14	204.12	2.15	2.02			
	15	189.07	2.19	1.57	155.87	2.11	2.15
1200 ppm CO_2 — no tides	16	172.62	2.17	2.04			
	17	215.03	2.14	2.03			
	18	188.25	2.16	2.19			
	19	114.21	2.14	2.01			
	20	221.95	2.16	2.22			

Tab. 18: DNA concentration [ng/µl] and its absorption at 260/280 and 260/230 nm of the plasmids extracted from positive *E. coli* colonies, containing a vector with an insert of the respective gene. Numbers (No.) give the respective number of positive colonies for each of the tested enzymes (RubisCO = Ribulose-1,5-bisphosphate carboxylase oxygenase, CA = Carbonic anhydrase, PEPCK = Phosphoenolpyruvate carboxykinase and glycolate oxidase).

Enzyme	DNA	No.	RNA concentration [ng/µl]	Absorption ratio 260/280 nm	Absorption ratio 260/230 nm
RubisCO 1	A6	1	72.38	2.04	1.79
	A8	2	31.83	1.96	1.35
CA	B1	1	116.58	1.89	2.10
	B2	2	134.34	1.95	2.01
	B3	3	162.44	1.93	1.77
	B5	4	58.88	1.92	1.47
	B7	5	95.68	1.96	2.05
	B10	6	158.39	1.94	1.93
	B11	7	83.53	2.01	1.58
RubisCO 2	C1	1	152.5	1.92	1.86
	C2	2	100.17	1.95	1.95
	C3	3	181.52	1.93	2.03
	C4	4	60.51	1.92	1.68
	C5	5	80.50	1.94	1.98
PEPCK	D1	1	144.84	1.95	1.97
	D2	2	74.99	1.88	1.08
	D3	3	78.75	1.91	1.89
	D4	4	71.41	1.88	1.54
	D5	5	77.35	1.94	2.04
	D6	6	71.46	1.87	1.66
	D7	7	145.81	1.92	2.05
	D8	8	58.17	1.91	1.83
	D9	9	70.34	1.91	1.87
	D10	10	80.41	1.98	1.94
Glycolate oxidase	E1	1	21.38	1.93	0.75
	E2	2	25.36	1.88	1.67
	E3	3	133.62	1.95	1.70
	E4	4	56.18	2.05	1.51
	E6	5	75.94	1.91	1.76
	E7	6	77.22	1.87	1.72

Tab. 19: C_t values of the spike-in gene MA (major allgergen) (reference) and different genes (target) of cDNA from *Fucus serratus* grown at different CO_2 concentrations and tidal regimes. Ct values were obtained by a quantitative real-time polymerase chain reaction (qRT-PCR). All results are presented as means (± SD) (n = 5).

Treatment		C_t value						
		MA	RubisCO1	RubisCO2	PEPCK1	PEPCK2	CA1	CA2
280 ppm	tides	29.9 (± 0.4)	22.7 (± 0.3)	28.4 (± 0.3)	23.6 (± 0.3)	23.2 (± 0.3)	24.4 (± 3.9)	19.3 (± 0.2)
	no tides	30.8 (± 1.8)	23.1 (± 2.3)	27.5 (± 0.5)	23.9 (± 2.8)	22.3 (± 0.5)	27.3 (± 5.4)	19.0 (± 0.3)
1200 ppm	tides	31.0 (± 0.9)	22.4 (± 0.3)	28.0 (± 0.8)	23.0 (± 1.1)	22.5 (± 0.8)	26.1 (± 4.2)	19.3 (± 0.8)
	no tides	29.7 (± 0.4)	22.0 (± 0.1)	26.3 (± 1.4)	22.4 (± 0.4)	21.7 (± 1.1)	24.5 (± 4.2)	19.0 (± 0.2)

Acknowledgement